EXTENT AND TIMING OF LAURENTIDE

GLACIAL LAKE MUSSELSHELL,

CENTRAL MONTANA

by

Nicole Kristina Davis

A thesis submitted in partial fulfillment
of the requirements for the degree

of

Master of Science

in

Earth Sciences

MONTANA STATE UNIVERSITY
Bozeman, Montana

July 2004

APPROVAL

of a thesis submitted by

Nicole Kristina Davis

This thesis has been read by each member of the thesis committee and has been found to be satisfactory regarding content, English usage, format, citations, bibliographic style, and consistency, and is ready for submission to the College of Graduate Studies.

Dr. William W. Locke

Approved for the Department of Earth Sciences

Dr. David R. Lageson

Approved for the College of Graduate Studies

Dr. Bruce McLeod

STATEMENT OF PERMISSION TO USE

Nicole K. Davis

July 15, 2004

ACKNOWLEDGEMENTS

This thesis would not have been possible without the support, advice and patience of a great number of people. Roger Colton, Dave Fullerton, and Bill Johnson from the US Geological Survey were especially helpful and provided materials and information that were central to the project. Rick Alexander was a tremendous help in the field. Bob Wegmann and Brian from the Soil Survey helped me to get oriented in the field and assisted with the soil study. Gary Landis of the USGS generously provided facilities for the ^{21}Ne analyses. I greatly appreciate the time and thought that Grace Sherwood-Winer, Marie-Luce Chevalier, Ken Pierce, Andy Hunt, Vinnie Mills-Herring, Cayce, Dan Miggins, Tom Guilderson, Joe Licciardi, and others gave to this project. Special thanks to my committee, Stephan Custer, Tom Keck, and Ken Pierce, my intrepid advisor Bill Locke, Bob Finkel from Lawrence Livermore, and to my family and friends.

I am also grateful to the residents of Petroleum and Garfield Counties for the generosity and trust that they showed me during my two field seasons. In particular, I would like to thank Phil and Delores Hill and family, Dave, Nancy, Bruce, Daisy and Dean Dutton and family, Skip and Diane Ahlgren, and Walter Manuel.

Most of the funding for this project was provided by the Center for Accelerator Mass Spectrometry at Lawrence Livermore National Laboratory. Additional support from the family of Barry C. Bishop, the Geological Society of America (GSA), the Quaternary Geology and Geomorphology Division of GSA, and the Association for Women Geoscientists made this work possible.

TABLE OF CONTENTS

LIST OF TABLES

LIST OF FIGURES

ABSTRACT

Glacial Lake Musselshell is the middle link in a chain of lakes that formed along the Pleistocene Laurentide ice margin in central Montana. It was first recognized because scores of glacially-transported boulders from the Canadian Shield are found in the Musselshell River basin, yet there is no evidence that the Laurentide ice sheet advanced that far south. For a century, the ice-rafted boulders remained the only physical evidence associated with the lake. No other features typical of other large, ephemeral lakes – varved lacustrine sediment, inflow deltas, or lake shorelines – had been identified for Lake Musselshell.

A sequence of nine river terraces and >100 previously located boulders provided the opportunity to place Lake Musselshell, and the corresponding Laurentide ice margin, in the context of regional and global chronologies. Terrace gradient and provenance, surface exposure ages of ice-rafted boulders, and identification of additional lake-related features were the most useful tools for establishing the extent and timing of Lake Musselshell.

Lake Musselshell probably existed as one or more short-lived stage(s) that reached a maximum altitude of ~920 m. The absence of varves, deltas and shorelines suggests against one or more stable levels. Deposits of sheet-like silt and fine sand are interpreted as slackwater sediment from one or more (hydraulically dammed?) lakes. The lake(s) drained under or in front of the ice sheet, down the modern Missouri River channel.

Strong evidence was found that Lake Musselshell existed during the Late Wisconsin stage. Twenty-seven ^{10}Be surface exposure ages from ice-rafted boulders are all Late Wisconsin and younger (5.2-21.7 ka). Canadian Shield gravel occurs only in the lowest (probably Late Wisconsin) Pleistocene terrace. Additionally, upstream convergence of the Musselshell River terraces implies that displacement of the Missouri River by the Laurentide ice sheet occurred only recently (possibly Late Wisconsin).

Pre-Late Wisconsin glacial advances into central Montana cannot be ruled out. Older deposits may be buried, removed or modified by erosion. However, the ice-rafted boulders and glacially-derived alluvium in the Musselshell basin are probably Late Wisconsin in age. Therefore, the Late Wisconsin Laurentide ice sheet may have been the most extensive Pleistocene ice sheet in central Montana.

INTRODUCTION

Over the last fifty years, significant advances have been made in our understanding of the extent and timing of late Cenozoic glaciation along the eastern half of the Laurentide ice sheet (Mickelson and Colgan, 2004), in the Cordillera (Cioppa et al., 1995; Karlstrom, 1999; Karlstrom, 2000; Booth et al., 2004), local glaciation in Yellowstone (Licciardi et al., 2001; Pierce, 2004), and in other alpine-glaciated areas (Kaufman et al., 2004; Pierce, 2004). Much work has also been presented on the recessional history of the western Laurentide ice sheet in Canada (Stalker, 1977; Jackson, 1980; Jackson et al., 1989; Liverman et al., 1989; Young et al., 1994; Jackson et al., 1997; Jackson et al., 1999; Young et al., 1999; Osborn et al., 2000; Little et al., 2001). Yet our understanding of the southwestern limit of Laurentide ice remains poorly dated.

At its maximum, the Laurentide ice sheet was the largest late Cenozoic ice sheet known to have existed, covering an area of <13.4 million km^2 (Andrews, 1975). Its presence had a profound affect on global climate and sea level (Clark et al., 1999; Clark et al., 2001; Clark and Mix, 2001), as well as regional geomorphology (Sugden, 1978; Fulton, 1989) and regional climate (Thackray et al., 2004). The timing of Laurentide glaciation on the northern Great Plains of Montana and North Dakota has not been well constrained over more than an 800 km stretch (Fullerton and Colton, 1986). It is possible to fill this gap by studying the extent and age of large ice-dammed lakes that interacted closely with the retreating and advancing ice sheet.

Boulders of Canadian Shield granite and gneiss litter the Montana plains in basins south of the farthest mapped ice margin. The boulders are presumably ice-rafted and their distribution provides direct physical evidence for at least six large proglacial lakes on the southern edge of the Laurentide ice sheet (Colton et al., 1961; Fig. 1). These lakes filled one or more times during the Pleistocene when ice advanced across the Missouri River and its tributaries. This caused large volumes of water to pond up against the ice until the lake overtopped a low pass or flowed out of the basin either beneath or along the edge of the ice, or the ice retreated allowing the water to spill out of the basin. Depending on the extent of Laurentide ice and the duration of ice damming, the lakes filled to different elevations during the various ice advances (Colton et al., 1961; Colton and Fullerton, 1986).

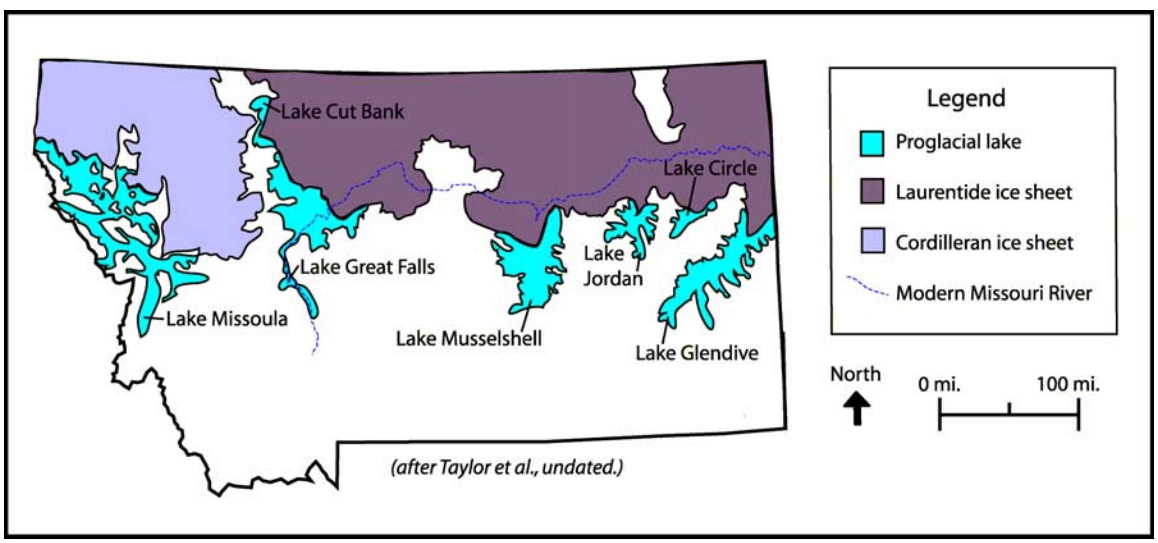

Figure 1. Maximum hypothesized Pleistocene ice and proglacial lake extent in Montana. Modern Missouri River shown for reference. Six major ice-dammed lakes existed on the Laurentide ice margin during one or more Pleistocene glaciations.

The age(s) and extent(s) of ice-dammed lakes in Montana are poorly understood, although they have been sporadically studied for more than a century (Calhoun, 1906; Alden, 1932; Colton et al., 1961; Colton and Fullerton, 1986; Fullerton et al., 2004). Very little field study and few attempts at numerical dating have been made with regard to these lakes. A flight of nine alluvial terraces and more than one hundred documented exotic boulders in the Musselshell basin (Johnson and Smith, 1964; Fig. 2) provide an excellent opportunity to obtain ages on the stand(s) of glacial Lake Musselshell, and therefore on the Laurentide ice front in central Montana.

Study Area

The study area is all of the land once covered by the highstand of glacial Lake Musselshell as depicted by Colton and others on the Glacial Map of Montana East of the Rocky Mountains (1961). This area covers portions of Fergus, Petroleum, Garfield, Musselshell and Rosebud counties (Fig. 3). Its northern border is the inferred ice margin responsible for blocking the Missouri River, resulting in the formation of Lake Musselshell (Colton et al., 1961). The rest of the lake highstand is delineated by the modern 960-meter (3150-foot) contour line, based on the altitude of the highest glacial boulder reported in the basin. The towns of Valentine, Winnett, Musselshell and Sand Springs all lie on the edge of the study area, and the towns of Mosby and Cat Creek are within the former lake boundary. The Musselshell River runs from south to north through the center of the study area.

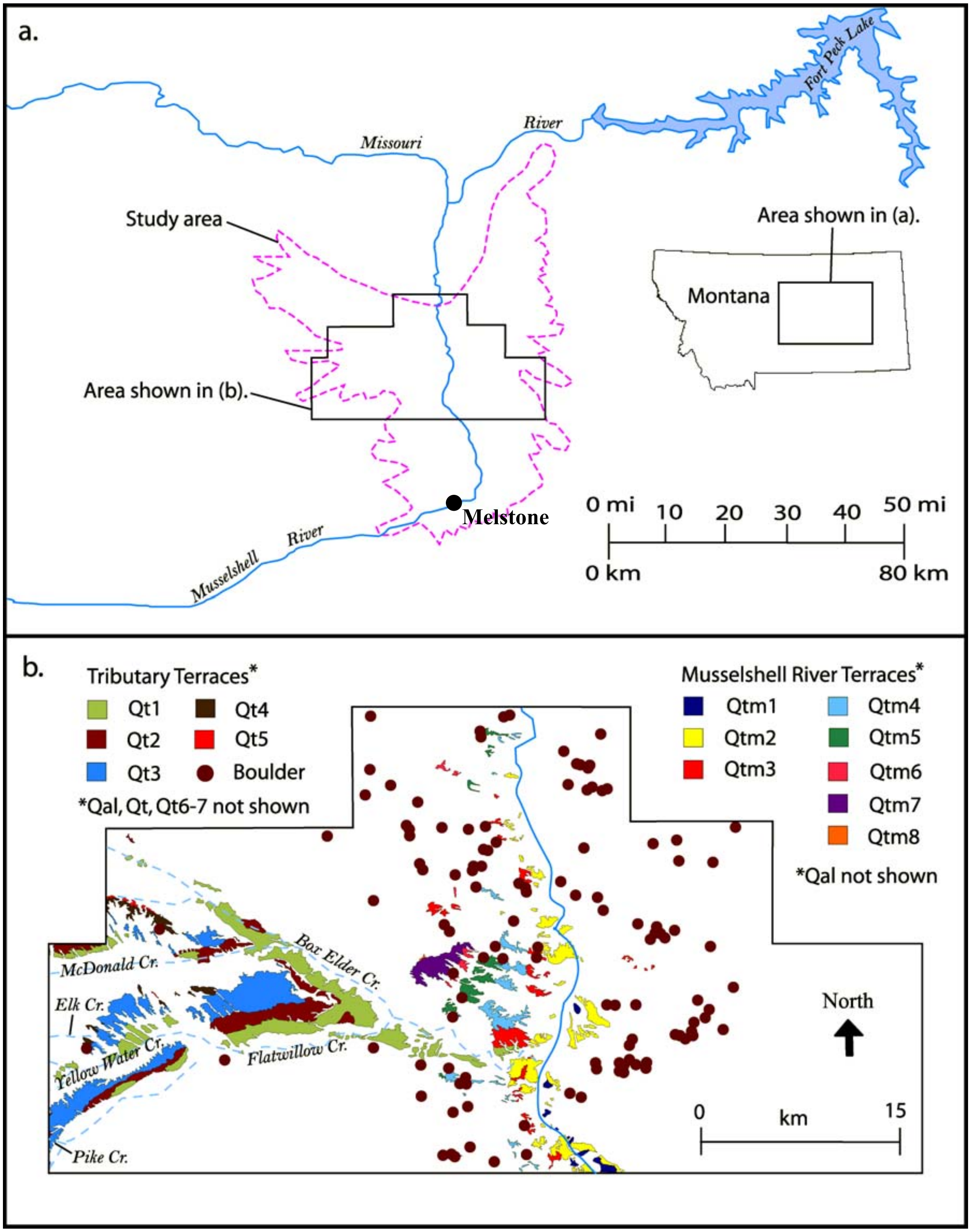

Figure 2. (a.) The study area is delineated by the outline of Lake Musselshell from Colton and others (1961). (b.) Gravel terraces and glacial boulders recognized in the Winnett-Mosby area by Johnson and Smith (1964).

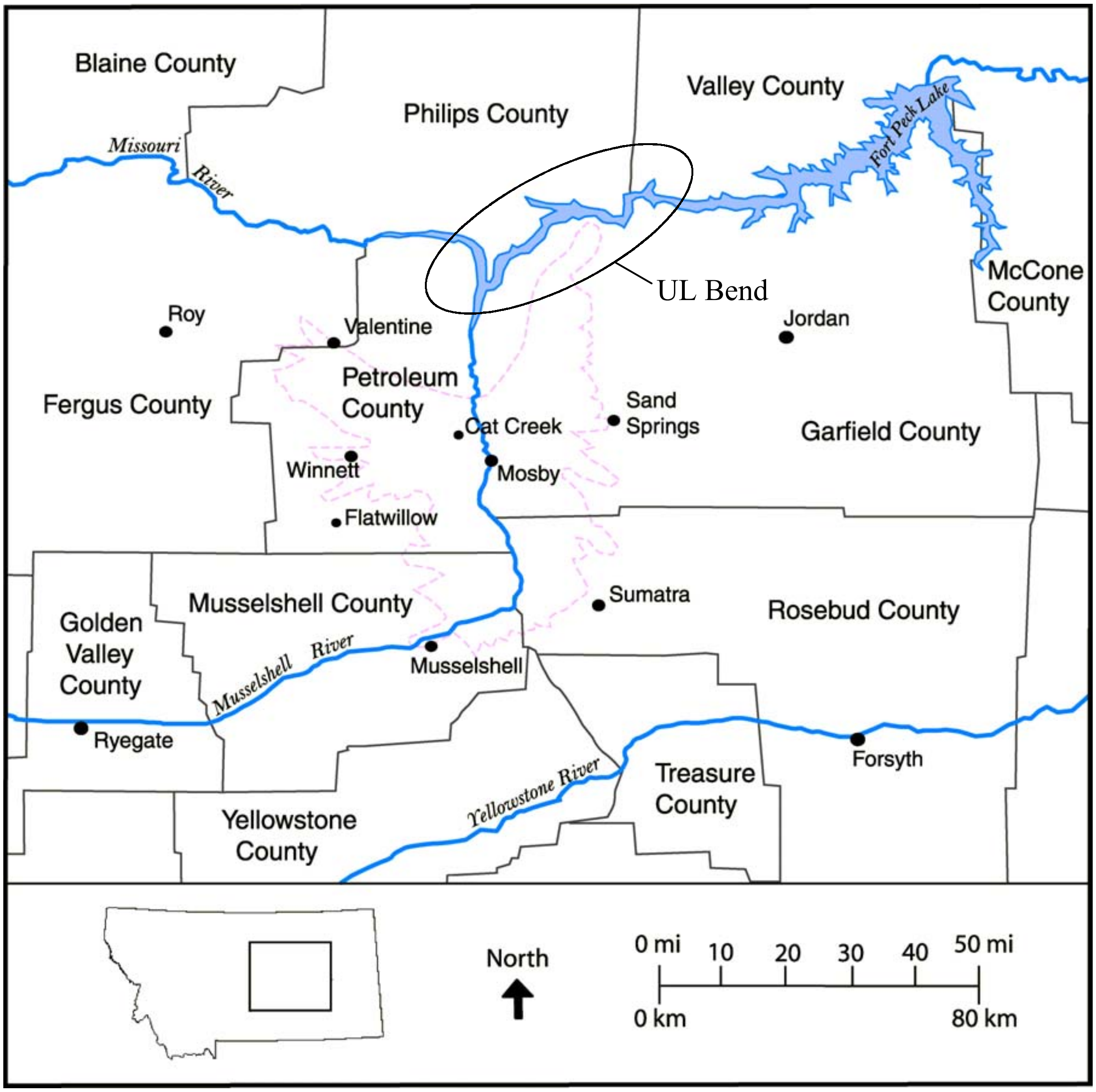

Figure 3. Counties and towns in the vicinity of the field area. Field area delineated by the outline of glacial Lake Musselshell from Colton and others (1961).

The modern Musselshell River begins in the Little Belt, Castle and northern Crazy Mountains (Fig. 4) and flows eastward for approximately 250 km parallel to the Yellowstone and Missouri Rivers. Tributaries from the Snowy and Bull Mountains (Fig. 4) join the Musselshell along this stretch. These source areas contain a variety of igneous, sedimentary and metasedimentary rock types (Fig. 5; Table 1). About 20 km downstream from the town of Musselshell, the river turns abruptly and flows north for 100 km to its confluence with the Missouri River at UL Bend (Fig. 3). Prior to joining the Missouri, the Musselshell is met by tributaries from the Snowy and Judith Mountains (Fig. 4). These tributaries contribute sedimentary and alkalic igneous rock types to the bedload of the river (Fig. 5; Table 1).

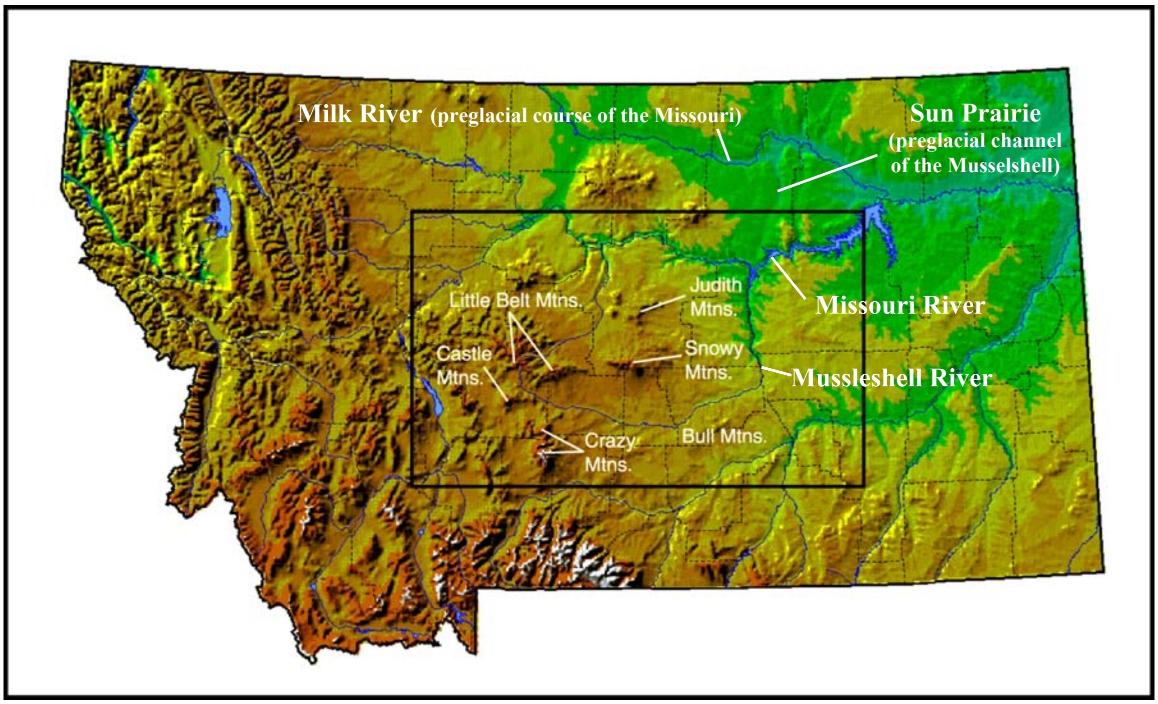

Figure 4. Shaded Relief Map of Montana (Montana Natural Resources Information System web site, 2004). Mountain ranges that serve as source areas for the Musselshell River are labeled. Boxed area is shown in Figure 5.

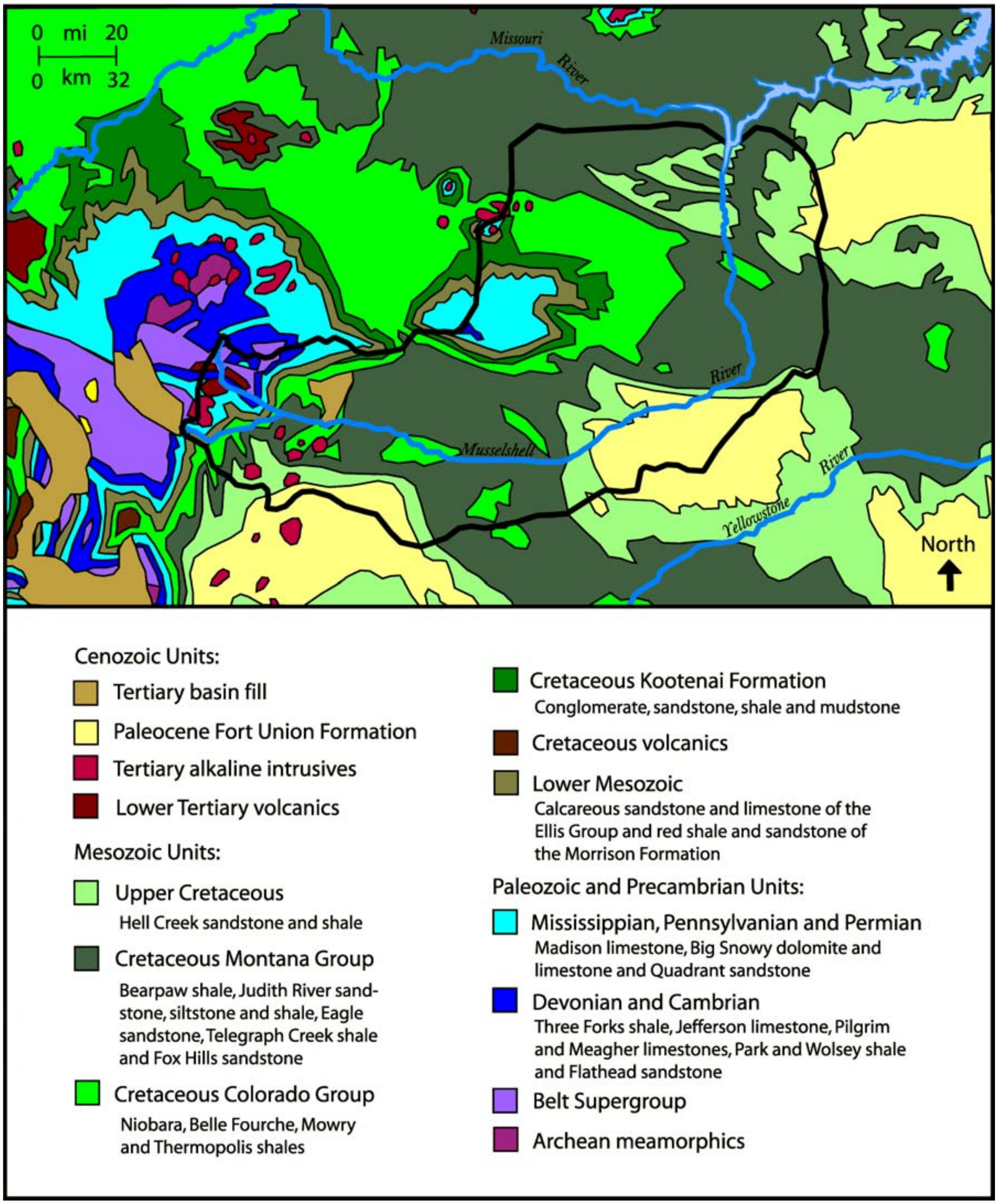

Figure 5. Bedrock geology of the Musselshell watershed and surrounding area (from Taylor et al., undated). The watershed is delineated by the thick black line.

TABLE 1. ROCK TYPES OF THE MUSSELSHELL RIVER BASIN.

Source area	Transport distance† (km)	Main rock types
Local‡	50-160	Calcareous and noncalcareous shale, sandstone, siltstone and mudstone, bentonite, concretions of limestone (some fossiliferous), sandstone and ironstone
Bull Mtns§	163-165	Coal-bearing Cretaceous Fort Union formation
Judith Mtns#	170-175	Alkaline intrusive igneous rocks, quartzite, shale, limestone, dolomite, sandstone, mudstone
Snowy Mtns††	175-290	Limestone, quartz sandstone, dolomite, siltstone, shale, small outcrops of lower Belt Supergroup (argillite, quartzite)
Little Belt Mtns‡‡	300-350	Belt quartzite and argillite, limestone, dolomite, and other sedimentary rock types
Northern Crazy Mtns§§	320-370	Alkaline, subalkaline, and silica-saturated to oversaturated intrusive rocks, small amounts of basalt, shonkinite (black syenite – mainly augite and orthoclase), and fenite (green metasomatic Fort Union shale)
Castle Mtns##	340-350	Eocene granite (phaneritic to porphyritic light pink granite with low mafic content), igneous sills, limestone, locally metamorphosed to white marble, Belt argillite

†Measured from the headwaters of tributary creeks in the source area to the end of the Musselshell River at UL Bend.
‡Rock types from Johnson and Smith, 1964, Porter, 1990, and Wilde and Bergantino, 1992.
§Rock types from Taylor and others, undated, and Porter and Wilde, 1999.
#Rock types from Baker and Berg, 1991 and Goddard, 1988.
††Rock types from Reeves, 1931, Roberts, 1986, and Porter and others, 1993.
‡‡Rock types from Weed, 1899, and Roberts, 1986.
§§Rock types from Harlan, 1986, and Alt and Hyndman, 1986.
##Rock types from Alt and Hyndman, 1986.

A buried channel running through the Sun Prairie north of UL Bend (Fig. 4) is probably the preglacial path of the Musselshell where it flowed north to meet the preglacial Missouri River (Colton et al., 1961). Many other underfit channels exist north of UL Bend, the confluence of the Musselshell and Missouri Rivers. Many of the tributaries of the Musselshell River south of UL Bend have overly large floodplains for their current size and strength (Bergantino, oral comm., 2001). This phenomenon can be explained by a number of glacial processes, including stream capture and downstream filling of a glacial lake.

The basin that held Pleistocene Lake Musselshell (Fig. 3) is in the lower (north-flowing) reach of the river. It is underlain mostly by highly erodible Cretaceous Colorado shale, Montana group sandstone, siltstone and shale, and Hell Creek sandstone and shale (Fig. 5; Table 1). The bedrock is gently folded and affected by local faults and joints. Johnson and Smith (1964) made the most comprehensive map to date of Quaternary features in the former lake basin. Their field area is shown as an inset map in Figure 2a, and the Quaternary features that they described in field notes and identified on large-scale (1:21,120) aerial photographs (Johnson and Smith, 1953-1956) are reproduced in Figure 2b. The primary purpose of their study was to detail the bedrock stratigraphy and structure for a US Geological Survey oil and gas investigation. However, they also identified a sequence of nine terraces and more than 100 glacial boulders in the former lake basin (see Fig. 2). The terraces are older than the erratics in the basin because the erratics rest on the terraces (Johnson and Smith, 1964; Fig. 2). Therefore the ages of the terraces, if determined, could offer a constraint on the age(s) of the lake. Surface exposure ages of the boulders themselves would also help to determine the age(s) of Lake Musselshell.

Musselshell River Terraces

Johnson and Smith (1964) distinguished nine terraces along the Musselshell and its major tributaries based on field observations and height above drainage (Fig. 2; Tables 2-3). On the Musselshell, a low terrace of fine-grained material was included with the modern floodplain alluvium (Q_{al}; not shown in Fig. 2). The highest eight terraces (Q_{tm1-8}; Fig. 2) are capped by ~2.5 m of gravel and interbedded sand overlain by 0.3-1.5 m of silt or clay. All of the gravel terraces are preserved only as fragments that are 1-20 km apart. Without plots of terrace altitude with distance downstream (longitudinal profiles), it is impossible to determine whether the correlation of individual terrace remnants by Johnson and Smith is accurate.

TABLE 2. TERRACES OF THE MUSSELSHELL RIVER.†

Terrace	Height above the modern Musselshell River (m)		
	Range (low/high)	Average	Variability (high-low)
Q_{al}	0-8	4	8
Q_{tm1}	12-17	14.5	5
Q_{tm2}	21-61	41	40
Q_{tm3}	44-90	67	46
Q_{tm4}	75-130	103	55
Q_{tm5}	122-137+	130	>15
Q_{tm6}	154-165+	160	>11
Q_{tm7}	165-178	172	13
Q_{tm8}	194	194	0

†From Johnson and Smith, 1964.

Q_{tm4}-Q_{tm8} are unpaired, and all fragments of these terraces are on the west side of the modern river (Johnson and Smith, 1964; Fig. 2). The highest terrace, Q_{tm8}, is represented by a single fragment that now tops the divide between the Musselshell and its tributary Box Elder Creek (Fig. 2). This signifies considerable topographic inversion since Q_{tm8} time. The fragments of each lower terrace are located to the east of the fragments of the pre-existing, higher terraces (Fig. 2). Q_{tm1-3} are exceptions. They exist on both sides of the modern Musselshell, and appear to be nested and paired (Fig. 2).

The tributary terraces proposed by Johnson and Smith (1964) have a more complex relationship than the Musselshell River terraces. Between three and seven terraces were identified in each of six tributary streams (Table 3; Fig. 2). Terraces were undifferentiated along Yellow Water Creek (Q_t) and in the valley bottoms (Q_{al}). Neither

TABLE 3. TERRACES IN SIX MUSSELSHELL TRIBUTARIES.[†]

Terrace	Associated tributaries[‡]						Height above adjacent tributary (m)		
	BE	MC	EC	YW	PC	FC	Range	Average	Variability
Q_{al}	X	X	X	X	X	X	0-18+	9	>18
Q_t				X			6-37	21.5	31
Q_{t1}	X	X	X	X			6-46	26	40
Q_{t2}	X	X	X			X	12-46	29	34
Q_{t3}		X	X			X	18-75	47	57
Q_{t4}		X	X		X	X	8-90	49	82
Q_{t5}	X	X			X		15-105	60	90
Q_{t6}					X		34-53	44	19
Q_{t7}		X	X				117-122	120	5

[†]From Johnson and Smith, 1964.
[‡]Box Elder Creek (BE), McDonald Creek (MC), Elk Creek (EC), Yellow Water Creek (YW), Pike Creek (PC) and Flatwillow Creek (FC). See Figure 2 for locations.

of the undifferentiated units is shown in Figure 2. Units Q_{t1-7} were designated roughly by height above drainage, but Q_{t6} appears to be out of sequence, and a different number and combination of these terraces was mapped in each of the six tributary valleys (Table 3). Only Q_{t1-5} are shown in Figure 2; Q_{t6-7} are off of the western and northern edges, respectively.

River gradients change over time because of variations in climate, lithology of the bed material, tectonics, and stream capture (Pierce and Morgan, 1992). Johnson and Smith (1964) reported that the terraces all converge upstream with their modern floodplains. The event(s) that caused this change in river gradient may relate to glaciation of the Montana plains, and to Lake Musselshell in particular. Therefore a study of the magnitude and timing of these events would be useful.

Correlation of Terraces with Late Cenozoic Climatic Events

There were twenty-one or more late Cenozoic glacial cycles, consisting of a glacial advance and an interglacial retreat. Figure 6 shows a reference time scale for the Quaternary Period ($\leq$1.65 Ma; Aguirre and Pasani, 1984), along with the marine oxygen isotope (MIS) record for the last 300 ka. The MIS record, a proxy for global ice volume, has been advocated as the most appropriate basis for Quaternary chronostratigraphy as it is well-dated and carries a minimal amount of regional asynchroneity and time transgression (Clark et al., 1993).

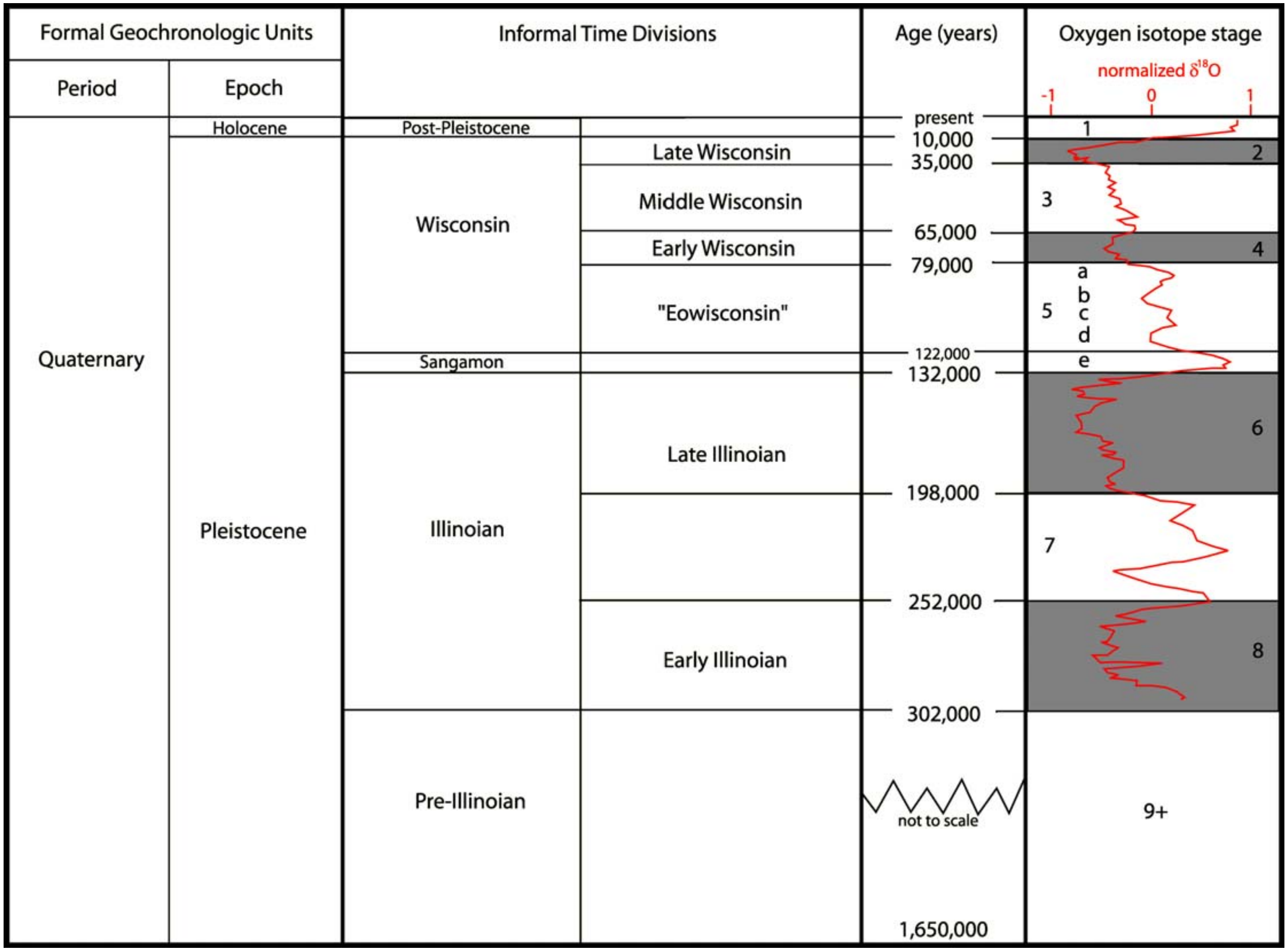

Figure 6. Quaternary time scale. Informal time divisions and their ages taken from Richmond and Fullerton (1986, p. 6). Marine Oxygen isotope stages and $\delta^{18}O$ record from SPECMAP (from Bradley, 1999, p. 211), a composite of seven marine records from different ocean basins.

Coincident with the onset of late Cenozoic continental glaciation, alluvial systems experienced a transition from net deposition to net incision. Extensive high gravel deposits like the Flaxville gravel of northeastern Montana reflect significant Tertiary-age aggradation. Sequences of seven or more terraces such as those in the northern Bighorn Basin of Wyoming and Montana (Reheis, 1984) and the Wind River basin of Wyoming (Chadwick et al., 1997) date to ≤2.1 Ma. These represent the overall incision that began in the Late Pliocene when late Cenozoic glacial conditions commenced.

During glacial maxima, heightened freeze-thaw action provided abundant gravel bedload for streams, while decreased evapotranspiration and longer winters increased and concentrated spring runoff (Pierce and Scott, 1982), resulting in episodes of alluvial deposition. Interglacial stages such as the Holocene epoch (≤10 ka B.P.; Hopkins, 1975) are times of river incision. Decreased gravel availability and somewhat lower discharge relative to glacial maxima cause interglacial rivers to downcut and create smaller floodplains (Pierce and Scott, 1982). Presumably, terrace sequences such as those in the Bighorn and Wind River basins were formed due to climatic controls: floodplains that were active during glacial stages were incised during and after deglaciation (Reheis, 1984; Chadwick et al., 1997). Similar terrace sequences in river systems such as the Musselshell, presumably also late Cenozoic in age, have the potential to provide a temporal reference for Quaternary surface processes in the basin.

TABLE 4. AGE OF TERRACES IN THE NORTHERN BIGHORN BASIN.†

Terrace	Height above Rock Creek† (m)	Height above Clarks Fork† (m)	Best age‡ (ka)	MIS†	Time division(s) or geochronologic unit(s)§
1	1.5-3	4.5-6	5±2	1	Holocene
2	6-9	12-15	20±10	2	Late Wisconsin
3	12-21	24-30	120±20	6-5	Late Illinoian-Eowisconsin
4	24-46	58-73	400±60	14-11	Middle Middle Pleistocene
5	40-61	85-101	660#	18-15	Early Middle Pleistocene
6	58-79	119-143	970±110	35-26††	Early Pleistocene
7	107-125	244-250	2100	86-85††	Late Pliocene

†From Reheis, 1984, unless otherwise noted.
‡Determined by Reheis (1984) using a combination of tephrochronology, correlation with deposits of previously known ages, and calculation of incision rates.
§From Bowen and others (1986); also see Figure 6.
The original age assigned to this terrace was 600 ka (Reheis, 1984). However, the age of Lava Creek B tephra, on which this age is based, has been revised to ~660 ka (Izett et al., 1992).
†† Estimated from equatorial Atlantic core ODP-607 benthic $\delta^{18}O$ record (Bradley, 1999).

In the Bighorn Basin (Table 4), the only obvious exceptions to the glacial aggradation-interglacial abandonment model are the Holocene terraces (5±2 ka). Because they consist of fine-grained material and are only a few meters above the modern floodplain, these terraces record a smaller event that will probably not be preserved in the long-term geomorphic record. The older terraces (2.1 Ma, 970±110 ka, 660 ka, 400±60 ka) may or may not fit the model; decreased resolution makes it difficult to constrain their formation to a single glacial-interglacial cycle (Reheis, 1984).

In the Wind River basin (Table 5), the ages of most of the younger terraces can be related directly to times of maximum glacial advance (Chadwick et al., 1997; Phillips et al., 1997). Terraces WR 3 and 1 can be traced to terminal moraines that yielded surface exposure ages ranging from 95-120 and 16-23 ka respectively, and WR 4 probably formed in conjunction with moraines dated to 100-130 or >130 ka. Terrace WR 7 may correspond with Sacagawea Ridge (MIS 16) moraines. The existence of terrace WR 2 implies an ice advance during early MIS 2, though moraines from this event were apparently not preserved. Moraines that were deposited at the same time as older terraces (WR 8-15) may have been lost to erosion.

TABLE 5. AGE OF TERRACES IN THE WIND RIVER BASIN.†

Terrace†	Height above river† (m)	Assigned age‡ (ka)	MIS†	Time division(s) or geochronologic unit(s)§
WR 1	6	16-23	2	Late Wisconsin
WR 2	12	28-46	2	Early Late Wisconsin
WR 3	40	100-125	5d	Eowisconsin
WR 4	43	122-152	6-5e	Late Illinoian-Sangamon
WR 7	124	640-680	16	Early Middle Pleistocene
WR 8	156	870	26#	Early Pleistocene
WR 9	167	950	30#	Early Pleistocene
WR 10	175	1000	34-33#	Early Pleistocene
WR 12	192	1100	38#	Early Pleistocene
WR 13	223	1300	48-47#	Early Pleistocene
WR 15	287	1700	68#	Late Pliocene

†From Chadwick and others, 1997, unless otherwise noted.
‡Determined by Chadwick and others (1997) using a combination of tephrochronology, ^{36}Cl surface exposure ages of terrace boulders (Phillips et al., 1997), and the linear incision rate model.
§From Bowen and others (1986); also see Figure 6.
#Estimated from equatorial Atlantic core ODP-607 benthic $\delta^{18}O$ record (Bradley, 1999).

Climate is not the only force responsible for terrace construction. Sudden changes in base level triggered by tectonics, stream capture or other processes can also result in terrace formation. In a basin such as the Musselshell, where glacial damming is suspected, factors other than climate must be considered when studying individual terraces within the sequence. Independent age controls on the terraces, such as tephrochronology or radiocarbon age constraints, or soil ages would allow approximate ages to be determined for the terraces using the linear incision rate model (Palmquist, 1983), similar to calculations made by Reheis (1984) and Chadwick and others (1997).

Terrace Soil Development

Reheis (1984, 1987) used the independently determined ages for the Rock Creek and Clarks Fork terraces (Table 4) to quantify the rate of soil development, assuming that the age of the soil was directly related to the age of the terrace in which it formed. She found a statistically significant relationship between soil age and several soil properties, including texture, pH and color (Reheis, 1987). Therefore, assuming a significant time span between the oldest and youngest soils (~2 Ma) to allow for measurable soil development in the Musselshell River terraces, the texture, pH, color, and other soil properties may be useful for determining terrace ages in the absence of other age controls.

Under deglacial and to a lesser extent interglacial conditions, available silt is reworked by wind and deposited as a loess cap over much of the landscape. In the central US, four middle and late Quaternary loess units have been identified and correlated with MIS 6 (Loveland Loess, ~100-160 ka), MIS 3 (Gilman Canyon Formation, 30-50 ka), MIS 2 (Peoria Loess, 11-25 ka B.P.), and MIS 1 (Bignell Loess; Busacca et al., 2004). Additional loess units, which have not been adequately dated, may extend the loess record into the early Pleistocene (Busacca et al., 2004). On the plains of Montana, abundant fine-grained material from erosion of the Cretaceous bedrock, glacial flour and proglacial lake sediment were available for transport by wind. Prevailing wind is from the northwest (Johnson and Smith, 1964), and the average wind speed is 5-7.5 m/s (Montana Natural Resources Information System web site, 2004). Given the available fines and winds to transport them, multiple episodes of loess deposition and removal may have occurred on the Musselshell terraces since the onset of late Cenozoic glaciation, adding complexity to and perhaps inhibiting the rate of soil development.

For carbonate-rich soils, the stages of calcium carbonate morphology (Gile et al., 1966; Machette, 1985) increase with age. Carbonate stages (Table 6) are another tool that can be used to estimate soil age. However, windblown dust is one of the predominant sources proposed for the origin of the carbonate in calcic soils in the southwestern United States (Machette, 1985). Therefore, an assessment of soil ages based on carbonate morphology would also be confused if multiple episodes of loess deposition and removal have occurred in the Musselshell basin.

Age(s) and Extent(s) of Lake Musselshell

In order to discuss the existing literature on Lake Musselshell, it is necessary to provide a brief overview of the current knowledge on the extent and timing of the Laurentide ice sheet, followed by specific discussions of the Laurentide along its western margin and, finally, along its southwestern margin in Montana. The ice lobe responsible for blocking the Missouri River to create Lake Musselshell (Fig. 1) may have advanced from different directions during different glacial stages. Fullerton and others (2004) proposed that ice approached the Musselshell basin from the northwest during MIS 2 and from the north/northeast during MIS 6 (Fullerton et al., 2004). Therefore, an understanding of glacial processes in southern Alberta and Saskatchewan is relevant to this study.

TABLE 6. STAGES OF CALCIUM CARBONATE MORPHOLOGY.[†]

Stage	Gravel content	Description	Maximum $CaCO_3$ content[‡]	Age of soil(s)[§] (ka)
I	High (>50%)	Thin, discontinuous carbonate coats sparse to common; usually on undersides of pebbles	Trace-2%	4
	Low (<20%)	Filaments sparse to common; faint coatings on faces of soil peds	Trace-4%	
II	High	Thin to thick, continuous carbonate coats common; on tops and undersides of pebbles; some carbonate in matrix; no induration	2-10%	20
	Low	Soft nodules common; 0.5-4 cm in diameter; little to no carbonate in matrix	4-20%	
III	High	Continuous carbonate in matrix; cementation possible	10-25%	120-290
	Low	Firm to moderate cementation; continuous carbonate in matrix; coalesced nodules	20-60%	
IV	High	Cemented, platy to weak tabular structure; indurated laminae (<0.2-1 cm thick); carbonate (K) horizon 0.5-1 m thick	>25	120-750
	Low		>60%	
V	High	Indurated, dense, strong platy to tabular structure; >1 cm thick laminae; thin to thick pisolites; some case-hardened surfaces; K horizon 1-2 m thick	>50%	750
	Low		>75%	
VI	Either	Indurated, dense, thick, strong tabular structure; multiple generations of laminae, breccia and pisolites; recemented; highly case-hardened; K horizon >2 m thick	>75%	none

[†]From Machette (1985, p. 5), modified from Gile and others (1966, p. 348) and Bachman and Machette (1977, p. 40), unless otherwise indicated. Criteria are for soils developed in noncalcareous parent materials under arid and semi-arid climates in the southwestern US.
[‡]In the <2 mm fraction.
[§]Ages are "assumed ages" compiled by Harden and Taylor (1983, p. 344).

Extents and Ages of the Laurentide Ice Sheet

Many reconstructions of the Late Wisconsin Laurentide ice sheet are available (Andrews, 1982; Denton and Hughes, 1981; Fulton, 1989; Clark et al., 1993; Clark and Mix, 2001; Dyke et al., 2002). Glacial geomorphologic evidence supports the view that Laurentide ice was composed of three coalescent ice centers which built up over broad lowland areas in Canada, and is thus divided into three sectors: the Keewatin Sector, which originated on the Canadian Shield northwest of Hudson Bay, the Labrador Sector, centered on the Canadian Shield east of Hudson Bay, and the Baffin Sector which developed over Baffin Island (Andrews, 1982; Fulton, 1989; Fig. 7). According to this model, the ice sheet might have advanced into the Musselshell basin from the northwest (from western Alberta) or the north/northeast (from eastern Alberta and Saskatchewan; Fig. 7). Either way, glacial ice flowing onto the Montana plains north of the Musselshell basin would have passed over the Precambrian igneous and metamorphic rocks of the Canadian Shield (Fig. 7).

Bowen and others (1986) proposed eleven major and four minor Quaternary advances of the Laurentide into the United States based on available field evidence and radiocarbon ages. The major advances proposed correspond to Marine Oxygen Isotope Stages (MIS) 22, 20 (812-790 ka), 18 (782-718 ka), 16 (687-630 ka), 14 (562-512 ka), 12 (480-428 ka), 8 (302-252 ka), 4 (79-65 ka), 2 (35-13 ka) and two in MIS 6 (198-132 ka). The four minor advances proposed fall within MIS 5b, 3 (65-35 ka), early stage 2 and early stage 1. During the most recent glaciation, the Wisconsin (MIS 5d-MIS 2; 122-10 ka), the southern Laurentide ice sheet did not reach its maximum until MIS 4 or, more likely, MIS 2 (Clark et al., 1993). Refer to Figure 6 for a partial MIS record, age assignments of glacial and interglacial stages, and informal nomenclature developed in the United States to describe the phases of the Laurentide ice sheet.

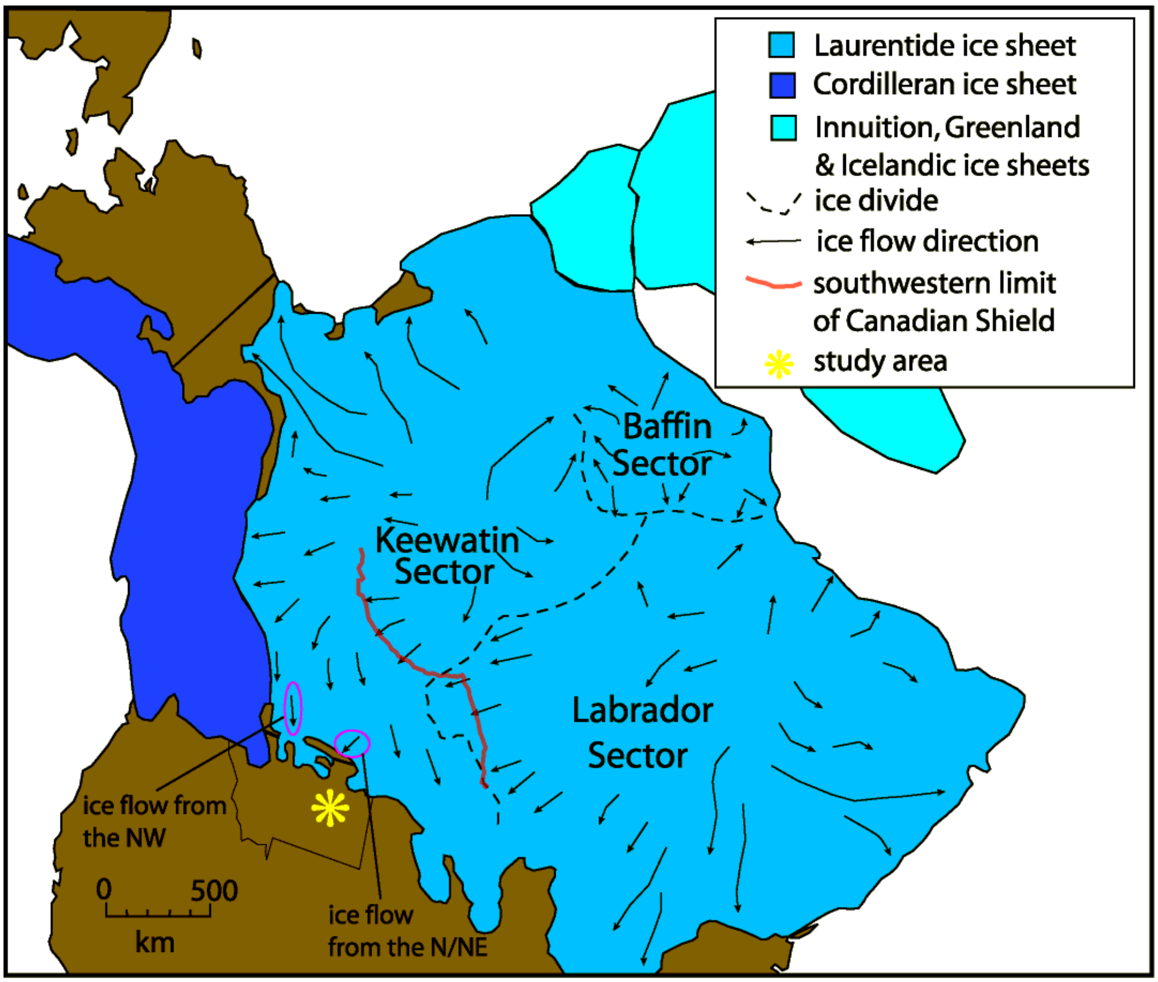

Figure 7. Source areas and flow dynamics of the Laurentide ice sheet during the last glacial maximum (after Fulton, 1989, p. 8). Location of Greenland ice sheet is approximate. Note that ice may have entered the study area from either the northwest or the north/northeast.

The Laurentide in Southwestern Alberta

Multiple hypotheses have been presented on the timing of the westernmost Laurentide glacial advance(s) and the existence during different ice ages of an "ice-free corridor" between the Laurentide and the Cordilleran ice sheet that covered the Rocky Mountains. Some research has indicated multiple coalescent Laurentide-Cordilleran ice advances (i.e. Jackson, 1980), while recent evidence points to the Late Wisconsin Laurentide ice sheet as the most extensive and the only ice sheet that closed the ice-free corridor (Liverman et al., 1989; Young et al., 1994; Jackson et al., 1997; Jackson et al., 1999).

Jackson (1980) identified four advances in southwestern Alberta based on till, glaciofluvial and glaciolacustrine stratigraphy. He considered the two oldest advances to be Illinoian in age based on land vertebrate chronology. He assigned a minimum age of Early Wisconsin to the third and Late Wisconsin to the final advance based on radiocarbon ages. Jackson (1980) found that Laurentide and Cordilleran advances were asynchronous during the oldest glacial advance, coalescent during the second and third advances, and non-coalescent during the final advance. Therefore he postulated that that the ice-free corridor was open during only the oldest and youngest of these episodes (Illinoian and Late Wisconsin).

In contrast, a single, Late Wisconsin ice advance may have been responsible for all glacial deposits in southwestern Alberta (Liverman et al., 1989; Young et al., 1994) as well as the closing of the ice-free corridor (Jackson et al., 1997). Recent work supports this hypothesis with a growing pool of radiocarbon and cosmogenic isotope ages (Liverman et al., 1989; Burns and McGillivray, 1989; Young et al., 1994; Young et al., 1996; Jackson et al., 1997; Jackson et al., 1999; Young et al., 1999).

Twenty-nine radiocarbon ages from a variety of materials excavated from the preglacial fluvial Saskatchewan gravel deposits range from 21.3 to 42.9 ka B.P. (Young et al., 1994). These workers assume that since the gravels contain no clasts of Canadian Shield origin, and since these deposits are accepted to be the basal Quaternary unit in the area, the Laurentide ice sheet had never covered the Edmonton, Alberta area prior to 21.3 ka B.P. They reason that if an ice sheet had been in the area prior to this time, Canadian Shield lithologies would have made up at least a small fraction of the Middle Wisconsin fluvial gravels. They therefore conclude that the Late Wisconsin Laurentide ice sheet is not only the most extensive of all of the Pleistocene ice sheets along its western margin, but that it is the only ice sheet to have extended farther west than Edmonton, closing the ice-free corridor to migratory animals, including *Homo sapiens*, during the Last (Late Wisconsin) Glacial Maximum.

Bone collagen from prairie dog fossils found in Quaternary sediment that caps the Hand Hills of Alberta gave radiocarbon ages of 22-33 ka B.P. (Burns and McGillivray, 1989). Young and others (1999) studied the stratigraphy of the sediment and found that the prairie dog colony postdates periglacial features and predates till of the Laurentide ice sheet. They conclude that the region was cold but ice-free during the early Middle Wisconsin, warm and dry during the late Middle Wisconsin when the prairie dogs inhabited the area, and then glaciated for the first time during the Late Wisconsin. Given the elevation of the Hand Hills and the direction of ice flow, they also concluded that Laurentide and Cordilleran ice were coalescent.

Eleven cosmogenic ^{36}Cl ages collected from Canadian Shield boulders deposited on the southern Alberta plains by the Laurentide ice sheet during its climax, as well as boulders deposited during less extensive continental glaciations in the same area, all yielded surface exposure ages between 12-18 ka (Jackson et al., 1999). The oldest subsurface till in the region is stratigraphically linked to this Late Wisconsin ice margin (Jackson et al., 1999), indicating that the Late Wisconsin ice sheet is the only one with known stratigraphic evidence to have reached this far west. Fullerton and others (2004) disagree with this interpretation. They state that the subsurface till, which Jackson and others (1999) consider to be stratigraphically continuous with the surface till that yielded Late Wisconsin surface exposure ages, is probably not all the same age.

The Foothills erratic train, deposited along the Rocky Mountain front in Alberta, represents the last and perhaps the only coalescence of Laurentide and Cordilleran ice. The erratic train was assigned to the Late Wisconsin stage based on seven of eight ^{36}Cl surface exposure ages that fell between 12-18 ka (Jackson et al., 1997). The older outlier had a Middle Wisconsin age, which was attributed to cosmogenic nuclides accumulated during a previous exposure (Jackson et al., 1997).

The Laurentide in Southeastern Alberta and Saskatchewan

The Late Wisconsin deglaciation of the Lethbridge area in southeastern Alberta occurred rapidly just before the deposition of the Glacier Peak G tephra (Vreeken, 1989).

This ash has generally been considered to date to ~12 ka B.P., though Mehringer and others (1984) suggest that its age be revised to ~11.2 ka B.P.

There is evidence for pre-Late Wisconsin glaciation in central Saskatchewan. In the Saskatoon area, a single till from an older glaciation is probably from a separate glacial stage than two younger till units (Christiansen, 1968). A zone of deep weathering of interglacial proportions separates the tills (Christiansen, 1968). If the young tills are Late Wisconsin in age, the older till might be Early Wisconsin, or Late or Early Illinoian. However, the till could also be from a much older (pre-Illinoian) glaciation.

The Laurentide in Montana

The southwestern sector of the Laurentide ice sheet is one of its least well-known margins. The eastern and central portions of the Late Wisconsin ice margin are fairly well constrained by radiocarbon dates. However, along the southwestern margin, even the Late Wisconsin advances are not adequately dated (Clayton and Moran, 1982). In Montana, even the extent of the ice sheet is not well-defined in places (Alden, 1932; Colton et al., 1961; Fullerton and Colton, 1986; Fullerton et al., 2004).

In general, deposits of till are found north but not south of the present-day Missouri River in Montana (Alden, 1932; Colton et al., 1961; Fullerton and Colton, 1986; Fullerton et al., 2004). An advance of the Laurentide ice sheet, possibly during the Illinoian stage (Fullerton et al., 2004), displaced the Missouri River from its preglacial channel (now occupied by the Milk River) to its present course (Fig. 4; Alden, 1932; Colton et al., 1961; Fullerton et al., 2004). Apparently, large sections of the current

Missouri channel were incised along the ice front (Colton et al., 1961; Colton and Fullerton, 1986). Therefore, the modern Missouri River channel has often been used as a first approximation for the southern limit of glaciation in Montana (Alden, 1932; Colton et al., 1961; Fullerton et al., 2004).

Clayton and Moran (1982) included Montana in their chronology of glaciation in middle and western North America based on radiocarbon dates on wood. Because no data was available from Montana, ice margins were assigned tentative ages based on data from other parts of the ice sheet and unpublished work of Fullerton and Colton. They described a pre-Wisconsin and possibly an Early Wisconsin ice margin as well as a Late Wisconsin maximum position (~20 ka B.P.) and recessional positions (Fig. 8a). Note that the 20 ka B.P. ice position (purple) is the same as the 15 ka B.P. position (dark blue) in the central and western portion of the ice sheet, and therefore only the younger ice is visible in Figure 8.

Fullerton and Colton (1986) suggest at least five Laurentide glaciations in Montana based on the identification of tills of different inferred ages. These tills had significantly different physical properties, weathering characteristics, and/or surface morphology. Ages were assigned to the five ice advances based on tentative correlation of Montana tills with tills of similar physical appearance and weathering characteristics, and in some cases stratigraphic order, in neighboring states and provinces. This correlation allowed the extension of age assignments made to tills outside Montana based on vertebrate chronology, ash deposits, and selected radiocarbon dates to tills in Montana.

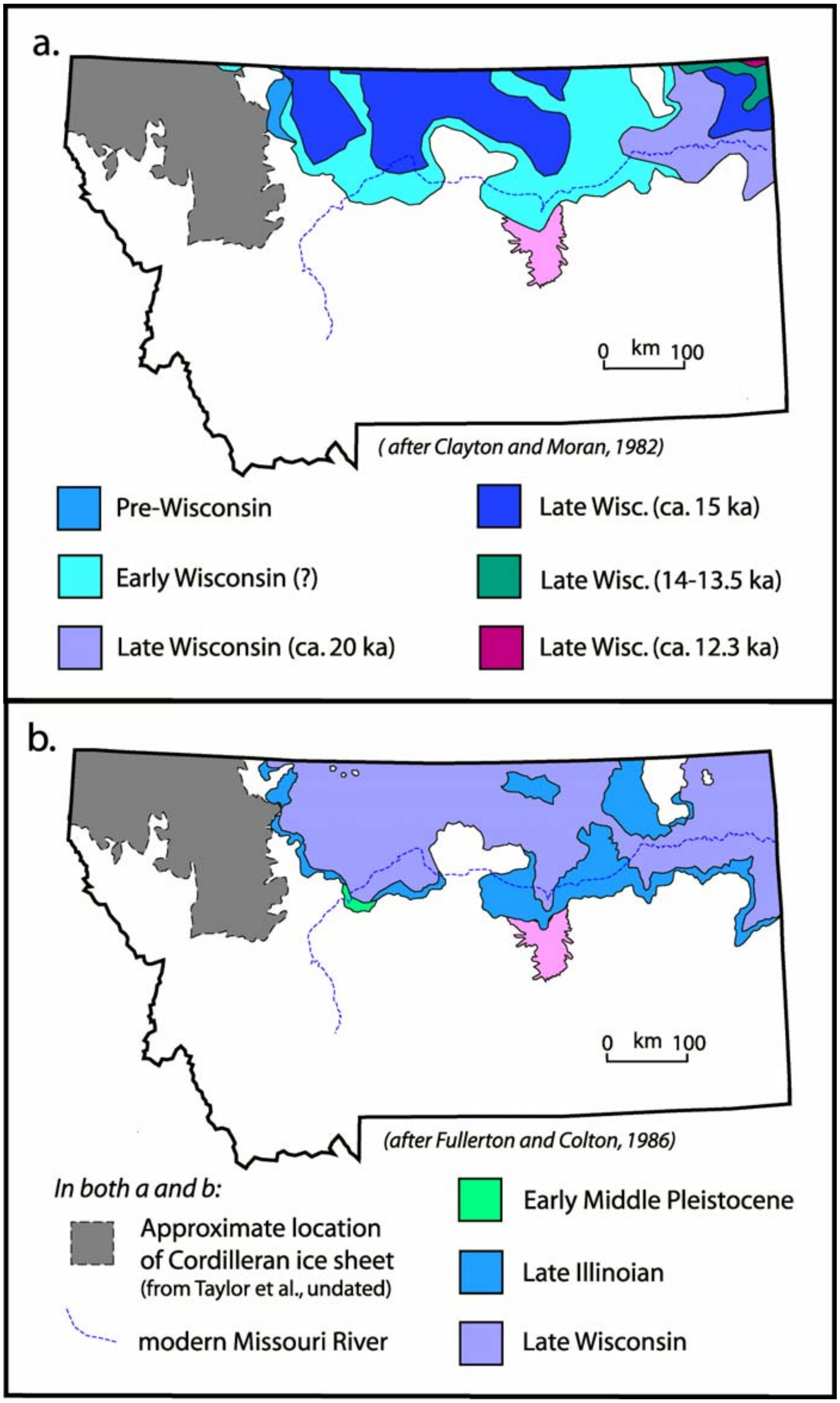

Figure 8. Ice marginal positions of the Laurentide ice sheet in Montana. Lake Musselshell (Colton et al., 1961) shown in pink.

The oldest glacial advance reported by Fullerton and Colton (1986), represented by the Sturgeon Bay till, is thought to be Early Pleistocene (790-812 ka; Marine Oxygen Isotope Stage (MIS) 20). An Early Middle Pleistocene (630-687 ka; MIS 16) and a Middle Middle Pleistocene (428-480 ka; MIS 12) glaciation are thought to be responsible for the deposition of the Perch Bay and Havre tills. During the Illinoian, the thin, discontinuous Kisler Butte, Markles Point and Herron Park tills were laid down on the plains. No Early or Middle Wisconsin tills were identified, but Late Wisconsin (MIS 2) till units, the Fort Assiniboine, Loring and Crazy Horse tills, and evidence of two Late Wisconsin readvances were found.

Fullerton and others (2004) refined the chronology of Fullerton and Colton (1986), proposing one Late Pliocene (MIS 82), two Middle Pleistocene (MIS 18 and 16; <778 ka, >639 ka; two Havre/Perch Bay/Archer tills separated by a paleosol), a Late Illinoian (MIS 6; Kisler Butte/Markles Point/Herron Park tills), and a Late Wisconsin (MIS 2; ~20 ka B.P.; Fort Assiniboine/Loring/Crazy Horse till) glaciation and a Late Wisconsin readvance (~14 ka B.P.). Because the Sturgeon Bay till, formerly thought to have reversed magnetic polarity, was reevaluated and has normal polarity, this unit was reassigned as part of the Perch Bay till (Fullerton et al., 2004).

Till on the plains of Montana is mostly thin and patchy (Fullerton et al., 2004). The timing of the Laurentide ice sheet in Montana has not been well constrained by radiocarbon or other types of age control (Fullerton and Colton, 1986). Tills have been identified and assigned a chronology based on physical properties and weathering characteristics (Fullerton and Colton, 1986; Fullerton et al., 2004), including dry color of the oxidized till matrix, extent and dry color of secondary iron and manganese oxide, extent of secondary carbonate and gypsum, compaction and induration, structure, fracture, joint patterns and prevalence of cobbles and boulders (Fullerton et al., 2004). According to Fullerton and others (2004), the surface till is of a variety of ages, ranging from pre-Illinoian to Late Wisconsin, contrary to the assumption (for which they did not cite a reference) that all surface till is of Late Wisconsin age. Fullerton and others (2004) state that the assumption (no reference given) that all of the physical properties of surface till in Montana are characteristic of Late Wisconsin till is incorrect. Fullerton and Colton (1986) and Fullerton and others (2004) consider the Illinoian ice sheet the most extensive overall (Fig. 8b). However, Fullerton and others (2004) also state that in some locations, Illinoian and Late Wisconsin till are indistinguishable. Although tills have been recognized and ice margins tentatively mapped (Fig. 8b), the ages of glacial advances are as yet only inferred.

The most abundant evidence of continental glaciation in Montana is the exotic boulders on the land surface. These boulders are mostly granite and gneiss transported from the Canadian Shield. Some were deposited directly by the ice sheet during recession, but south of the Missouri River high-elevation exotics are found in basins south of the farthest mapped ice margin. These deposits have been explained historically as iceberg deposits from large proglacial lakes (Calhoun, 1906; Alden, 1932; Colton et al., 1961). At least six major lakes (see Fig. 1), formed on the edge of the Laurentide ice sheet as it blocked the Missouri River and its tributaries, are cited in widely accessible sources pertaining to Montana geology (e.g. Alt and Hyndman, 1986). As the Missouri is the approximate southern limit of glaciation, the lakes could only have existed when the ice sheet was near its maximum position. The Missouri River is the headwaters of the largest watershed in the United States. This chain of lakes filled and drained down the ice front, sending enormous volumes of cold water down the Missouri River to the Mississippi. Surprisingly little is known about the sequence of these discharge events and their potential influence on global climate.

Glacial Lakes Glendive, Circle, Jordan, Musselshell, Great Falls and Cut Bank (Colton et al., 1961) were mapped based on small-scale aerial photos, limited quadrangle-scale mapping and regional reconnaissance mapping of surface morphology (Fullerton and Colton, 1986). Lacustrine sediments have been identified from Lakes Great Falls and Cut Bank, abandoned drainage channels have been found at the margin of Lake Great Falls, and one delta has been identified in Lake Glendive. Optically stimulated luminescence (OSL) dates on lacustrine sediments indicate that the most recent stage of glacial Lake Great Falls existed between 13-15 ka (Feathers and Hill, 2001; Hill, 2001). A great deal of additional field study and numerical dating is necessary to reconstruct the history of these lakes. This research addresses both the timing and local extent of Late Cenozoic glaciations on the plains of Montana through mapping and dating of ice-rafted boulders and other deposits of glacial Lake Musselshell.

Lake Musselshell was one of the largest, yet paradoxically poorly documented, glacial lakes at the margin of the Laurentide ice sheet in Montana. As it is most commonly mapped, this lake spanned as much as a hundred-kilometer stretch of the ice front and inundated more than 5,000 square kilometers of the Montana plains (Colton et al., 1961; Fig. 3). Nonetheless, the most recent compilation map of the area (Soller, 1994) showed Musselshell as an inferred lake, citing the scarcity of known lake deposits in the Musselshell River drainage and the potential complications encountered as a result of extrapolating sediment type and thickness for a large lake for which there is insufficient geologic data (Soller, 1992).

Extent(s) of Lake Musselshell

The extent of this lake was inferred (Alden, 1932; Colton et al., 1961; Fig. 9a) based on the distribution of cobbles and boulders of Canadian Shield lithology found in the modern Musselshell River basin. These clasts, assumed to be ice-rafted erratics, are the primary physical evidence associated with the lake. Alden (1932) mapped the lake based on the location of the majority of boulders known to exist in the basin. Subsequent location of boulders (including those located by Johnson and Smith, 1964) and availability of improved topographic data (Colton, 1959) allowed Colton and others (1961) to remap Lake Musselshell. Because the erratics were all found at elevations below 960 m (3150 ft), Colton (1959) suggested this as the maximum lake level and Colton and others (1961) used the 960-meter (3150-foot) contour line in the Musselshell basin as the limit of the Lake Musselshell highstand. Johnson and Smith (1964, p. 60; Fig. 2) mapped more than 100 boulders in the Winnett-Mosby area and found that most lie between 777-930 m (2550-3050 ft) in elevation. Modern divides exist along the southern and eastern basin margins at or below 940 m (3085 ft), suggesting that either

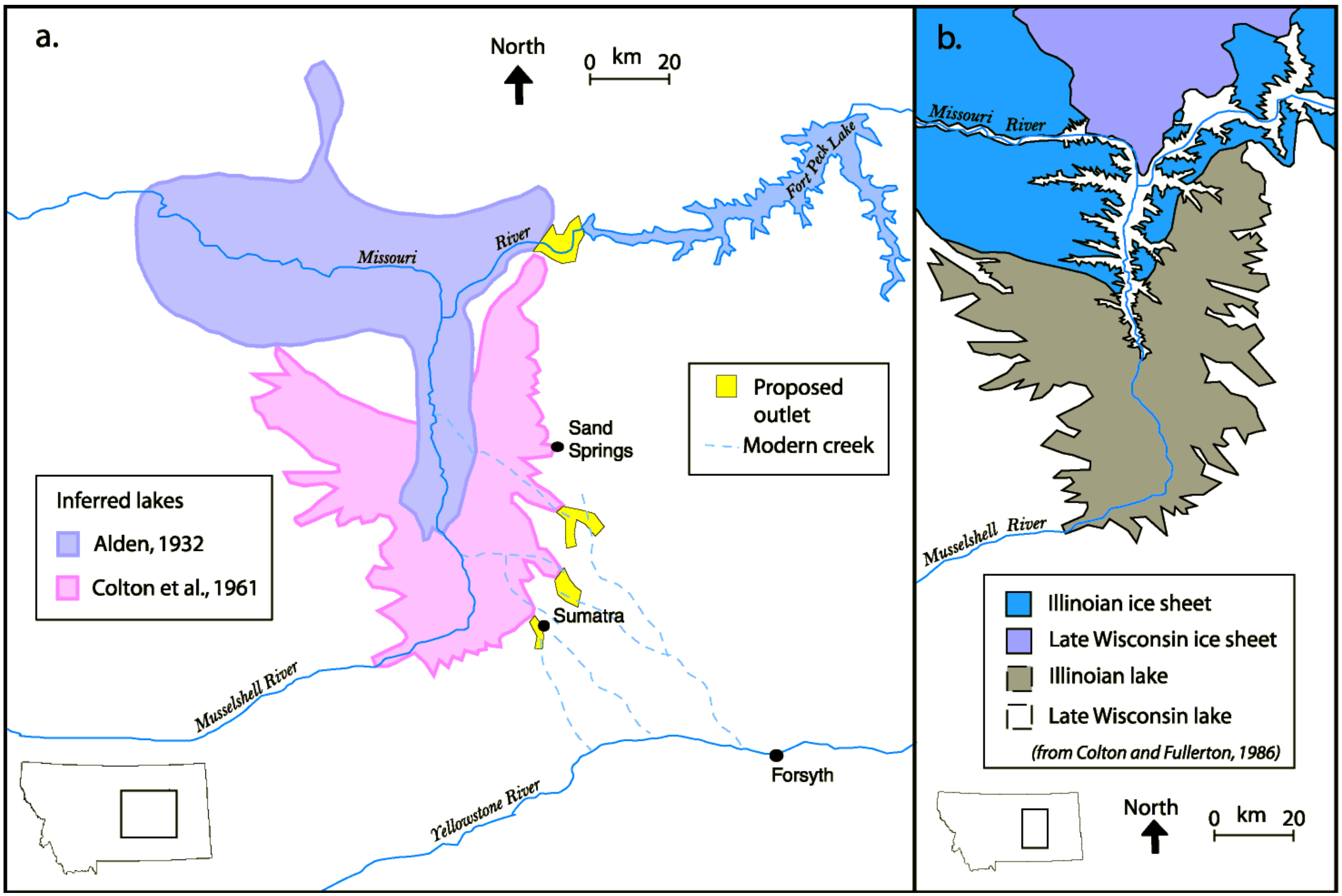

Figure 9. Various depictions of glacial Lake Musselshell and potential outlets.

Colton (1959) estimated too high a boulder elevation or that significant divide-lowering occurred during or after the drainage of the lake.

One important attribute of ephemeral lakes such as Lake Musselshell is the manner in which they drained. Models from other ephemeral lakes in the western United States demonstrate four different drainage processes, all of which are plausible for Lake Musselshell: spillway-control, subglacial drainage, hydraulic control, and ice-marginal drainage (Table 7). Lake Bonneville was a relatively long-lived lake (1-3 ka) with a stable outlet (Hamblin, 2003). Lake Missoula filled for an average of 30 years and catastrophically drained at least forty times underneath its own ice dam (Waitt, 1985). “Lake Lewis” filled for hours or days each time Lake Missoula drained because the water could not pass efficiently through the narrow, downstream Wallula Gap (Waitt, 1980). Lake Great Falls, which was comparable in size and probably existed around the same time(s) as Lake Musselshell, drained catastrophically along the ice margin, carving multiple channels that are now perched on the flanks of the Highwood Mountains (Fullerton et al., 2004).

In contrast, the draining of Lake Musselshell left no obvious evidence (Alden, 1932). Reconstructions of Lake Musselshell imply water input from the Missouri, Musselshell, and tributaries (Colton et al., 1961; Colton and Fullerton, 1986). Drainage of a lake of this size, be it ice-marginal, subglacial, or outflow over a low bedrock divide, would have produced a channel large enough to hold the combined waters of the proglacial Missouri and Musselshell Rivers. Boulders and gravel would have been deposited downstream, perhaps as flood bars, when the water from this lake was released.

TABLE 7. CHARACTERISTICS OF SELECTED LARGE, EPHEMERAL LAKES.

Lake	Age	Max. size†	Stratigraphic evidence	Drainage
Pluvial Lake Bonneville‡	20-23 ka B.P. 14.5-16 ka B.P.† 13.5-14.5 ka B.P. 10-11 ka B.P.	Depth: 320 m Area: 51.8* 10^3 km^2	4 major shorelines (beaches, spits, bars, deltas, sea-stacks, caves, wave-cut and wave-built terraces); >17 minor shorelines (narrow beaches, barrier bars, wave-cut terraces and sea cliffs)	Spillway at Red Rock pass: 100 m of rapid incision through unconsolidated sediment to bedrock;‡ erosion of broad valleys and deposition of fields of boulders downstream
Glacial Lake Missoula§	Multiple 20-100 yr lakes between 12.7-15.3 ka B.P.	Depth: 670 m Volume: 2.5* 10^3 km^3	Varves totaling <2.5 ka of annual deposition, shorelines, ice-rafted boulders; deltas are small and "smeared" over a range of elevations due to the frequent fluctuations in lake level	Buoying of the Purcell Trench ice lobe by the lake water triggered periodic, catastrophic, subglacial drainage of Lake Missoula; deposition of giant ripples, bar forms, and Touchet bed rhythmites, and erosion of the Channeled Scabland downstream
Hydraulically-dammed "Lake Lewis"§	Multiple episodes of slackwater sedimentation between 12.7-15.3 ka B.P.	Volume: 1.1* 10^3 km^3	≥40 slackwater rhythmites ("Touchet beds") with up-valley paleocurrent indicators deposited over the course of hours by ≥40 jökulhlaups from glacial Lake Missoula; ice-rafted debris; no varves or shorelines	These short-lived slackwater "lakes" backfilled upstream from a constriction (hydraulic dam) in the valley (Wallula Gap) and emptied through this same constriction, depositing sub-fluvial deltas on the downstream side of Wallula Gap
Glacial Lake Great Falls#	~140 ka† ~20 ka B.P. 13-15 ka††	Depth: ~200m Area: ~5*10^3 km^2	Varves, ice-rafted boulders; shorelines have been proposed	Deep, wide ice-marginal channels were carved by the catastrophic floodwaters of this lake; these ice-marginal channels (i.e. the Shonkin Sag) are now abandoned or remarkably underfit
Glacial Lake Musselshell#	~140 ka† ~20 ka B.P.	Depth: ~200m Area: ~5* 10^3 km^2	Ice-rafted boulders; no other stratigraphic evidence reported prior to this study	Southeast drainage over a low pass into the Yellowstone River or east down the modern Missouri River channel

†Maximum lake stage.
‡Data from Hamblin, 2003.
§Data from Waitt, 1980, Waitt, 1984, Waitt, 1985, and Bjornstad, 2004.
#Data from Alden, 1932, Colton and Fullerton, 1986, and Fullerton and others, 2004.
††Based on optically stimulated luminescence ages (Feathers and Hill, 2001; Hill, 2001).

Neither a channel of suitable size, nor downstream flood deposits have been identified for glacial Lake Musselshell (Alden, 1932; Colton et al., 1961).

In the absence of an obvious outlet for Lake Musselshell, Alden (1932, p. 88) surmised that the lake overtopped a low pass and drained southeastward into the Yellowstone River a few miles west of Forsyth (Fig. 9a). He noted that drainage could have also been straight eastward down the Missouri River (Fig. 9a). Colton (1959) cited discovery of additional erratic boulders that supported Alden's hypothesis that the lake drained to the Yellowstone west of Forsyth. He noted three potential spillways (Fig. 9a) on high-altitude aerial photographs. These are located 3 km west of Sumatra, 16 km northeast of Sumatra, and 26 km south of Sand Springs. The latter two join Alden's channel west of Forsyth. Colton (written comm., 2001) visited the lowest of these potential spillways in search of exotic boulders, but was unable to locate any. He determined that a boulder in that vicinity cited by Alden (1932, p. 81) as evidence for southeastward drainage, had probably been moved to a nearby homestead (Colton, written comm., 2001). Although four outlets had been proposed, the true outlet for Lake Musselshell was not determined.

If Lake Musselshell existed some time during the Quaternary, multiple types of stratigraphic evidence should have been preserved in the former lake basin. Other ephemeral lakes in the western US left behind shorelines, deposits of varved lacustrine silt and clay, deltas and ice-rafted debris (Table 7). Of these, only ice-rafted boulders have been reported from Lake Musselshell. The soft bedrock in the basin is particularly susceptible to wave erosion, indicating that a lake that was long-lived enough to have significant ice-rafting would have been able to carve shorelines. The erodible Cretaceous bedrock and erosive Laurentide ice sheet would have provided ample silt and clay for varves. Well-preserved alluvial terraces in the basin (Johnson and Smith, 1964; Fig. 2) attest to both adequate preservation and sufficient gravel bedload to form deltas at lake level. No deltas, lacustrine sediments, or shoreline ridges have been identified in the basin despite favorable conditions for the formation of these features.

If the gravel deposits mapped by Johnson and Smith (1964; Fig. 2) are indeed terraces of the Musselshell River and its present-day tributary streams as proposed by Johnson and Smith (1964), then the rock types represented should be consistent with bedrock types in the Musselshell watershed (Fig. 5; Table 1). However, it is possible that some of the gravels mapped as terrace deposits are actually deltas of glacial meltwater streams into Lake Musselshell. If this is the case, clasts of Canadian Shield origin might be found in the gravel deposits. Therefore, a study of the provenance of gravel deposits in the Musselshell basin might aid in the identification of Lake Musselshell deltas. The location and elevation of ice-rafted debris, glaciolacustrine deltas, lake sediments, and beach ridges, and spillway channels would illuminate the nature of the outlet(s) and help to determine the extent(s) of glacial Lake Musselshell.

Age(s) of Lake Musselshell

The age(s) of the stand(s) of Lake Musselshell have never been directly determined. The major lake stage (Fig. 9a) has generally been depicted as pre-Late Wisconsin in age (Calhoun, 1906; Alden, 1932; Clayton and Moran, 1982) based on the age assignment given to the local maximum of the Laurentide ice sheet. Calhoun (1906) and Alden (1932) regarded the lake as Illinoian or "Iowan." According to Clayton and Moran (1982), Early Wisconsin ice covered the Missouri at its confluence with the Musselshell, while the terminus of Late Wisconsin ice was north of the Missouri (Fig. 8a), supporting an Early Wisconsin age for the lake.

More recent interpretations of the ice terminus (Fullerton and Colton, 1986; Fig. 8b; Fullerton et al., 2004) suggest a lower Late Wisconsin lake in addition to an Illinoian or older stage (Fig. 9b). This inferred lake was not caused by an ice dam in the Musselshell basin. Instead, Colton and Fullerton (1986) suggest that the ice sheet blocked the Missouri River farther east to create a Late Wisconsin stand of Lake Jordan. The water level in Lake Jordan exceeded the capacity of that basin and therefore also occupied part of the Musselshell basin to the west. Colton and Fullerton (1986) mapped this combination Lake Jordan/Lake Musselshell using the 793-meter (2600-foot) contour line.

The youngest stage of glacial Lake Great Falls (Fig. 1) was determined to be 13-15 ka based on optically stimulated luminescence of lake sediment (Feathers and Hill, 2001; Hill, 2001). A lake may also have been trapped in the Musselshell basin at this time. The advance of the Laurentide ice sheet that was responsible for damming a lake in the Great Falls area might have been roughly coincident with ice advance to the east.

Surface Exposure Ages of Musselshell Boulders As mentioned above, the only recognized physical remnants of a glacial lake in the Musselshell valley are exotic

(Canadian Shield lithology) boulders deposited by icebergs. Because the location of >100 of these glacial boulders were documented by previous workers, these were the only lake-related features certain to be located during this study. For this reason, a main focus of the current research was on obtaining and interpreting surface exposure ages of the Musselshell boulders.

The concentration of cosmogenic isotopes in certain minerals on the surface of the earth increases at an approximately constant rate. Therefore, the technique of counting these isotopes gives an exposure age for the surface (Cerling and Craig, 1994; Lal, 1991; Gosse and Phillips, 2001). Assuming that the surface of a glacial boulder was freshly exposed and has been continuously exposed to cosmic radiation since it was deposited, the age of the glaciation that deposited the boulder at its present position can be determined from the concentration of cosmogenic nuclides in the boulder (Gosse and Phillips, 2001).

Many factors can cause a boulder's surface exposure age to be younger or older than the glaciation responsible for deposition of the boulder (Table 8). Because many of the sources of uncertainty tend to result in a surface exposure age that is lower than the age of the event in question, cosmogenic surface exposure ages are often considered minimum ages. However, there are some factors – particularly the inheritance of cosmogenic isotopes from non-cosmogenic sources or from a previous exposure – that cause surface exposure ages to be older than the event of interest. The uncertainty of each surface exposure age must be assessed relative to other surface exposure ages from the same geomorphic feature (i.e. moraine), and relative to relevant, available ages obtained using different geochronologic tools such as Radiocarbon dating.

TABLE 8. MAIN SOURCES OF ERROR FOR SURFACE EXPOSURE AGES.

Source of error†	Effect on exposure age	Techniques for minimizing uncertainty†
Calculation of nuclide half-life	Increase/ decrease	None
Calculation of production rate (which varies with geomagnetic latitude, atmospheric depth, etc.)	Increase/ decrease	Determine latitude and altitude of sample and apply currently accepted scaling factors; also report uncorrected data
Laboratory error	Increase/ decrease	Careful sample preparation; correct for contamination using blanks
Mass spectrometric error	Increase/ decrease	Correct using standards; make multiple measurements on the same sample
Difficulty removing non-cosmogenic components	Increase	Improve sample preparation and use stepwise heating procedure for ^{21}Ne
Topographic shielding	Decrease	Measure in the field and apply correction
Dip of sample surface	Decrease	Same as above
Differences in sample thickness and density	Increase/ decrease	Calculate average sample thickness and density of the rock and apply correction
Irregular sample geometry	Decrease	None
Displacement	Decrease	Avoid during sample selection
Previous shielding by snow or sediment	Decrease	Avoid during sample selection; estimate duration and calculate corrected ages; quantify using the ratio of two nuclides
Surface erosion	Decrease	Same as above
Inheritance from a previous exposure	Increase	None

†See text for discussion and references.

Errors from half-life and production rate uncertainties are system-wide (Gosse and Phillips, 2001), and our ability to better understand and quantify these is critical to an accurate interpretation of cosmogenic nuclide data (Bard, 1997). In the meantime, it is important to reference the production rate, latitude and altitude scaling factors used in any calculation of surface exposure ages. It is also helpful to report or archive uncorrected nuclide concentrations, so that ages can be recalculated as our understanding of systematic error sources improves.

The main sources of laboratory error are from imprecision in weighing the samples and adding carrier (Gosse and Phillips, 2001). Contamination by atmospherically-produced nuclides, which is particularly problematic in ^{10}Be analysis, is greatly reduced by using blanks (Gosse and Phillips, 2001).

The random error associated with mass spectrometric measurements is the square root of the number of counts (Gosse and Phillips, 2001). Therefore, precision is higher for samples with high isotopic ratios or long run times, and when corrections are made using standards interspersed with the sample measurements (Gosse and Phillips, 2001).

A special consideration in measuring cosmogenic ^{21}Ne is the difficulty of removing non-cosmogenic components (Graf et al., 1991; Gosse and Phillips, 2001; Niedermann, 2002). Non-cosmogenic ^{21}Ne accumulates from several sources, some of which are active from the time of crystallization of the quartz (Poreda and Farley, 1992; Niedermann et al., 1994; Hetzel et al., 2002; Niedermann, 2002). Non-cosmogenic ^{21}Ne is especially problematic in granitic rocks, where α-particles from normal levels of uranium and thorium produce enough nucleogenic ^{21}Ne to drown out the cosmogenic signal in old rocks with short surface exposure histories (Niedermann et al., 1994). The problem of contamination by non-cosmogenic ^{21}Ne can be addressed by using a stepwise heating and crushing procedure and neon three-isotope plots (Niedermann et al., 1994; Hetzel et al., 2002; Niedermann, 2002), though more work is necessary to perfect the technique. A larger sample size (~5 g quartz) would increase the resolution of cosmogenic vs. nucleogenic ^{21}Ne in rocks with a small cosmogenic component. Rigorous etching of grain surfaces with hydrofluoric acid, such as that described by Kohl and Nishiizumi (1992) may help to remove the nucleogenic ^{21}Ne produced from neighboring mineral grains (Niedermann, 2002).

Topographic shielding, dip, and geometry of the sample surface can be measured and corrected for (Gosse and Phillips, 2001). However, recent evidence shows that current geometric corrections, which assume that the surface is flat and of uniform depth, are not sufficient (Masarik et al., 2000; Masarik and Wieler, 2003). An irregular sample shape can result in underestimation of the cosmogenic nuclide production rate by up to 12% (Masarik and Wieler, 2003).

Displacement, temporary burial, and surface erosion of a boulder after its deposition in the basin can often be avoided by careful sample selection (Gosse and Phillips, 2001). Boulders may roll and shift as the underlying landscape erodes. They may be overturned during road construction. Boulders in isolated locations, on high, flat or otherwise stable landforms should be chosen over those in drainage bottoms, on slopes, or on post-glacial landforms. In addition, a carbonate coat on the bottom of the boulder is evidence that the top has remained unchanged over geologic time. To avoid complications from former burial by snow or sediment, samples should be chosen that are taller than the maximum estimated height of regional snow or loess cover. Boulders are unlikely to have had significant surface-lowering if they have glacial striations, uniformly smooth surfaces and retain a rounded morphology from glacial transport. Likewise, boulders that have not been subjected to weathering by fire-spalling, freeze-thaw action and other processes are desirable samples.

Sometimes it is possible to estimate the duration of prior snow or sediment shielding. In these situations, ages corrected for the maximum estimated shielding can be given alongside uncorrected ages (Jackson et al., 1999; Benson et al., 2004). In the same manner, corrected ages using estimates of maximum surface erosion have also been reported (Jackson et al., 1997; Jackson et al., 1999; Phillips et al., 1997). However, sometimes there is no indication of past shielding or surface erosion other than exposure ages that are consistently younger than expected. In order to test whether samples have been affected by *either* shielding (Gosse et al., 2003) *or* surface-lowering (Phillips et al., 1997), two cosmogenic nuclides with sufficiently different half-lives can be measured (Gosse and Phillips, 2001). If one or both of these processes affected the sample, the ratio of the two nuclides will deviate from the ratio expected for a sample that has never been buried or eroded. However, only geologic evidence can determine the *cause* for the deviation.

Inevitably, some boulders carry a cosmogenic signal that was inherited from a prior exposure. The spallogenic production of cosmogenic isotopes in earth surface materials decreases approximately exponentially with depth beneath the surface (Gosse and Phillips, 2001). The attenuation depth of the cosmic radiation varies with the density of the rock and the energy of the incoming radiation, but for ^{10}Be in a quartz arenite, production is reduced by an order of magnitude at a depth of ~1 m, and by two orders of magnitude at ~3 m (Gosse and Phillips, 2001). Not all boulders transported in an ice sheet are plucked from a depth greater than 3 m and some boulders are remobilized from previous glacial deposits. Inheritance is very problematic. So far it has been discussed only when one or two surface exposure ages are significantly older than the rest, especially when the problematic age(s) fall within an interglacial stage (Jackson et al., 1997; Phillips et al., 1997). In order to recognize inheritance statistically, a large number of samples ($n \geq 30$) should be analyzed. However, given the time-consuming and cost-prohibitive nature of each analysis, a sample size of this magnitude is often out of the question. Sample sizes in recent cosmogenic studies (Gosse et al., 1995; Jackson et al., 1997; Jackson et al., 1999; Licciardi et al., 2001; Benson et al., 2004) range from one to sixteen samples from each geomorphically distinct landscape feature (i.e. moraine or, in this case, lake level).

The ice-rafted boulders in the Musselshell basin are quite suitable for the cosmogenic isotope technique because of their mineralogy and size, and the local climate and topography. The majority of the boulders are granite (~52%) and gneiss (~34%) (Johnson and Smith, 1964), so they contain ample quartz, a resistant mineral with simple chemistry that accumulates four commonly measured cosmogenic nuclides: ^{21}Ne, ^{10}Be, ^{26}Al and ^{14}C. Of these four, the first two may be used to date surfaces with relatively long (>2 Ma) exposure histories (Gosse and Phillips, 2001). Given that Late Cenozoic glaciation of the Montana plains is thought to extend into the Pliocene (Fullerton et al., 2004), and that the most recent interpretation shows both a Late Illinoian (132-198 ka) and Late Wisconsin (10-35 ka) stage of Lake Musselshell (Colton and Fullerton, 1986), the stable isotope ^{21}Ne and the long-lived isotope ^{10}Be were selected for this study.

The large boulders in the study area range from 1.2 to 2.4 meters in diameter (Johnson and Smith, 1964). Their size makes displacement and prolonged shielding by snow or sediment unlikely. However, the turbid waters of a glacial lake would have shielded any boulders on the floor of the lake from cosmic rays in the same way as snow or overlying rock. Thus, a lake that covered an ice-rafted boulder for a prolonged period of time would reduce the surface exposure age of the boulder by a noticeable amount.

Typical of a midlatitude steppe climate, the region experiences a pronounced difference between extreme high and low temperatures, and is only frost-free for 1/3 of the year (Soil Survey Staff, 1993). Therefore, freeze-thaw action must be considered a potentially significant surface-lowering agent. However, the aridity of the climate reduces the likelihood of chemical and physical (freeze-thaw related) weathering of boulder surfaces.

In a steppe environment, abrasion and polishing by windblown sand and silt are common. Most eolian material is transported within 2 m of the ground (Ritter et al., 2002), therefore wind erosion has likely affected the Musselshell boulders. Saltation of silt-sized particles would have polished the corners of the boulders, perhaps lowering them by 1-2 mm, but probably has not removed enough material from boulder tops to be considered a significant source of error in cosmogenic dating.

Sparse forests of ponderosa pine and scrub cedar exist on higher terrain, and some cottonwoods are found on the floodplains (Johnson and Smith, 1964), but for the most part vegetation is low and sparse, reducing the risk of fire-spalling on the tops of large boulders or shielding of cosmic rays by a dense canopy. There is very little regional relief in the lower Musselshell basin, negating the effects of topographic shielding of incoming cosmic radiation. The terrain is not mountainous; however, local relief due to gully incision could be significant in this semi-arid terrain underlain largely by Cretaceous shale. Boulders situated in or near gullies may have rolled since their time of emplacement, thus their current surface would contain only those cosmogenic nuclides that had accumulated since the time of rolling as opposed to the total accumulation since the time of deposition in Lake Musselshell. To avoid sampling surfaces which would yield erroneously young surface exposure ages, only large boulders in topographically stable landscape positions (i.e. gravel terraces or resistant bedrock ridges), that do not show evidence of prior burial or overturning, and whose surfaces appear to have undergone minimal to no erosion since glacial transport should be selected for sampling.

Numerical dates for glacial deposits associated with glacial Lake Musselshell would be useful in constraining the age of past glacial advances of the Laurentide ice sheet in an area with very few published ages. In order to best attain this goal, the current study included:

- age determination and provenance studies of alluvial terraces,
- mapping, evaluation of landscape position and surface weathering characteristics, and exposure age dating of exotic boulders, and
- a search for spillways, shorelines, deltaic and lacustrine sediments.

METHODS

This study consisted of four parts. Longitudinal profiles of the Musselshell River terraces were constructed using altitude and location data from Johnson and Smith (1964), and the thickness and bedding, rounding, grain-size distribution, and provenance of the terrace gravel was studied in field exposures. A pilot study was performed in an attempt to determine the ages of the terraces using the degree of soil development (Harden, 1982; Harden and Taylor, 1983; Reheis, 1984; Reheis, 1987). Lake-related features in the former Lake Musselshell basin were studied in the field and on topographic maps. Finally, sample collection and laboratory analysis of surface exposure ages – five using cosmogenic ^{21}Ne (Niedermann, 2002) and twenty-seven using cosmogenic ^{10}Be (Kohl and Nishiizumi, 1992; Gosse and Phillips, 2001; Bierman et al., 2002) – was conducted on ice-rafted boulders from Lake Musselshell.

Terrace Correlation and Provenance

The major remnants of gravel terraces attributed to the Musselshell River (Q_{tm1-8}; Fig. 2; Johnson and Smith, 1964) were located on 1:24,000-scale topographic maps. Their altitude and distance upstream from the town of Melstone, MT were determined from the maps. Melstone was chosen because it marks the approximate location of the point where the Musselshell turns north, and both the area covered by Johnson and Smith (1964) and the current study area lie in this north-flowing stretch (Fig. 2). Longitudinal profiles were constructed using the location and altitude of the remnants. A profile of the modern floodplain was constructed for comparison. The correlation of some individual terrace remnants was revised based on their height above the river and distance downstream. All changes were checked on the topographic maps to ensure that the new correlations are consistent with the geographic positions of other terraces mapped nearby. Profiles were used to test for upstream convergence and to correlate new terraces located during this study.

Exposures of the Musselshell River terraces were described at Sites A, E-J, L-M, P, Q, and W-Y (see Fig. 10 for locations). In particular, the thickness, bedding characteristics, rounding, and grain size distribution of the gravel was noted. Some of the sites were described only by Johnson and Smith (unpublished field notes, 1953-1956; Sites P, Q, and X). Two of the sites (W and Y) were described by Johnson and Smith and revisited during this study. The rest of the sites were unique to this study.

Eleven sites were evaluated for provenance (Fig. 10). The sites were located in modern Musselshell alluvium (Site E), Q_{tm2} (Sites F and G), Q_{tm3} (Sites J and W), Q_{tm7} (Site Y) and Q_{tm8} (Site L), and gravel deposits not identified by Johnson and Smith (Sites H, I, M and N). In order to quantitatively determine the provenance of the Musselshell terrace gravel, cobble counts were performed in exposures of seven terrace fragments in the Musselshell basin (Sites E-J and L; Fig. 10). At each site, one hundred cobbles were pulled from the exposure and evaluated for lithology and size. A cobble count was also performed in a thick gravel deposit at Site K. This deposit is discussed separately because it is not a terrace (see Chapters 3 and 4). Several other gravel sites were

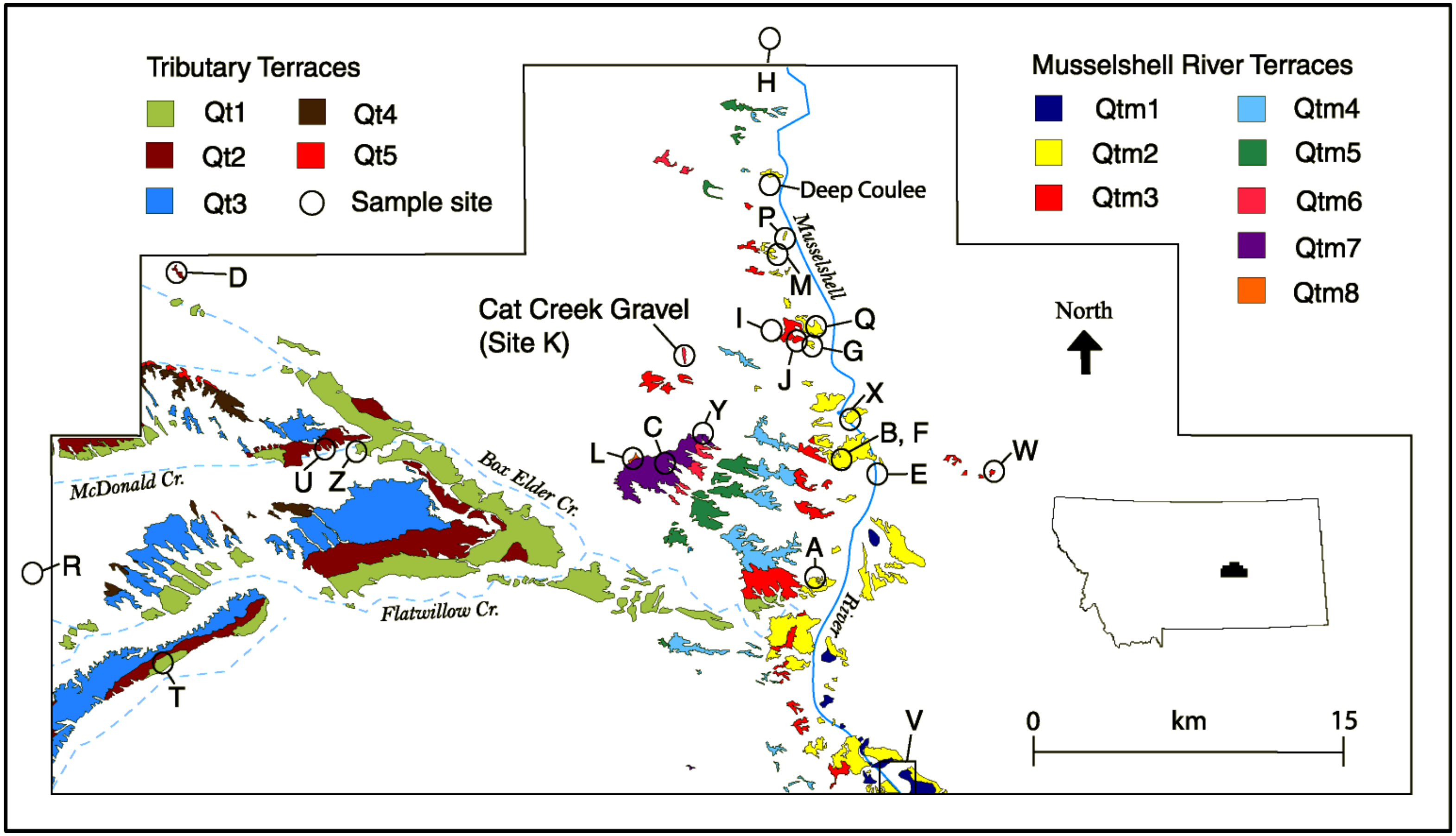

Figure 10. Terraces of the Musselshell River valley and locations of Sites A-Z. Site E is in the modern alluvium of the Musselshell River. Site H is exactly two miles (3.2 km) north of the map boundary. Site N (not shown) is 6.35 mi (10.2 km) north of Site H on the west side of the Musselshell River. Site S (not shown) is probably 9.25 mi (14.9 km) west of Site T. Site V is somewhere in the section delineated by the box. Note that there is no Site O.

evaluated for provenance during this study (M, N, W and Y; Fig. 10), but no cobble counts were performed there.

Johnson and Smith (unpublished field notes, 1953-1956) performed five cobble counts in the Musselshell River terraces (n=25-58; Sites P, Q, and V-Y) and described the exposure at Site W. Unfortunately, they did not specify in their field notes which terraces they studied, giving only the location of the Township, Range and section of the exposures. Using these locations, their sites were correlated to Q_{tm2or1} (Site V), Q_{tm2} (Sites P, Q and X), Q_{tm3} (Site W), Q_{tm6} (Site K), and Q_{tm7} (Site Y; Fig. 10). The results from Sites P, Q, X, and Y were used in the current study.

Most of the terrace fragments mapped by Johnson and Smith (1964) were identified based on observations of abundant gravel lying on a flat surface. Only in a few cases was an exposure visible in a gravel pit or road cut. Because gravel is commonly used in this area for surfacing roads, and because even the least-traveled parts of the study area are used for ranching, it seemed prudent to perform cobble counts only where the deposit was exposed in cross-section. This ensures that the gravel was in place prior to counting. Sites E-K, M-N, W and Y all had exposures. Site L did not have an exposure, but observations of cobble lithology and size were made on five clasts found on the surface and in an animal burrow at this site because this is the only remnant of the highest terrace of the Musselshell (Q_{tm8}). No pits were dug to perform cobble counts in gravel deposits without pre-existing exposures.

No cobble counts were performed in the tributary terraces (Q_{t-t7}; Fig. 10) during this study. However, Johnson and Smith (unpublished field notes, 1953-1956) did perform five cobble counts in these terraces (n=25-60; Sites R-U and Z). Again, based only on Township and Range locations, these were tentatively correlated with $Q_{t?}$ (Site S), Q_{t1} (Site Z), Q_{t2or1} (Site T), Q_{t2} (Site U), $Q_{t3or4?}$ (Site R). Correlation was especially problematic at Sites S and R because they are located outside of Johnson and Smith's map area (see Fig. 10). This data was reviewed during this study and general conclusions were drawn. However, because the relationships between the tributary terraces of Johnson and Smith (1964; Q_{t-t7}) were unclear as discussed in Chapter 1, these terraces were not studied any further. The tributary terraces have a history that is likely related in part to glacial Lake Musselshell, but that story is beyond the scope of this thesis.

Terrace Soil Development

The Profile Development Index (PDI; Harden, 1982; Harden and Taylor, 1983) is a semi-quantitative tool that can be used to determine the ages of a chronosequence of terrace soils. A soil chronosequence is a related set of soils for which four of the five main factors that contribute to the rate of soil formation (topography, biological activity, climate, and parent material) are essentially constant, and time is the only variable that contributes significantly to differences in the degree of soil development (Jenny, 1941). Terrace soils such as those in the Musselshell basin can be considered a chronosequence if they are shown to have developed in topographically, biologically and climatically similar settings, as well as in similar parent material (i.e. fluvial gravel of similar sorting and composition). In general, this is a reasonable assumption to make. The Musselshell terraces are all similar in gradient and aspect, though their altitudes vary more than 194 m from the highest terrace to the modern floodplain (Johnson and Smith, 1964; Table 2). Terraces along the Clarks Fork, where Reheis (1984) demonstrated a statistically significant relationship between soil age and soil properties, spanned 250 m in elevation. Therefore, the range in terrace altitude in the Musselshell basin should not be too great for effective application of soil development as a technique for determining the absolute age of the terraces. Vegetation is similar on the terraces of the Musselshell. Trees occupy parts of the modern floodplain, while the upper terraces are colonized by sparse grassland vegetation such as short grasses, prickly pear cactus, sagebrush and other small shrubs (Johnson and Smith, 1964). The lower Musselshell basin is a midlatitude steppe, characterized by semi-arid climate conditions. The closest upwind topographic barrier that could cause significant differences in the local distribution of precipitation (the Judith Mountain range) is 90 km west of the highest Musselshell terrace. No mountains exist to the south or east of the terraces for more than 150 km. Thus, there is no evidence that small-scale climate variations within the Musselshell basin exceed those in basins where the PDI technique was developed and applied (Harden, 1982; Harden and Taylor, 1983; Reheis, 1984). No great differences exist in the grain-size distribution or lithology of the Musselshell terrace gravels (Johnson and Smith, 1964), so the gravelly parent material is probably similar for all of the terraces. However, water or wind may add or remove surface material, thus altering the upper portion of the parent material and potentially working against soil development processes (Gosse et al., 2003).

Four sites (A-D; Fig. 10) in the Musselshell and tributary terrace sequences were selected for the soil development study based on a combination of accessibility and relative age distribution. Soils were sampled from Q_{tm2} (Sites A and B), Q_{tm7} (Site C) and Q_{t2} on Box Elder Creek (Site D). At each site, vegetation, topography, and local bedrock type were described. Soils were sampled to the top of the 2C (gravel) horizon using a 7.6-cm (3-inch) diameter auger rather than digging soil pits. The depth of the 2C was inferred to be at or slightly below the depth at which the auger became impossible to operate, presumably due to increased gravel content. The 2C horizon was not directly observed except at Site A where it was exposed nearby. The soils were described and samples were collected from each horizon (above the 2C horizon) for laboratory analysis. Two members of the Natural Resources Conservation Service Soil Survey staff assisted with soil sampling and field descriptions during this pilot study.

The potential age indicators used in this study were calcium carbonate morphology (Machette, 1985), texture, pH and soil color (Harden, 1982; Harden and Taylor, 1983; Reheis, 1984; Reheis, 1987). Calcium carbonate morphology was evaluated in the field by direct observation and application of dilute hydrochloric acid. Texture, pH and soil color were determined in the laboratory using the dry fine-earth fraction (<2 mm). The texture of each horizon was analyzed using hydrometer analysis (Bouyoucos, 1936). Samples were tested for pH using a field method based on indicator dyes that change colors over specific pH ranges. The indicators used were Bromthymol Blue, Creosol Red and Thymol Blue. Dry colors were determined using standard Munsell soil color charts.

A study of terrace soils was both a logical and potentially fruitful approach to gain information on Lake Musselshell. Previous workers have developed and tested quantitative criteria for correlation of soil properties with age (Gile et al., 1966; Harden, 1982; Harden and Taylor, 1983; Reheis, 1984; Machette, 1985; Reheis, 1987). Unfortunately, this technique was not effective in the Musselshell basin, probably due to complications caused by eolian deposition and erosion. In reality, the rate of soil development is seldom a linear function of one or more variables. Instead, the rate may increase, decrease, or even reverse through time as a result of local or regional shifts in topography, biological activity, climate, and parent material. The results of the terrace soil study will still be presented and discussed in the upcoming chapters, despite the inconclusive outcome. However, a combination of surface mapping and cosmogenic isotope dating yielded the most useful data for interpreting the history of Lake Musselshell.

Lake-Related Features in the Musselshell Basin

Previously located and proposed lake-related features (Alden, 1932; Johnson and Smith, 1964; Colton, written comm., 2001) were studied in the field and on topographic maps. A search for additional lake-related features was also conducted. The potential lake-related features investigated in the Musselshell basin were ice-rafted debris, spillways, deltas, lake sediments, and shorelines.

Ice-Rafted Boulders

Johnson and Smith (1964) mapped the locations of 123 exotic boulders in the Musselshell basin (see Fig. 2b). The original low-altitude aerial photographs (approximate scale 1:21,120) used as base maps by Johnson and Smith were used to relocate many boulders. Locations of boulders were transferred from these photographs to 1:24,000 scale topographic maps in order to obtain their latitude, longitude and altitude. Boulders at high altitudes or at the eastern or western margin of the mapped area would be particularly useful in defining the farthest extent of the lake. Thorough searches for these key boulders were made using the topographic maps and a Trimble GeoExplorer 3 Global Positioning System (GPS).

A Mylar overlay prepared as an update of the Glacial Map of Montana East of the Rocky Mountains (1961) showed the location of some of the high boulders at the 1:500,000 scale (Colton, written comm., 2001). These were plotted onto 1:24,000-scale maps and investigated with the help of Colton's original notes (written comm., 2001). Conversations with area residents, planned traverses and incidental discovery were responsible for the location of many more boulders.

Boulders were located using a Trimble GeoExplorer 3 GPS. Postprocessed differential correction was applied to the data using GPS Pathfinder Office 2.80. After differential correction, this GPS unit has a horizontal accuracy of 1-5 m + 2 ppm (varies with distance from the base station) and a vertical accuracy of 2-5 times the horizontal accuracy. The base station used was the Charles M. Russell National Wildlife Refuge GPS Community Base Station in Lewistown, MT. Given the distance of ~150 km from this station to the farthest mapped boulder, the largest error possible is 5.3 m in the x- and y-planes (horizontal) and 26.5 m in the z-plane (vertical). Because of the large z-coordinate error, x and y-coordinates were plotted on 1:24,000 scale USGS topographic maps using the "Coordinate Locator" option in the National Geographic TOPO! software. Elevations were read off of these maps, which are generally considered to have a horizontal accuracy of 12.2 m and a vertical accuracy of half the contour interval (USGS, 1999). The contour intervals for the 7.5' maps used were 20 or 40 ft. Therefore, the vertical error was either 3 or 6 m, not accounting for the additional amount due to the horizontal error. The horizontal error was considered negligible because a visual inspection of boulder locations on topographic maps in the field ensured that their positions were accurate relative to nearby landmarks.

Potential Outlets

Two of the three spillways proposed by Colton (1959; Fig. 9a) were visited, and a search was made therein for gravel and exotic boulders transported by the floodwaters of Lake Musselshell. The other potential outlets were studied on 7.5-minute topographic maps. The main criteria for evaluating the proposed outlets were:

1. Their altitude relative to other lake-related features in the Musselshell basin.
2. Their morphology and sedimentology as compared with that of the established drainage channels of glacial lakes Great Falls and Missoula and pluvial Lake Bonneville (Table 7).

Deltas, Lake Sediment, and Shorelines

Deltas, lacustrine sediment and shorelines have been identified in other proglacial lake basins but had never been described in the Musselshell prior to this study. A search was made for these features using information from county officials and residents, observation while on foot, horseback and automobile, and conversations with and/or field notes of geologists William D. Johnson, Howard R. Smith, Roger B. Colton and David S. Fullerton (US Geological Survey), Robert N. Bergantino (Montana Bureau of Mines and Geology) and James R. Wild (University of Calgary). When identified, these features were located and studied in the field and on topographic maps and aerial photographs, and compared with similar features from other proglacial lakes.

Surface Exposure Ages of Musselshell Boulders

One hundred and twenty-five recovered and previously unmapped exotics were located in the study area. Surface exposure ages were obtained for twenty-seven of these boulders: five using both ^{21}Ne and ^{10}Be, and the remaining twenty-two with ^{10}Be only. Samples were selected based on altitude and the likelihood that the top surface had remained unchanged since the existence of Lake Musselshell.

Under the influence of prevailing winds, icebergs typically ground and melt near the margin of a water body. For this reason, ice-rafted debris tends to accumulate in a "bath-tub ring" at or slightly below the shoreline. If multiple stages of Lake Musselshell existed, the deposits of the different lake stages should be separable by altitude. To test whether the Musselshell boulders cluster by altitude, the boulder elevation data was compiled into histograms. A maximum of five altitude clusters were identified. If all or some of these correspond to separate lake stages, these altitude clusters should produce distinct sets of surface exposure ages. Therefore, each of these five groups was treated as a separate population for sampling purposes. Several boulders (3-11) were sampled from each altitude cluster to reduce the chance for outliers to be considered representative.

The mineralogy and dimensions of each boulder, as well as the topography and vegetation of the surrounding area were described in the field. Each boulder was rated "very low," "low," "moderate," "high" or "certain" based on the likelihood that it had undergone one or more of the following processes in the time since its deposition in the basin:

1. Displacement (by humans or naturally, such as by rolling into a gully)
2. Surface-lowering (by chemical weathering, spalling or ventifaction)
3. Previous burial (by loess or another temporary cover)

Multiple quantitative and qualitative criteria were used to rate the boulders (Table 9). For many boulders (in fact, for all but those rated "very low" and "certain"), these criteria were extremely difficult to evaluate. Even the "quantitative" criteria were devised subjectively and therefore have a large degree of associated error. Nonetheless, the rating system aided in selecting boulders that would yield the most accurate surface exposure ages. Boulders that were certain to have undergone one or more of these processes were not sampled. Sampling preference was given to boulders with low or very low ratings. However, about half the time, a boulder with a high likelihood in one category was sampled either because it was rated very low in another category, it was at a key altitude, or it was rated lower overall than other boulders in its altitude group. In one case, a boulder that was rated high in two categories was sampled because it appeared to have its original surface.

TABLE 9. CRITERIA FOR RATING THE LIKELIHOOD OF DISPLACEMENT, EROSION AND SHIELDING.

Process	Likelihood is: Very low	Low	Moderate	High	Certain
Displacement	If boulder appears to be in place[†] or top is indicated by a carbonate coat[‡] or lichen line[§]	If boulder is on a stable landform far from roads +/ fence lines, or its geometry indicates that rolling is unlikely	If boulder is near a road or fence line or on a gentle slope	If boulder is in a gully side, partly buried in slopewash, or on a steep slope	If boulder has bulldozer marks or a carbonate coat on the top
Surface - lowering	If the boulder has a weathering rind[#] or appears to have its original surface[††]	If the surface appears[‡‡] to have eroded only 1-2 mm	If the surface appears[‡‡] to have eroded 2-5 mm	If the surface appears[‡‡] to have eroded >5 mm	If broken pieces of the surface are lying on the ground nearby
Prior burial[§§]	If boulder height is $\geq$1 m	If boulder height is 0.5-0.95 m	If boulder height is 0.25-0.45 m	If boulder height is 0.1-0.2 m	If boulder height is <0.1 m

[†]Boulders on a high and/or flat surface removed from roads and fence lines are considered to be in place.
[‡]In one case, a boulder with a tilted carbonate coat was sampled. The displacement was measured and corrected for by sampling from the former top, so this boulder is considered to have a very low chance for displacement.
[§]Fairly continuous lichen or other discoloration above a line ("lichen line") was treated the same as a carbonate coat.
[#]The presence of a weathering rind was considered a sign of long-term stability of the surface.
[††]Uniformly smooth or striated surfaces are considered original.
[‡‡]The amount of surface-lowering on boulders was estimated in different ways for different boulders. Sometimes it was possible to compare of the height of the top surface with that of original surface on the side of the boulder. In other cases, a minimum estimate could be obtained from the depth of surface roughness, pitting, and fractures.
[§§]The height of the boulder top above the present land surface was used to rate the likelihood of prior burial. Because $\leq$0.5-1 m of fine material was observed capping some terrace gravels, boulders whose tops were $\geq$0.5 m but <1 m off the present land surface were rated low and $\geq$1 m were rated very low. Other cutoffs are arbitrary divisions of the remaining 0.5 m.

Cosmogenic ^{21}Neon Ages

One boulder from each altitude cluster was selected for ^{21}Ne analysis. Four of these were collected using a sledgehammer and chisel (Fig. 11a). One sample, E54, was collected using a paleomagnetic coring device (Fig. 11b). Samples were collected from the top of the boulder. The approximate quartz composition (usually 20-30% for granite and 15-25% for gneiss) was used to calculate a sample weight sufficient to yield 0.5 grams of quartz after purification. Quartz separation was performed in the Department of

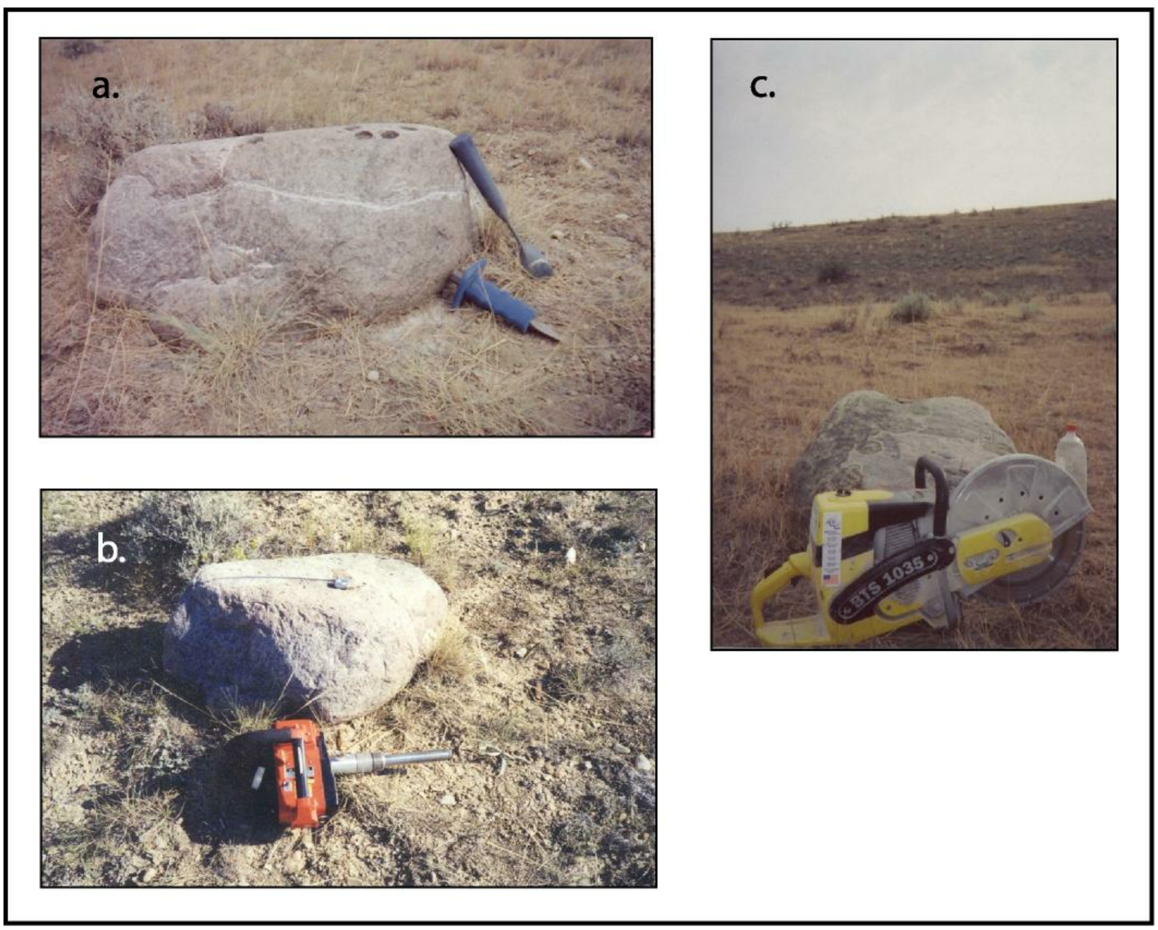

Figure 11. Sampling techniques for cosmogenic isotope dating: (a.) hammer and chisel (b.) paleomagnetic coring device, and (c.) concrete saw.

Earth Sciences at Montana State University and at the Argon Geochronology Laboratory of the United States Geological Survey in Denver, CO. Specifics of the quartz separation techniques used in this study are given in Appendix A.

Analyses were conducted using a Noble Gas Mass Spectrometer (MAP 215-50 gas-source mass spectrometer) at the US Geological Survey Noble Gas Laboratory, Denver, CO. The total neon concentration and the isotopic makeup of the neon were measured. The extraction used was a low-pressure process (1×10^{-9} torr) in which the sample was purified in a vacuum. Next, the sample was fused in a modified Turner double-walled vacuum furnace at $1600^{o}C$ over the course of an hour to release the gas. An air standard of known volume and pressure was also measured in order to calibrate the amount of ^{22}Ne. In order to correct the measured ratio of $^{21}Ne/^{22}Ne$, the atmospheric ratio of 0.029 (Eberhardt et al., 1965) was subtracted and that number was multiplied by the measured amount of ^{22}Ne to calculate the amount of excess ^{21}Ne.

In this study, none of the steps recommended by Niedermann (2002) and others (see Chapter 1) were taken to account for the presence of ^{21}Ne from non-cosmogenic sources. Samples were melted in the furnace without crushing or stepwise heating. Small sample sizes (0.2 g) were used. Samples were leached with hydrofluoric acid at room temperature for only 15 minutes as opposed to the multiple 9-hour sub-boiling leaches recommended by Kohl and Nishiizumi (1992). Therefore, the measured ^{21}Ne concentrations included both non-cosmogenic and cosmogenic components, and ages calculated from these data are not reflective of the exposure time of the boulder surfaces.

Cosmogenic ^{10}Beryllium Ages

Three to eleven samples per altitude cluster were collected for ^{10}Be analysis using a gas-operated Demolition concrete saw with a diamond-tipped blade (Fig. 11c). Angled cuts were made in a triangle or diamond shape on the top of the boulder. Hammer blows were applied to a chisel inserted in one of the cuts until the sample “popped out.” One kg or more of rock was collected from the upper 7 cm of each boulder. The objective was to collect enough rock to have 30 g of clean quartz after purification. The five rocks that were analyzed for ^{21}Ne were resampled for ^{10}Be analysis. Topographic shielding and angle of incidence of the sample surface was measured in the field.

Quartz separation and isotopic extraction of ^{10}BeO was performed at Lawrence Livermore National Laboratory in Livermore, CA. The quartz separation methodology that was used produced high-quality quartz. Atomic Absorption Spectrometer (AAS) analysis of a granite (E100) and a gneiss (E16) demonstrated aluminum contents <100ppm, attesting to the purity of the quartz after separation (Kohl and Nishiizumi, 1992). The quartz separation techniques followed those of Kohl and Nishiizumi (1992) and Gosse and Phillips (2001), with modifications and specifications as described in Appendix B.

Twenty-seven samples and four blanks were analyzed in the 10 MV Tandem Van de Graff Accelerator Mass Spectrometer at Lawrence Livermore National Laboratory. The measurements were normalized to the ^{10}Be/^{9}Be ratio in an ICN standard diluted by Kuni Nishiizumi, which has an estimated error of ~5% (R.C. Finkel, written comm., 2004). A sea level, high latitude (SLHL) production rate of 5.16 ^{10}Be atoms g^{-1} yr^{-1} was used to calculate ages. This is the ^{10}Be production rate from the Sierra Nevada (6.01 atoms g^{-1} yr^{-1}; Nishiizumi et al., 1989) rescaled by Owen and others (2002, but note that a computer program error resulted in an initial overestimation of the rescaled value, 5.2 atoms g^{-1} yr^{-1}, used in that paper; R.C. Finkel, written comm., 2004). Corrections were applied for latitude and altitude (Stone, 2000), sample thickness (assumed attenuation coefficient of ~160 g/cm^2), and any topographic shielding or surface dip in excess of 10 degrees (Nishiizumi et al., 1989; Brown et al., 1992). E122 was the only sample affected by >10^o of shielding, and E33 was the only sample with a surface dip >10^o. A density of 2.7 g/cm^3 was used for all of the samples.

The data was also adjusted for variations of the magnetic field intensity and the position of the geomagnetic pole using data from Ohno and Hamano (1992), McEllhinny and Senanayake (1982) and the SINT-800 record (Guyodo, and Valet, 1999) and the technique of Nishiizumi and others (1989). In calculating the new (geomagnetically corrected) set of ages, it is appropriate to use a SLHL production rate that has also been corrected for variations in the magnetic field >13 ka (the calibration age for the Sierra Nevada production rate calculation; Owen et al., 2002). Therefore, 5.06 ^{10}Be atoms g^{-1} yr^{-1}, with an associated error of ~6% (Stone, 2000) was used.

RESULTS

Several sets of data pertaining to the extent and timing of glacial Lake Musselshell are presented in this chapter. First, longitudinal profiles, provenance data, and a summary of the morphology and sedimentology of the Musselshell River terraces are given. The potential lake outlets and two notable deposits that may be related to Lake Musselshell, the "Cat Creek gravel" and the "Deep Coulee deposit," are described. In addition, information on the distribution and surface exposure ages of ice-rafted boulders is presented. Data from selected soils developed on the Musselshell River terraces is also contained in this chapter. However, the results of the soil study did not provide insight into the age of the terraces themselves or of Lake Musselshell.

Terrace Correlation and Provenance

The first round of longitudinal profiles of the Musselshell River terraces (Fig. 12) shows the terraces as mapped by Johnson and Smith (1964). On these profiles, Q_{tm1}, Q_{tm2}, Q_{tm3} and Q_{tm7} converge upstream with the modern Musselshell River, while Q_{tm4}, Q_{tm5} and Q_{tm6} have a gradient similar to that of the modern river. However, the significant scatter in the data for Q_{tm1-4} and Q_{tm6} (linear R^2 values <0.90; Fig. 12) indicated that some revisions were in order. The profiles were revised as follows:

1. The southernmost fragment correlated with Q_{tm7} (Fig. 12) was instead correlated with Q_{tm6}.

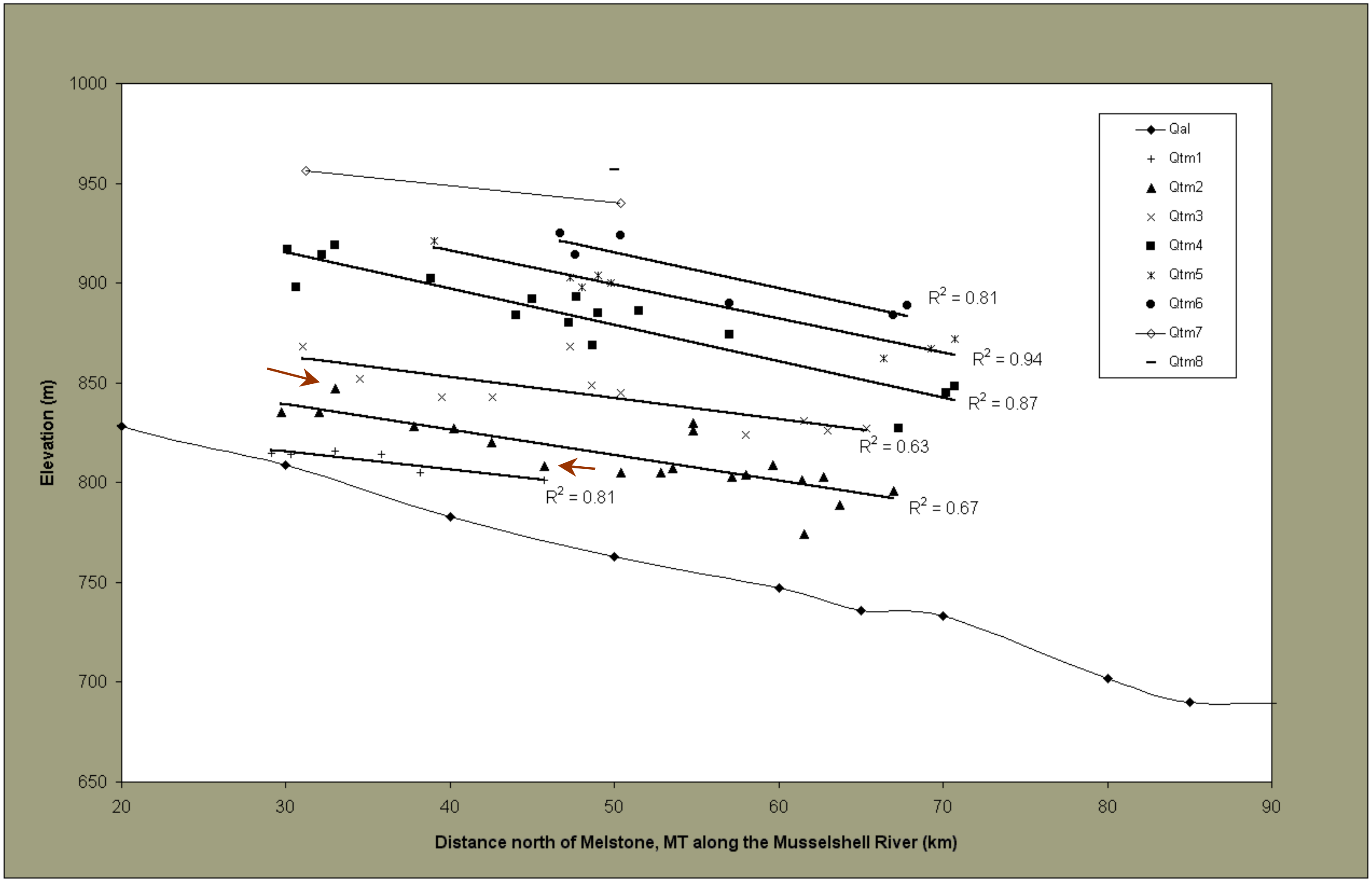

Figure 12. Longitudinal profiles of the Musselshell River terraces (Q_{tm1-8}) and the modern Musselshell River (Q_{al}) based on data from Johnson and Smith (1964). Arrows point to terrace remnants that cannot be revised (details in text).

2. The gravel deposit at Site K was removed entirely from the terrace data set. This deposit, (the Cat Creek gravel) is discussed in detail later in this chapter.
3. The lowest remnant mapped as Q_{tm4} was instead correlated with Q_{tm3}.
4. The two high fragments correlated with Q_{tm2} located ~55 km downstream of Melstone were instead correlated with Q_{tm3}.
5. The lowest fragment mapped as Q_{tm2} was grouped with Q_{tm1} instead.

The geographic location of each of the revised fragments was checked on the topographic maps to ensure that it is consistent with the locations of nearby terrace fragments. Two terrace fragments that appear to be miscorrelated when looking at the longitudinal profiles alone were not revised because the new correlation would have put them in an awkward geographic position relative to nearby terraces. These are marked with arrows on Figure 12.

During this study, additional terrace remnants were identified at Sites H, I, M and N. These sites were correlated with the most appropriate terrace as follows:

1. Site I was correlated with Q_{tm2}.
2. Sites H and M were correlated with Q_{tm1}.
3. Site N did not correlate well with any of the terraces mapped by Johnson and Smith (1964).

On the revised profiles (Fig. 13), the high terraces (Q_{tm4-6}) are approximately parallel to the modern gradient, while the low terraces (Q_{tm1-3}) converge upstream. This indicates that the Musselshell and its tributaries are now graded to a lower base level than

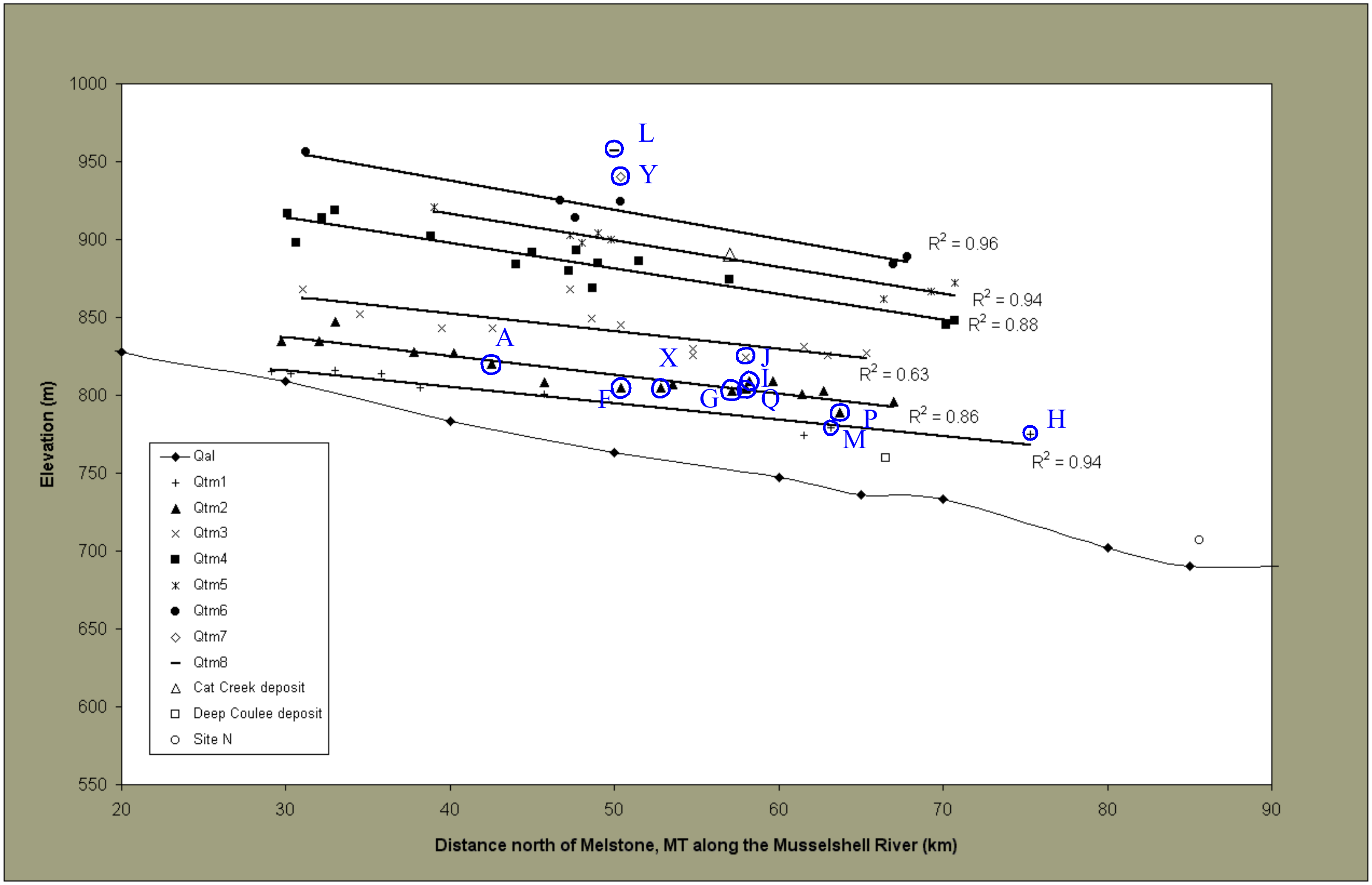

Figure 13. Revised longitudinal profiles of the Musselshell River terraces (Q_{tm1-8}) and the gradient of the modern Musselshell (Q_{al}). See Fig. 10 for geographic location of sites A, F-J, L-N, P, Q, X, and Y.

they were when the lower (now abandoned) floodplains were active. The changes improved the R^2 values for Q_{tm6} and Q_{tm1}. However, the R^2 values for Q_{tm2} (0.86), Q_{tm4} (0.88), and particularly Q_{tm3} (0.63) remained low relative to those of the other terraces ($\geq$0.94). Terrace fragments with large, flat tops are scattered at various altitudes between Q_{tm4} and Q_{tm2}. The terrace fragments between Q_{tm2-4} may actually be from three, rather than one terrace. The addition of three new terraces, Q_{tm3a}, Q_{tm3b} and Q_{tm3c} (Fig. 14), in place of Q_{tm3} is favored because it is consistent with geomorphic relationships on the topographic maps and increases the linear R^2 values to $\geq$0.87 for all terrace levels. However, a field investigation of the key terrace fragments is necessary before $Q_{tm3a-3c}$ are accepted as valid terraces. Such an investigation is outside the scope of the current study.

The thickness, bedding characteristics, rounding, and grain size distribution of the Musselshell terraces were studied at Sites A, E-J, L, M, P, Q, X, and Y in Q_{al}, Q_{tm1-3}, and Q_{tm7-8} (Fig. 10; Table 10). These characteristics were also studied at Site W, which was originally correlated with Q_{tm3} (Johnson and Smith, 1964). However, this deposit does not appear to be part of the Musselshell River terrace sequence at all. The gravel at Site W is different from the gravel at all other sites. It is angular rather than predominantly subrounded, and it is derived from bedrock in the immediate area rather than from mountain ranges to the west and south (Fig. 4; Table 1). The deposit is probably associated with a nearby tributary that enters the Musselshell from the east rather than with the Musselshell River itself. Therefore, no evidence exists that Q_{tm3} is a paired terrace, or that Q_{tm2} and Q_{tm1} are nested within Q_{tm3}.

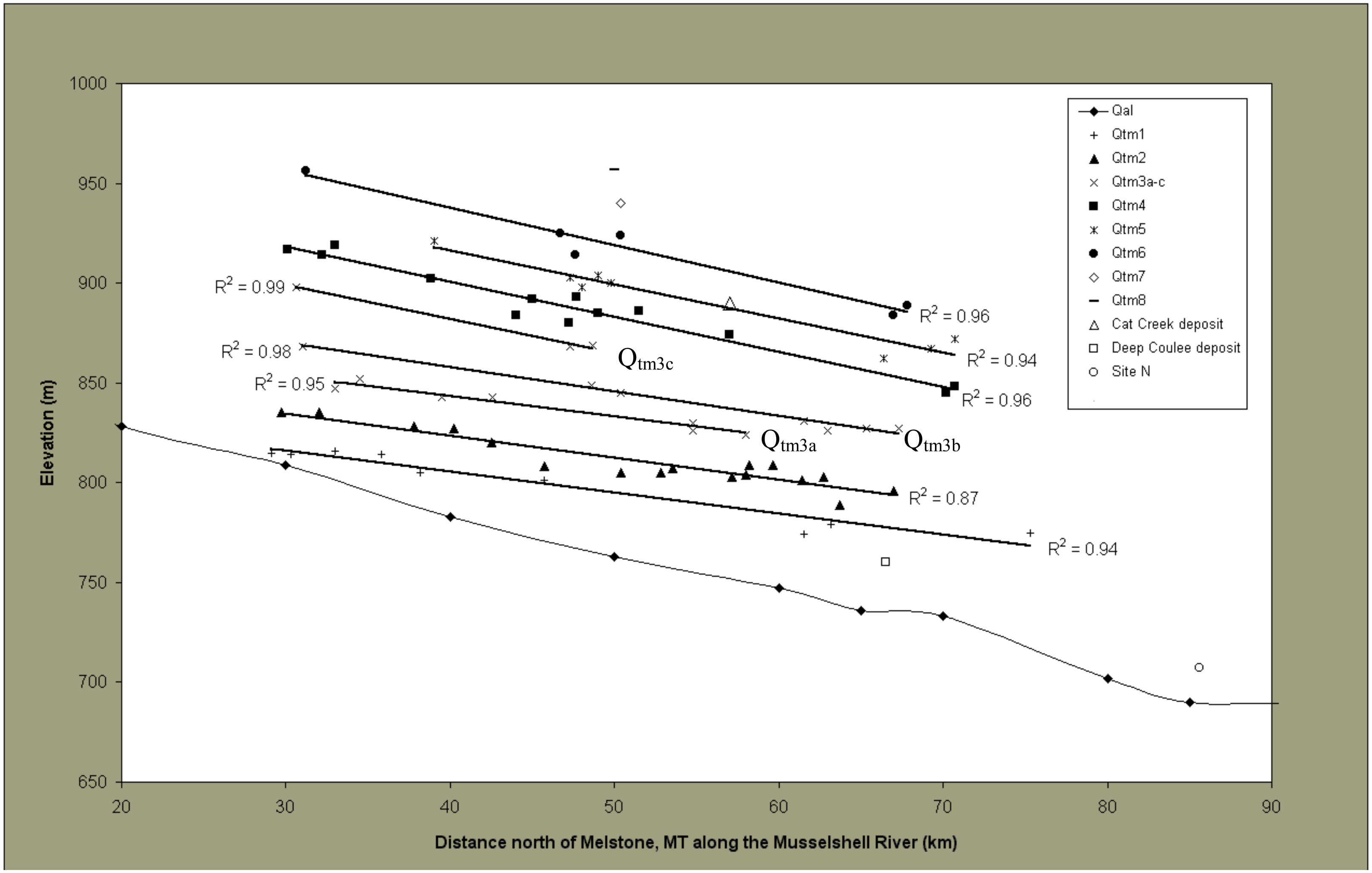

Figure 14. Revised longitudinal profiles of the Musselshell River terraces showing proposed terraces Q_{tm3a-c}.

TABLE 10. CHARACTERISTICS OF THE MUSSELSHELL RIVER TERRACES AND FLOODPLAIN.

Unit	Site	HAR† (m)	Site description, including thickness and bedding characteristics	% Sub-rounded	% Sub-angular	Size‡ (cm) Avg.	Size‡ (cm) Range	Source area(s)‡
Q_{al}	E	0	Gravel bar in the modern Musselshell River	-	-	5.5	≤12.5	MT
Q_{tm1}	H	59	5-7 m of imbricate, graded gravel and cross-bedded sand and gravel beds	92	8	5.9	≤50	MT/CN
	M	44	4 m of imbricate gravel	-	-	-	≤15	MT/CN
Q_{tm2}	A	43	Clast-supported gravel (thickness unknown) overlain by 0.7 m of pebbly fines with soil development	-	-	-	-	MT
	F	28	1 m of imbricate, clast-supported, graded gravel with scour and fill features underlain by a bed of laminated fine-medium sand	97	3	5.0	≤10	MT
	G	49	1 m of imbricate, clast-supported gravel with slabs of locally-derived sandstone and shale; gravel is overlain by fines with soil development and underlain by bedrock	88	12	5.3	≤22.5	MT
	I	63	1-2 m of imbricate, clast-supported gravel overlain by 3.8 m of finely laminated silt and interbedded clay; silt and clay is overlain by 0.4 m of imbricate gravel capped by 0.3 m of fine material with soil development	99	1	4.3	≤10	MT
	P§	56	1.5-2 m of gravel	-	-	3.4	≤10	MT
	Q§	55	1.5-2 m of gravel	-	-	2.6	≤7.5	MT
	X§	43	2.7 m of subangular to subrounded gravel	-	-	-	most <5	MT
Q_{tm3}	J	75	3.7 m of imbricate, clast-supported gravel with sand lenses (not laminated)	94	6	4.5	<10	MT
Q_{tm7}	Y	156	3 m of gravel overlain by 0.6 m of pebbly fines with soil development	-	-	-	2.5-12.5§	MT
Q_{tm8}	L	198	~1-3 m of gravel; no good exposure	-	-	-	-	MT

NOTE: No data is available for categories containing a dashed line.
†HAR: Height above the Musselshell River.
‡See Appendix C for size and provenance data.
§Data from Johnson and Smith (unpublished field notes, 1953-1956); see Appendix C.

The highest terraces (Q_{tm2-3} and Q_{tm7-8}) have a thin layer (1-4 m) of imbricate, clast-supported gravel with a fine to medium sand matrix (Fig. 15). Some exposures display scour and fill marks, graded bedding, or interbedded sand layers. At four sites, the gravel is overlain by 0.3-0.7 m of fine material that displays some degree of soil development. At most sites, the gravel is subrounded and has a smaller range in size than the modern Musselshell alluvium. However, at Site G, large, subangular slabs of locally-derived rock are present (Fig. 16a). Also at Site G, the contact between the gravel and the underlying bedrock is visible (Fig. 16b). The lower contact is covered at the other sites (for example, Site F in Fig. 15).

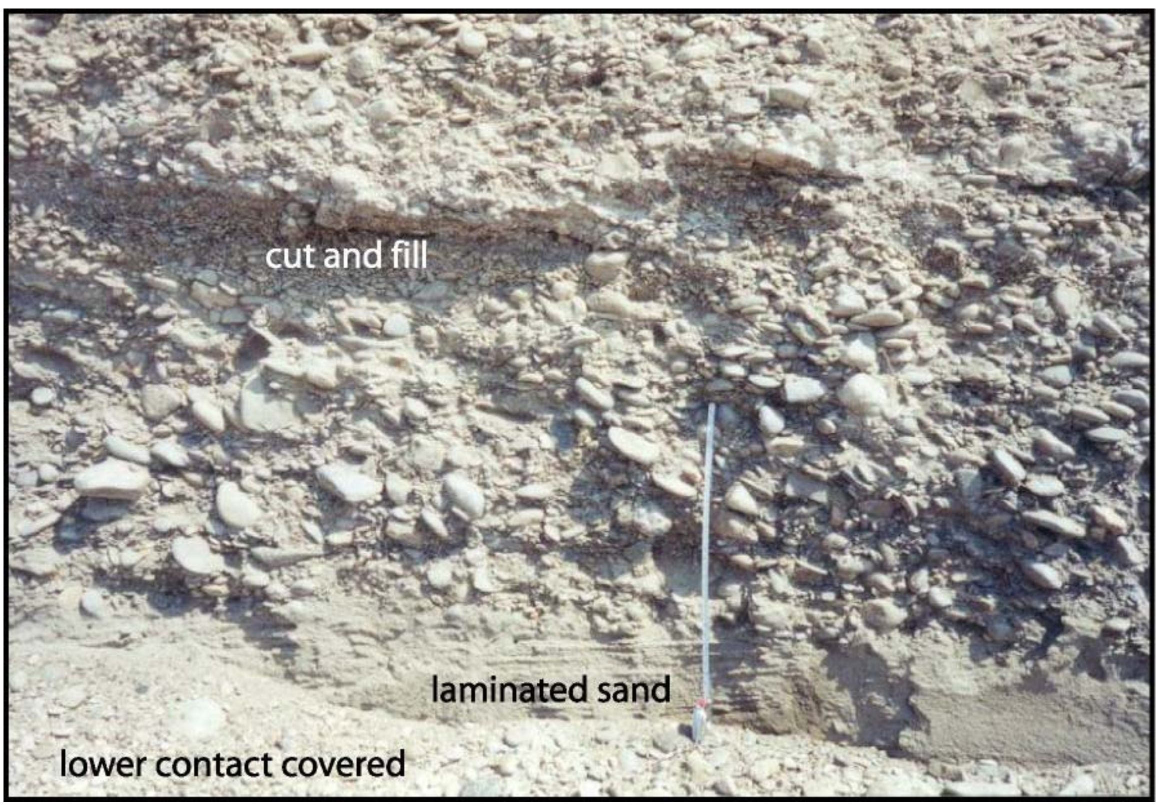

Figure 15. Terrace gravel and laminated sand at Site F, in Q_{tm2}. Gravel is generally clast-supported and subrounded with a sandy matrix. Tape measure is 0.3 m for scale.

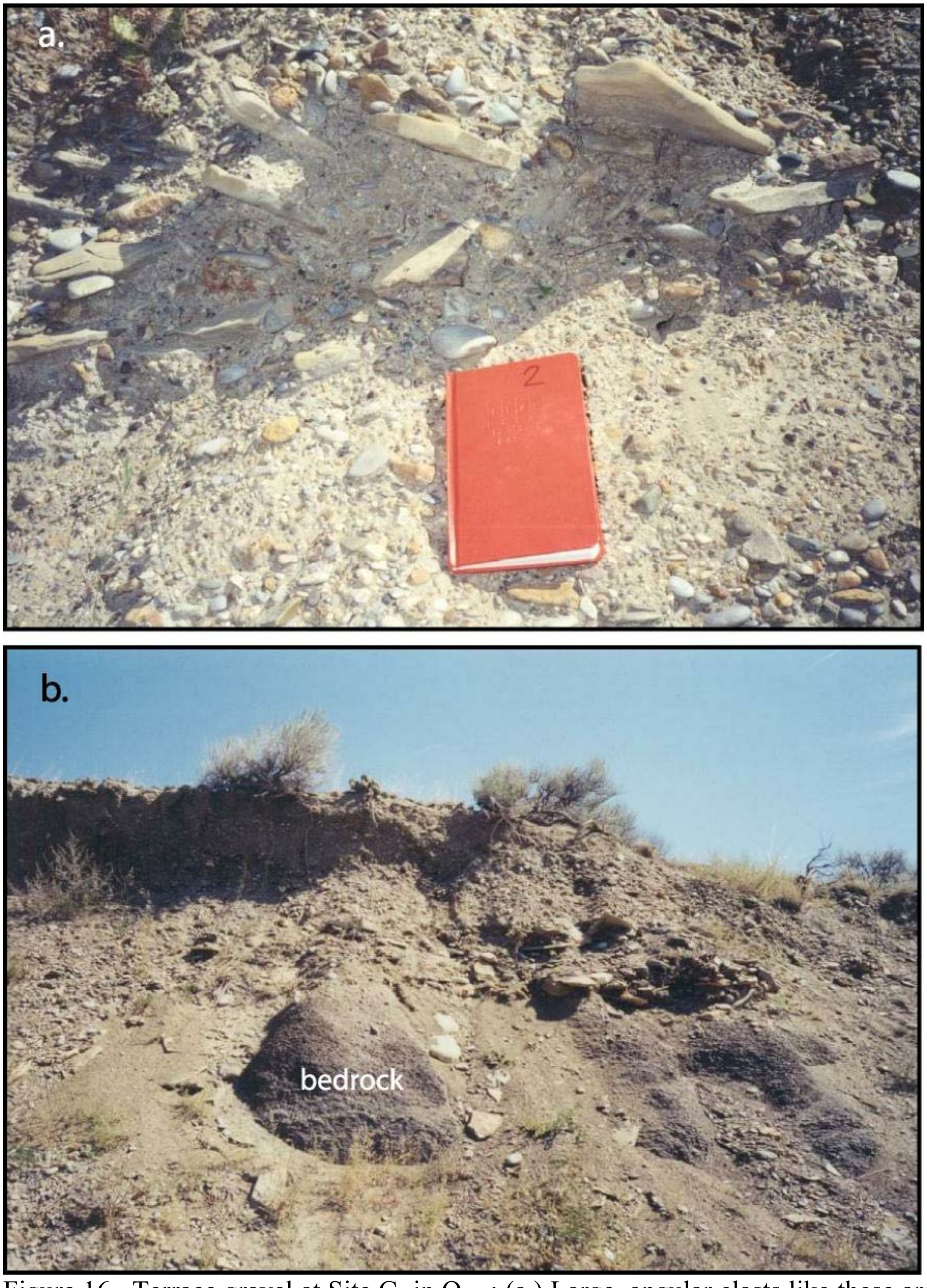

Figure 16. Terrace gravel at Site G, in Q_{tm2}: (a.) Large, angular clasts like these are found only locally in the Musselshell terraces; most of the gravel is subrounded. Field book is 0.2 m for scale. (b.) The gravel is thin (~1 m) and rests on bedrock.

The gravel in Q_{tm1} is also imbricate, but is slightly thicker (4-7 m) and contains more matrix than the higher terraces (Fig. 17). At Site H, multiple distinct beds, some of which are cross-bedded or graded, imply that this unit might have formed as a valley fill rather than as a strath (Fig. 17). The deposits of Q_{tm1} are nested within Q_{tm2} (Fig. 10).

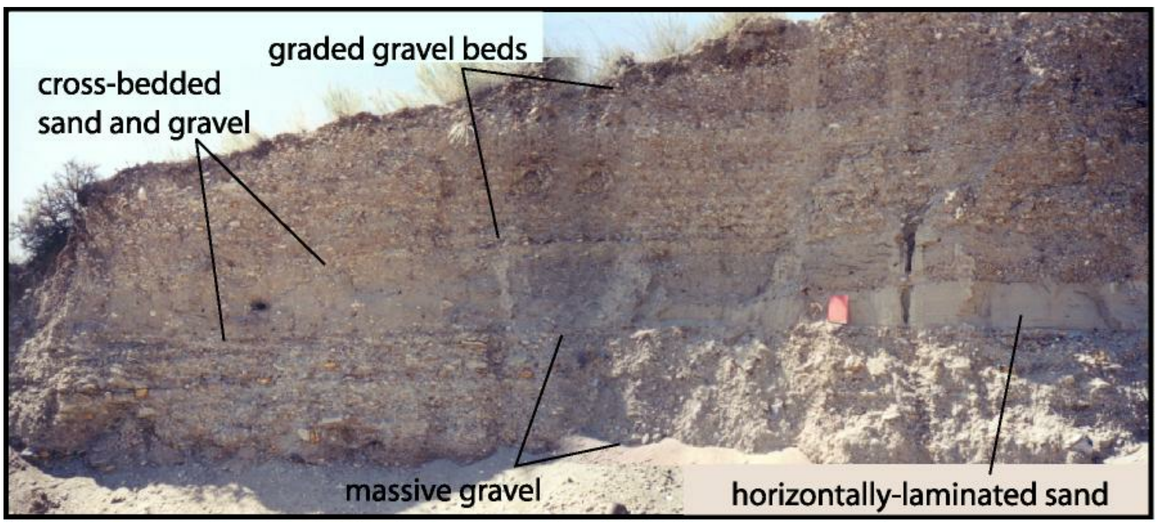

Figure 17. Terrace gravel at Site H, in Q_{tm1}. This terrace may be a valley fill, because of its thickness and multiple beds of gravel and sand. Some of the beds are imbricate and/or graded, and one bed has north-dipping cross-beds. Field book is 0.2 m for scale.

A low terrace (≤8 m above the Musselshell River) that consists of predominantly fine alluvium, was observed along the Musselshell River (see Appendix C for a description). Johnson and Smith (1964) included this low bench with their Q_{al}. Because low benches have been distinguished from the modern alluvium and assigned a Holocene (MIS 1) age in other river valleys (Pierce and Scott, 1982; Reheis, 1984), a similar distinction is made here.

Four of the Musselshell terraces (Q_{tm2}, Q_{tm3}, Q_{tm7} and Q_{tm8}) and the modern alluvium (Q_{al}) consist of all Montana-source gravels (Table 10), including rock types found in the Bull, Judith, Big and Little Snowy, northern Crazy, Little Belt and Castle Mountains and clasts derived from the local bedrock (see Figs. 4-5 and Table 1). The modern alluvium consists of 21% limestone and 40% igneous rocks, with lesser amounts of chert, sandstone, quartzite and shale. The majority of the clasts in Q_{tm2}, Q_{tm3}, and Q_{tm7} are Montana-source limestone (24-40%) and alkaline igneous rocks (28-38%) with some chert, sandstone and Precambrian quartzite and argillite of the Belt Supergroup. See Appendix C for the cobble count data.

Q_{tm1} includes a small but unmistakable percentage of crystalline Canadian Shield lithologies at Sites H and M (Table 10). Site H contains granite (<6%), gneiss (<3%) and biotite schist (<1%), but the majority of the gravel (90%) is from source areas in Montana (Appendix C, Table 24). Individual exotic clasts observed at this site were subrounded and ranged in size from 2.5-17 cm, with an average size of 7.5 cm. Two subrounded, 15 cm long Canadian Shield clasts (a pink granite and a pink gneiss) were observed at Site M. No cobble count was performed at this site.

At Site N, 1.5 m of imbricate gravel was observed (Fig. 18). The gravel is not capped by fine material; it is the uppermost layer in the exposure. It is underlain by $\geq$3 m of laminated fine sand, silt and clay with some cobble-rich layers. The contact between the two units is sharp and planar (Fig. 18). Two exotic boulders, much larger than the surrounding gravel, were buried 0.2 m in the gravel deposit (Fig. 18). No cobble count was performed at Site N. However, aside from the two boulders, the deposit appeared to have come from Montana source areas. Site N is at a much lower elevation than the downstream projection of Q_{tm1} (see Fig. 13), and therefore cannot be correlated with that terrace. This site is located about 5 km south of UL Bend (the Musselshell/Missouri confluence; see Fig. 3), north of the ice margins mapped by all workers since Colton and others (1961; Fig. 8). The gravel at Site N may therefore be related to the river, the lake, or the ice sheet. Further investigation is required to properly classify this deposit.

Figure 18. Imbricate gravel and underlying fine material at Site N. This site is too low to be correlated with Q_{tm1}. Two Canadian Shield boulders are buried 0.2 m in the gravel.

Johnson and Smith (unpublished field notes, 1953-1956) performed five cobble counts in the tributary terraces ($Q_{t-t7;}$ Sites R-U and Z; Appendix C). In general, the terraces of Box Elder, Flatwillow and the other tributaries are composed of Montana-source gravel. The potential exception is Site U (Appendix C, Table 35), in Q_{t2}, at 47° 00' N and 888 m elevation. That cobble count included two small "granitic" clasts (2 and 10 cm), but the color or deduced origin for the granite was not specified. These are probably not from the Castle Mountains, because Site U is in the terrace of a tributary that drains the Snowy and Judith mountains, which have sedimentary and alkalic igneous bedrock. None of the other cobble counts performed in the tributary terraces ($Q_{t1\text{-}3or4}$; see Appendix C) contained any exotic clasts. Perhaps these clasts were misidentified by Johnson and Smith, or perhaps the term "granitic" was used loosely to refer to a coarse-grained alkalic igneous rock. Because these clasts were not observed during this study, no further speculation will be made on the significance of this data. Additional study of the gravel benches in the tributary basins is outside the scope of the current research. However, such a study could be quite informative about the history of glacial Lake Musselshell.

Terrace Soil Development

Soil development did not provide an effective means to date alluvial gravels in the Musselshell basin. If the mapping and inferred geomorphic relationships of gravel deposits are valid, terraces at Sites A, B and D (Q_{tm2} and Q_{t2}) are approximately the same age, while the terrace at Site C (Q_{tm7}) is much older (Johnson and Smith, 1964; Fig. 10). However, soils at Sites A, B and D showed neither a similarity to each other nor a characteristic difference from Site C in terms of clay film development, carbonate morphology, or other properties observed in the field (Table 11; Appendix D). Laboratory analyses of the texture, pH and dry color of these four soils also did not reveal any obvious patterns with age (Fig. 19; Appendix E). Instead, the soils appear to show the signature of the local bedrock geology, particularly at Sites B and D, where soils are heavy-textured and contain gypsum. This is characteristic of soils formed in Colorado shale (Soil Survey Staff, 1993).

TABLE 11. SELECTED SOIL FIELD CHARACTERISTICS AT SITES A-D.[†]

Site	A horizon thickness (cm)	Clay films[‡]	Gypsum	Carbonate[§]	Thickness above terrace (cm)	Local rock type(s)
A (Q_{tm2})	10	moderate	None	Filaments	69	Judith River formation
B (Q_{tm2})	20	well	Filaments	Present	76[#]	Colorado shale
C (Q_{tm7})	10	moderate	None	Filaments	89[#]	Eagle sandstone, Claggett shale
D (Q_{t2})	6	well	Filaments	Filaments	122[#]	Colorado shale

[†]See Appendix D for full field descriptions.
[‡]Moderate or well-developed (R. Wegmann, oral comm., 2002).
[§]Detected using dilute hydrochloric acid.
[#]The terrace was not observed directly at these sites (see Chapter 2 for details).

Additional soil profiles were observed in exposures at Sites K (Cat Creek gravel) and Y (Q_{tm7}; Fig. 10). The upper 0.5-2 m of the exposures at these two sites was composed of fine sand, silt and clay with <10% rock fragments. Below this layer there was an abrupt transition to a gravel-dominated deposit. The gravel deposits were clast-supported, with fine to medium sandy matrix. The fine cap showed development of A and B horizons, but the only sign of soil formation in the gravel was the presence of carbonate coats (<3 mm thick) on the undersides of many gravel clasts. Soils were not described in any more detail or analyzed for texture, pH and color at Sites K and Y.

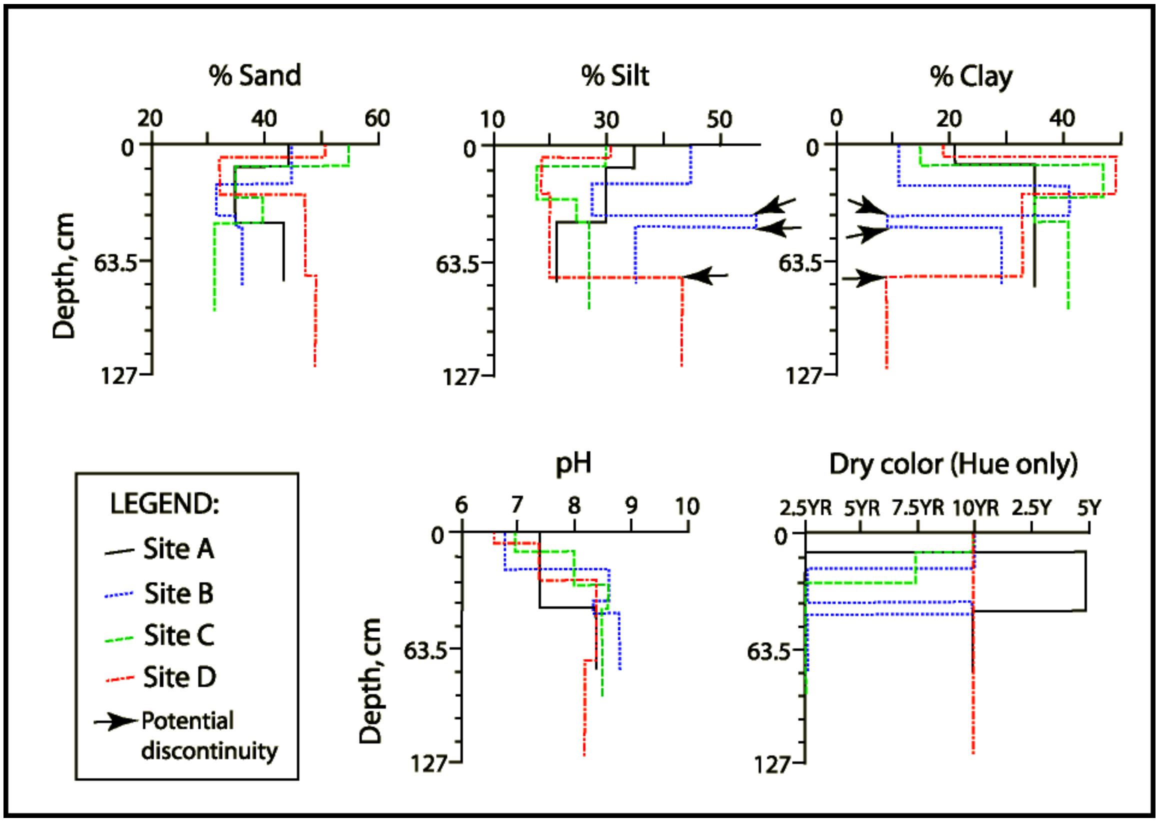

Figure 19. Texture, pH and hue of soils at Sites A-D. Arrows point to the locations of texture discontinuities discussed in the text. See Figure 10 for site locations.

Because the calcium carbonate content was not measured in the laboratory, the soils cannot be placed quantitatively into a carbonate stage (Gile et al., 1966; Machette, 1985). However, all six soils observed fit the field description for Stage I (see Table 6). At Sites A-D, at least one horizon in each soil effervesced in dilute HCl and filaments were present at Sites A, C and D (Table 11). At Sites K and Y, thin carbonate coats (<3 mm) were observed on the undersides of cobbles. No carbonate nodules, cementation or carbonate coating entire cobbles were observed at any of the sites.

The parent material of the soils studied is not the terrace gravel itself. Soils were developed in a cap of fine material that overlies the gravel. The cap was approximately 0.5-2 m thick and, at Sites A-D, it consisted of 30-55% sand, 20-55% silt, and 10-50% clay in all horizons (see Appendices D and E). Gravel was present throughout the fine cap, but its total volume was less than 10%. The gravel may have migrated into the cap from the underlying gravel deposit. Such upward migration has been demonstrated in the laboratory through repeated wetting and drying of a sandy-skeletal loam (Springer, 1958), but can also result from freeze-thaw, growth and decay of salt crystals or expansion and contraction of soil air (Buol et al., 1997). Only the material in the cap was analyzed for carbonate morphology, texture, pH, and dry color.

Discontinuities are present in the texture data at two sites, indicating that the cap of fine material could record multiple episodes of deposition and possibly erosion. The soil at Site B has an increased silt/decreased clay content between 38 and 45 cm (Fig. 19; Appendix E). A similar "silty layer" occurs below 71 cm at Site D (Fig. 19; Appendix E). Alternatively, these apparent discontinuities might simply be the result of poor disaggregation of flocculated clay particles during hydrometer analysis. Repeat hydrometer measurements would be necessary to test for this.

Origin of the Fine Material Capping the Terraces

The cap of fine material observed at Sites A-D, K and Y may be of alluvial, eolian, colluvial, or a combination of origins. The absence of a soil-age relationship at these sites implies that the age of the fine caps are not closely related to the age of the terraces they cover. It is therefore unlikely that each of the caps is simply fine-grained alluvium deposited during terrace formation. Also, if the entire cap was laid down at all of the sites at the same time(s) from the same source, the six soils would be more similar to each other in texture, pH and color. This rules out a common origin, such as constant or episodic deposition of regional-scale loess.

Instead, the fine material seems to have a complex origin that is different at each site and includes multiple episodes of deposition, burial and/or truncation of locally-derived alluvium, loess and/or colluvium. Any of the above origins would have incorporated material from nearby bedrock types. However, the young (Stage I) carbonate morphology indicates that the influx of carbonate may have occurred at the same time – and recently – at all six sites. One method for the simultaneous, recent addition of carbonate is regional deposition of wind-blown material during MIS 2-1 on top of pre-existing fine material of various origins. Despite this speculation, an evaluation of the timing of eolian, alluvial and/or colluvial sediment deposition on the Musselshell terraces is beyond the scope of this study.

Ice-Rafted Boulders

It was the presence of glacial boulders and absence of till that first indicated to geologists that glacial Lake Musselshell had existed (Calhoun, 1906; Alden, 1932). The location and altitude of these exotics has traditionally been used to define the boundaries of the lake (Colton et al., 1961). In this study, 35 re-located boulders and 90 newly located boulders were used to determine the extent and age of the former stage(s) of Lake Musselshell.

Previously Located Boulders

Thirty-five of the 123 boulders located by Johnson and Smith (1964) were re-located during this study. Unsuccessful attempts were made to locate 12 others (Fig. 20), including the three at the highest altitudes. The highest boulder at 940 m (3085 ft; JS1; Fig. 20) could not be found despite thorough searches and conversations with the landowners. The second highest boulder at 927 m (3042 ft) east and slightly north of Winnett was relocated (E71; Fig. 20). However, this boulder has probably been broken and moved by humans. E71 is small, has angular, unweathered surfaces and is next to a road along a fence. All other boulders mapped by Johnson and Smith (1964) were <920 m (3020 ft).

In 2001, Roger Colton generously supplied me with his original files from the 1950's pertaining to his work on glacial Lake Musselshell. The files included a map with 21 boulder locations (Fig. 20) on which he based the outline of glacial Lake Musselshell

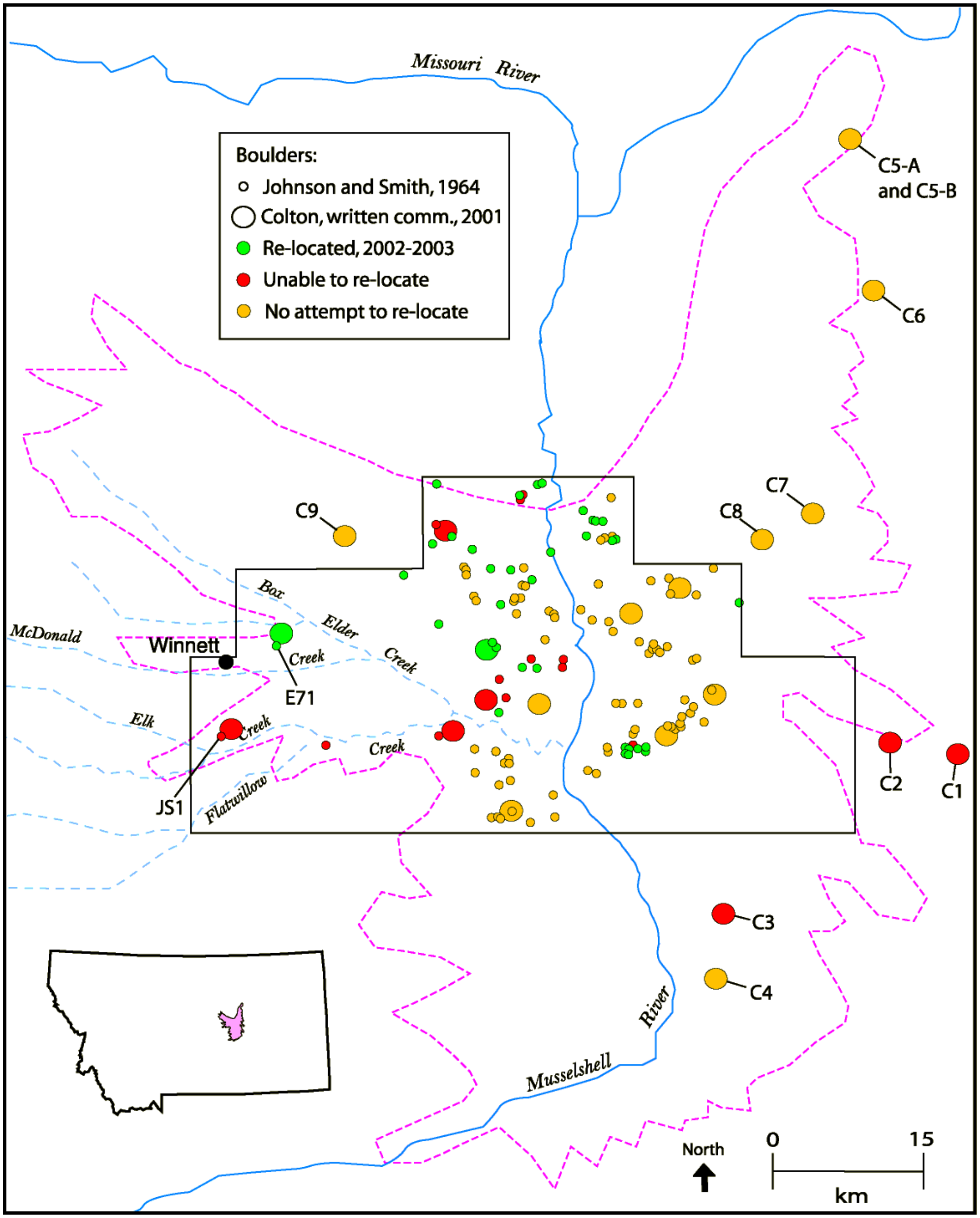

Figure 20. Location of glacial boulders mapped by other workers. Labeled boulders are discussed in the text. The outline of Lake Musselshell (Colton et al., 1961) and the study area of Johnson and Smith (1964; also shown in Figs. 2 and 10) are shown for reference.

for the Glacial Map of Montana East of the Rocky Mountains (Colton et al., 1961). These were plotted based on section, Township and Range locations given to Roger Colton by various geologists and soil scientists working in the area. Unfortunately, not all of the section locations were included in the files, so many of the boulders at key locations could not be precisely transferred to the 1:24,000-scale topographic maps.

The highest boulder on Colton's map was from Alden (1932; C1; Fig. 20). It was mistakenly reported as being in sec. 9 T13N R34E (Alden, 1932, p. 81), but was actually in NE ¼ SE ¼ SW ¼ sec. 4 (information from files received from R. Colton, 2001), where the highest topography is approximately 963 m (3160 ft). This boulder has never been re-located despite attempts by Colton and others, and Colton concluded that the boulder had been moved to a nearby homestead (according to his notes from the 1950's).

Boulders C3-4 (Fig. 20) were probably reported to Roger Colton by H.R. Smith, who, according to Colton's notes (received in 2001), located about ten erratics 10 miles northeast of Melstone on aerial photographs as part of the Alice Dome mapping project (Smith, 1962). As part of the current study, a search was made for high boulders mapped near Proposed Spillways 2 and 4 (C1-3; Fig. 20), but none were found. Boulder C4 was not investigated because it was at a lower elevation (<884 m).

The locations and altitudes of two boulders given to Roger Colton by G. Anderson in September, 1960 plot precisely as described in a note from G. Anderson to R. Colton (Colton's files, received 2001) on the 1:24,000 topographic maps (C5; Fig. 20). Anderson described these as a pink fine-grained granite, 1.5 feet in diameter at 924 m (3032 ft) altitude and a "red granite gneiss," 2.5x1.5x3 feet at 919 m (3016 ft) elevation.

Another set of granitic erratics described by Anderson and mapped by Colton (C6; Fig. 20; elevations 920-940 m (3020-3086 ft)) were rather small (max. 38 cm) and were in and on top of a gravel deposit. There were no details given in Roger Colton's files regarding the location of the three remaining boulders (C7-C9; Fig. 20).

Twelve of Colton's 21 boulders are within the area mapped by Johnson and Smith (1964; Fig. 20). Probably due to the error associated with transfer of data between maps of different scales, these twelve boulders do not all overlap with a boulder mapped by Johnson and Smith on Figure 20, though it is likely that these twelve locations were taken from the work of Johnson and Smith (1964). Two of these were re-located in 2002, but four others could not be found.

Lithology, Size and Geographic Distribution

The 125 boulders located and re-located in this study are pink granite (51%), pink gneiss (35.5%), white granite (3.5%), white gneiss (3.5%), shonkinite (2.5%), biotite schist (2.5%) and fossiliferous limestone (1.5%). The largest boulder (E106) is 1.5 m long, 1.5 m wide and 1.5 m high. The average boulder dimension is 0.75x0.55x0.37 m. Many cobbles of exotic lithologies were observed, but in general only rocks with one axis $\geq$0.3 m long were considered boulders. The latitude, longitude, altitude, lithology, and dimensions of all 125 boulders used in this study are reported in Appendix F.

Glacial boulders are located between 725 and 927 m (2379 and 3042 feet) above sea level, a span of 202 m. A histogram of boulder altitude using 3-meter bins was used to separate the boulders into five altitude clusters (Fig. 21). Only 93 of the 125 boulders were included in the histogram. Some boulders were excluded because of small size or because they were thought to have been moved >3 m in elevation by humans. A maximum of five former lake levels were discerned from this histogram: Cluster 1 at 722-796 m (2370-2610 ft), Cluster 2 at 808-838 m (2650-2750 ft), Cluster 3 at 844-878 m (2770-2880 ft), Cluster 4 at 878-899 m (2880-2950 ft), and Cluster 5 at 902-930 m (2960-3050 ft).

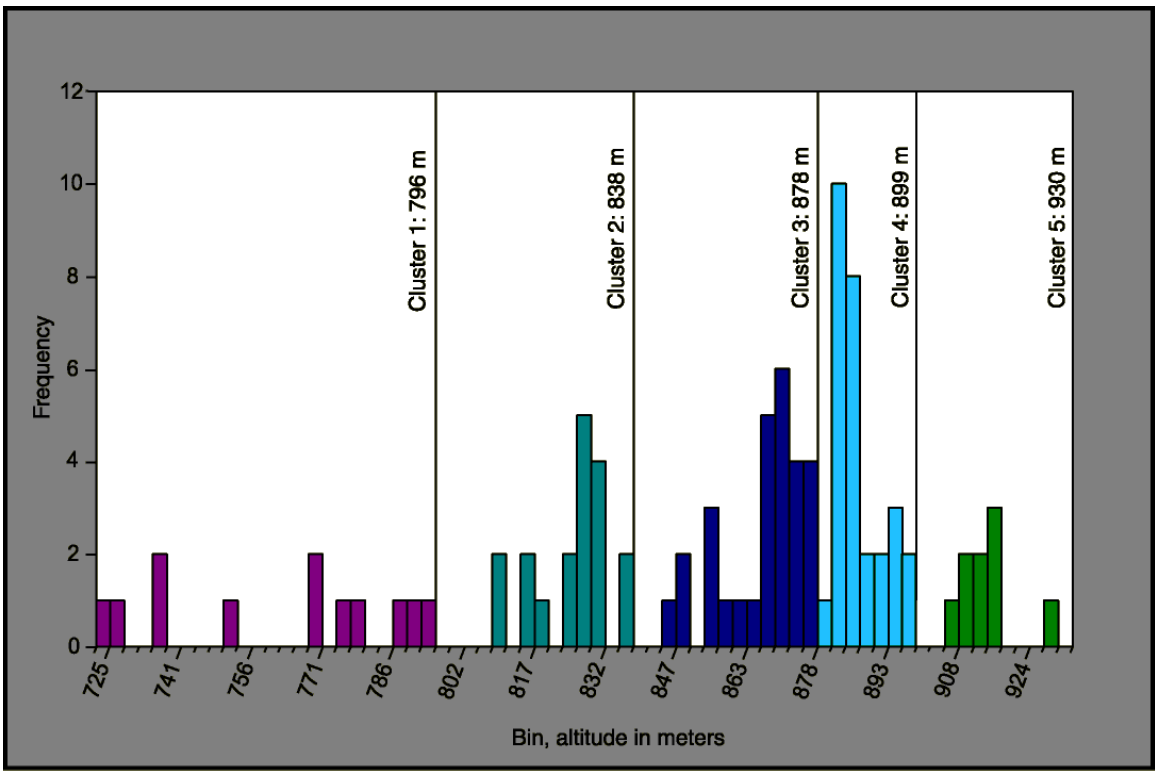

Figure 21. Histogram of Musselshell boulders with 3-meter altitude bins. Boulders are divided into five altitude clusters.

It was prudent to entertain the maximum number of altitude clusters (Fig. 21) for the purpose of sample collection. If lakes of different levels existed at different times in the past, the deposits from these lakes should be separable by altitude and age. The altitude clusters were used as a first approximation to separate the ice-rafted boulders into as many potential lake levels as possible. Obtaining surface exposure ages on multiple samples from each of the five altitude clusters ensured that sufficient surfaces were examined from each potential lake level. However, the clusters are only important if the surface exposure ages from boulders in two or more of the altitude clusters are distinct. Thus, the surface exposure ages were used to test the hypothesis that there were multiple lake levels represented by altitude clusters of ice-rafted debris. The altitude clusters will be discussed further when the surface exposure age results are presented.

The maximum extent of Lake Musselshell can be inferred based on the location of the highest ice-rafted boulders (Table 12). However, six of the eleven highest boulders have either been moved by humans or may have been deposited by the ice sheet itself rather than an iceberg in Lake Musselshell. The highest boulder, E71 appears to have been broken and placed along a fence line by humans. Boulders E84 and E85 are within the area thought to have been glaciated by the Laurentide ice sheet (Colton et al., 1961; Fullerton et al., 2004). E94, C5-A and C5-B are close to the lake-ice contact (Colton et al., 1961).

The remaining five exotic boulders, E116, E115, E113, E72 and E40, are ≥20 km south of the ice margin and do not appear to have been moved by humans. These boulders are the most reliable evidence available to define the maximum stage of Lake Musselshell. In order for these five ice-rafted boulders to be deposited between 911 and 917 m, the lake must have reached at least 917 m. In fact, it was probably higher, because the bottom of an iceberg can hit the lake bottom before the edge of the iceberg has reached the shore.

TABLE 12. HIGH-ALTITUDE BOULDERS IN THE MUSSELSHELL BASIN.

Boulder	N Latitude	W Longitude	Altitude (m)	Comments
E94	47° 10' 41"	108° 04' 47"	908	Within 1 km of the ice margin
E84	47° 20' 53"	108° 08' 16"	910	North of ice margin
E40	47° 01' 19"	108° 00' 45"	911	~20 km south of ice margin
E72	46° 58' 54"	108° 00' 19"	913	~25 km south of ice margin
E113	46° 58' 50"	107° 32' 45"	913	~35 km southeast of the ice margin
E115	46° 59' 30"	107° 33' 29"	916	~35 km southeast of the ice margin
E85	47° 20' 56"	108° 08' 20"	917	North of ice margin
E116	46° 59' 30"	107° 33' 28"	917	~35 km southeast of the ice margin
C5-B[†]	~47° 31' 27"	~107° 33' 34"	919	Within 5 km of the ice margin
C5-A[†]	~47° 31' 51"	~107° 33' 21"	924	Within 5 km of the ice margin
E71	47° 01' 27"	108° 16' 43"	927	Probably moved by humans

[†]Locations for boulders C5-A and C5-B are approximate. They are based on the section, Township, Range, altitude and sketch maps given to Roger Colton by Gerry Anderson (see text for discussion). The given section, Township and Range locations match with the given altitude when plotted on modern 1:24,000 scale topographic maps. Thus, the altitudes are considered reliable.

All of the boulders are within the boundaries of either the ice margins or the lakes drawn by Colton and others (1961) and Colton and Fullerton (1986; Fig. 22). Many boulders are found outside the lake mapped by Alden (1932; Fig. 22) suggesting that his boundary needs revision. The prevailing westerly winds in central Montana would have carried the majority of the icebergs to the southeastern shore. However, easterly katabatic winds have been modeled for the Wisconsin Laurentide ice sheet (Kutzbach and Wright, 1985; Glasgow et al., 1998). This would make the northwestern shore the lee

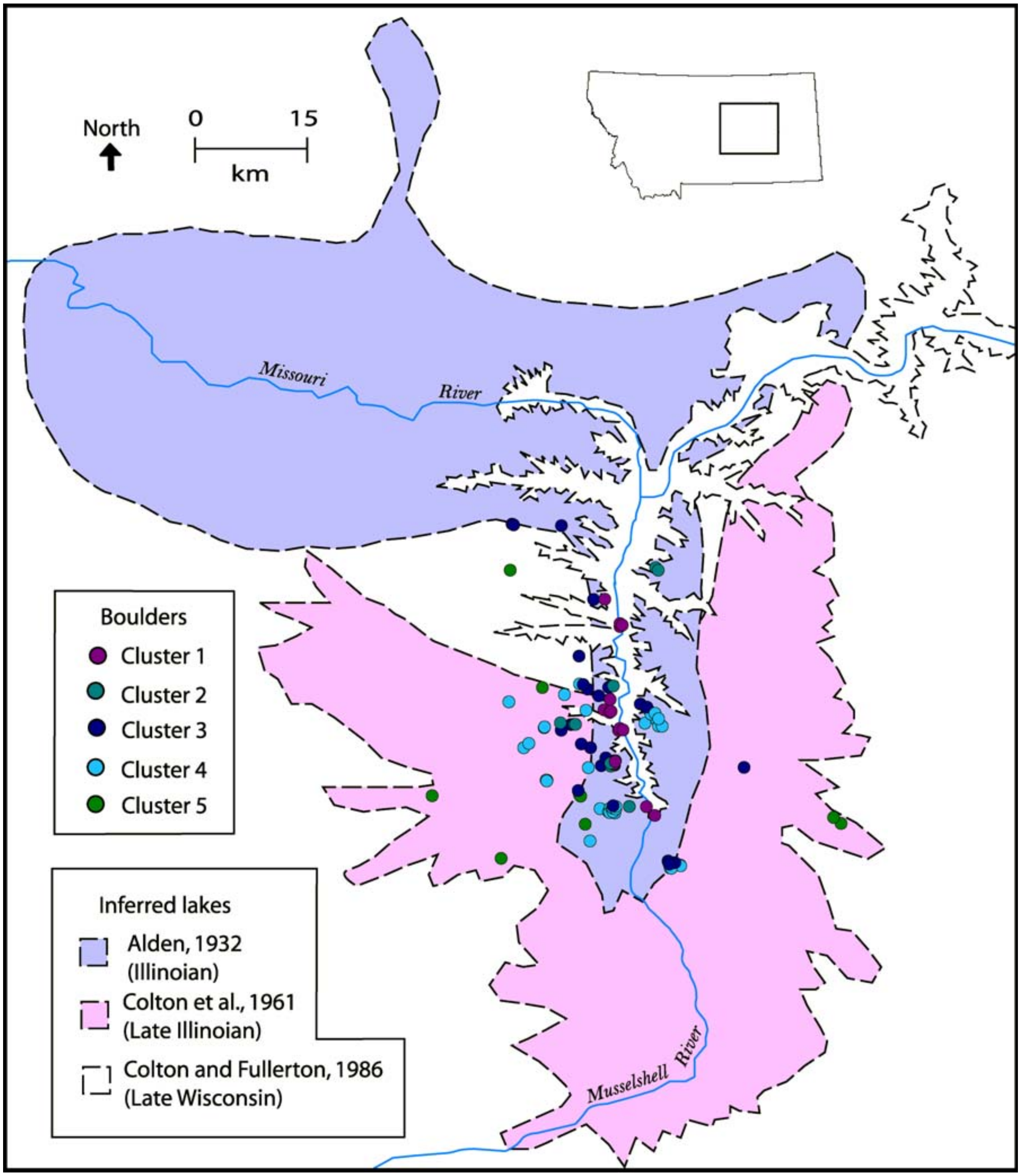

Figure 22. Locations of exotic boulders mapped during this study. Boulders grouped by altitude into Clusters 1-5 (see Fig. 21). Latitude, longitude and elevation of each boulder are given in Appendix F.

shore and thus the habitual iceberg grounding area. No boulders were found in the southeast and northwest sections of the lake mapped by Colton and others (1961) despite limited field investigation of these areas. The southwest portion of the lake was not visited due to lack of time. None of the 21 boulders reported by Roger Colton are in the southwest portion of the lake basin (Fig. 20). The northeast portion was not visited due to poor accessibility. However, Roger Colton's location for two boulders in the northeast sector (C5-A and C5-B; Fig. 20) seems reliable.

Buried Boulders on the Musselshell-Winifred Divide

Exotic boulders buried at altitudes between 980 and 1064 m (3220 and 3490 ft) were uncovered during road construction in the summer of 2002. More than twenty 0.3-0.76 m long boulders were unearthed from the upper 4 m of the landscape during widening of Highway 19. The boulders were excavated along a 20-km stretch south of Roy in the Box Elder, Bear and South Fork Bear Creek watersheds (Fig. 23). Cretaceous bedrock is exposed along this stretch of the highway, and the fine sediment observed in the area looked like weathered bedrock. The boulders were pink granite and gneiss, shonkinite, and one pink pegmatite. They were not highly weathered, nor did they display carbonate coats that could help to determine their age. The construction crew had piled the boulders east of the road and has subsequently removed them from the site.

No exotic boulders have ever been reported on the surface at this altitude this far south. North of Roy, north of the mapped (Late Illinoian) ice margin (Fig. 23), abundant

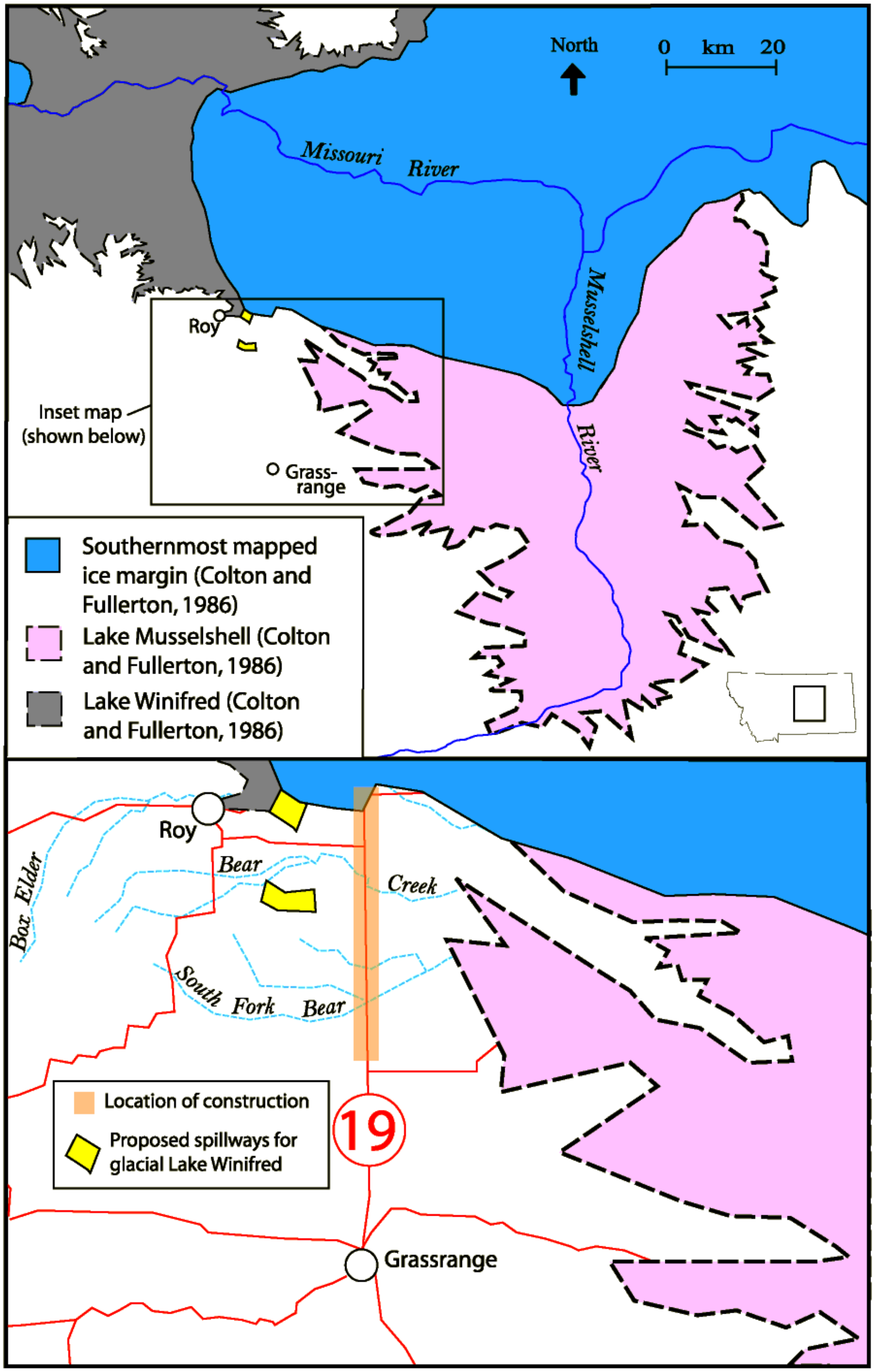

Figure 23. Location of proposed glacial Lake Winifred and spillways relative to Lake Musselshell. Inset map shows location of 20-km stretch of highway excavation that unearthed glacial boulders along Hwy 19.

exotic boulders are visible on the land surface. Neither glacial ice nor a glacial lake has been mapped south of Roy. However, another large proglacial lake, Lake Winifred, was suggested by Colton and Fullerton (1986; Fig. 23) between lakes Great Falls and Musselshell. Lake Winifred was thought to exist at 1067 m (3500 ft) during the Late Illinoian stage, and was probably invoked to explain lake sediments that had been reported west and south of the Little Rocky Mountains (Colton and Fullerton, 1986). The spillways for this lake are shown east of Roy (Fig. 23; Colton and Fullerton, 1986) in the vicinity of the highway construction.

Potential Outlets for Lake Musselshell

Roger Colton (1959) proposed that the three lowest passes on the southeastern edge of the Musselshell drainage divide might have accommodated the hypothetical draining of Lake Musselshell into the Yellowstone River. The current study did not attempt to rigorously test this hypothesis by coring channel bottoms to look for exotic clasts, or by looking for a large deltaic deposit in the Yellowstone River west of Forsyth (Fig. 9a). However, a limited study of these three passes in the field and on 1:24,000 topographic maps does not support the idea that Lake Musselshell drained to the Yellowstone.

^{10}Be surface exposure ages of 27 ice-rafted boulders indicate that Lake Musselshell existed during the Late Wisconsin. Because Lake Musselshell and Lake Bonneville are of comparable age, the outlet of Lake Musselshell should be fairly similar to that of Lake Bonneville (Red Rock pass; Table 7) if Lake Musselshell was spillway-controlled. However, rolling hills or bedrock knobs, as opposed to cliffs like those in Red Rock pass, flank each of the three passes to the Yellowstone (Table 13; Fig. 24). At present, the floor of each of the three passes to the Yellowstone is at or above 940 m (Table 13). Reliable boulder altitudes indicate that the highest stage of Lake Musselshell was not much more than 917 m above sea level (Table 12). When the water from Lake Bonneville overtopped its spillway, it incised ~100 m into the unconsolidated sediment in Red Rock pass (Hamblin, 2003; Table 7). If the passes to the Yellowstone were once active spillways, the enormous volume of water in glacial Lake Musselshell would have cut deeply into the erodible Cretaceous bedrock, lowering the divide to a level well below

TABLE 13. PROPOSED OUTLETS FOR LAKE MUSSELSHELL.†

Proposed outlet	Location	Altitude	Morphology
1.) Modern Missouri channel	47° 37'28" N 107° 29' 54" W	685 m (2250 ft)	Bounded by >220 m cliffs; currently under Fort Peck Reservoir
2.) 3 km west of Sumatra‡	46° 37' 48" N 107° 35' 2" W	969 m (3180 ft)	Bounded by rolling hills; now occupied by Hwy 12 and an abandoned railroad trench
3.) 16 km northeast of Sumatra‡	46° 44' 57" N 107° 26' 27" W	969 m (3180 ft)	Bounded by rolling hills
4a.) 26 km south of Sand Springs; west fork‡	46° 54' 02" N 107° 28' 46" W	940 m (3085 ft)	Bounded by bedrock knobs 40 m high on both sides
4b.) 26 km south of Sand Springs; east fork‡	46° 54' 0" N 107° 24' 45" W	950 m (3116 ft)	Bounded by rolling hills

†Shown in Figure 9a.
‡Flows into the Yellowstone west of Forsyth.

that of the maximum lake surface. Colton's three proposed spillways could perhaps be interpreted as older (pre-Late Wisconsin) outlets, but they do not have the morphology expected of a young (MIS 2) spillway.

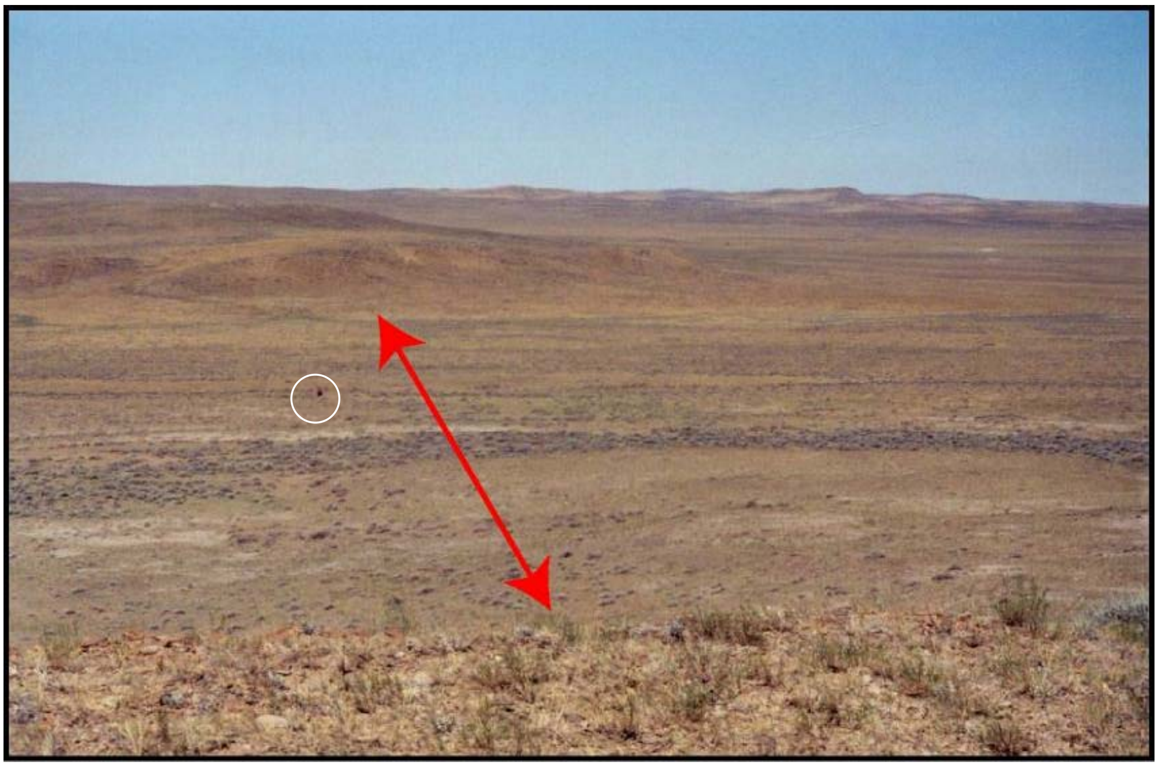

Figure 24. Photograph of the lowest of the proposed outlets that drains southeast to the Yellowstone River. Person (circled) for scale.

The only other proposed outlet for Lake Musselshell is a steep-walled segment of the modern Missouri River channel downstream from UL Bend, the Musselshell-Missouri confluence (Fig. 9a; Fig. 25). The modern Missouri is the only channel preserved on the periphery of the former lake basin that could have accommodated the draining of Lake Musselshell. The bend in the Missouri River channel at this location

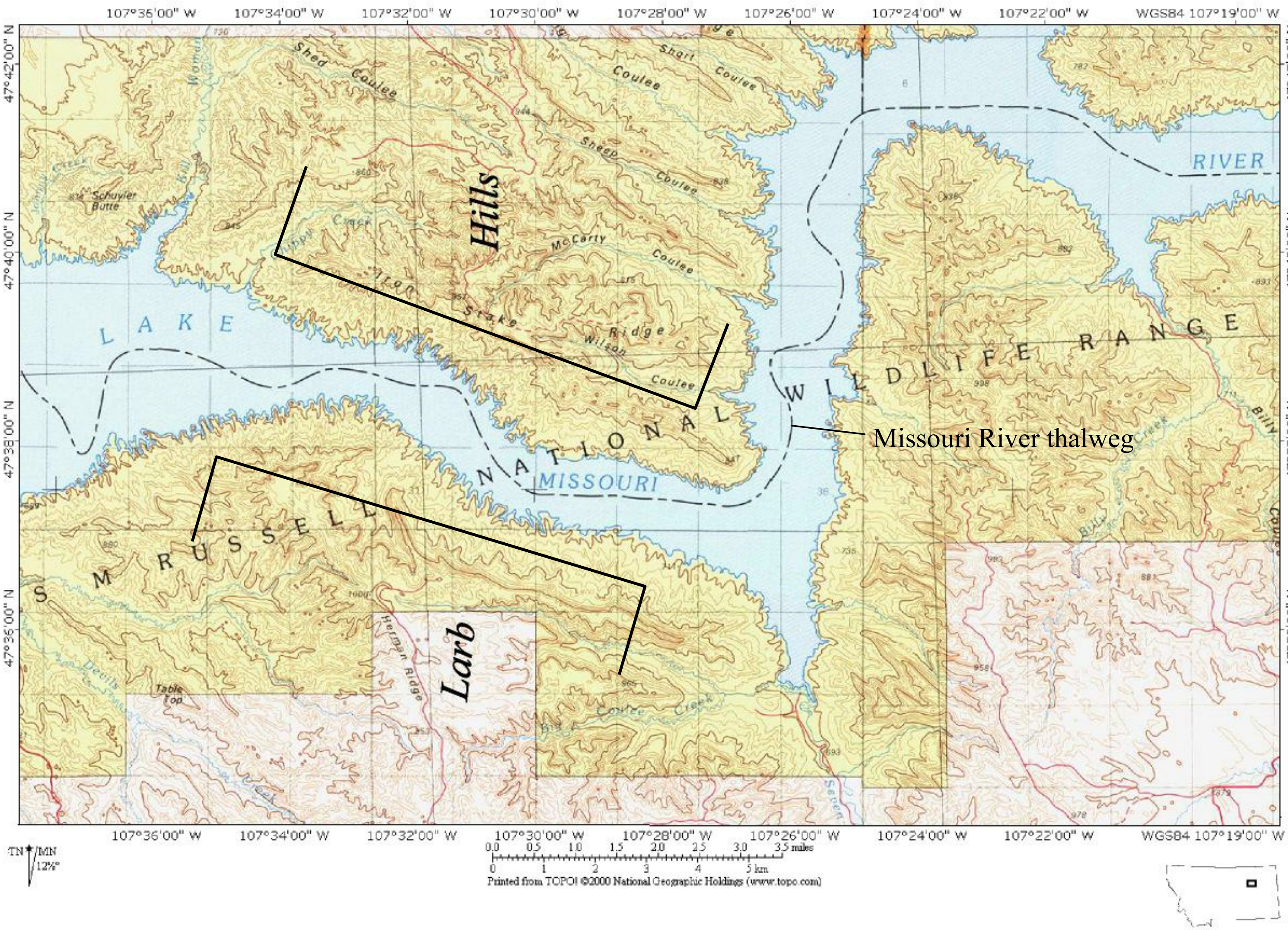

Figure 25. 1:100,000-scale topographic map showing the location of the proposed outlet for Lake Musselshell in the modern Missouri River channel. Contour interval is 20 m.

(the “L” in UL Bend) is evidence that this portion of the channel could have been created catastrophically. However, post-glacial channel modification by the Missouri River makes it extremely difficult to assess whether drainage was subglacial, ice-marginal or spillway-controlled. Because the Musselshell River currently drains into the Missouri upstream from the “L,” the floor of this former lake outlet is now, of course, lower than the rest of the Musselshell basin. The channel bottom, though it cannot be observed because it is now inundated by Fort Peck Reservoir, is below 685 m (Fig. 25; Table 13).

The proposed outlet is where the Missouri River passes through a low mountain range known as the Larb Hills (Fig. 25). The current altitude of the Larb Hills divide is between 900 and 940 m, approximately the same altitude as the lake highstand (~917 m). Thus, the lowest pass in the Larb Hills may have once been the lowest point on the periphery of Lake Musselshell, and acted as either a subglacial or subaerial spillway. This requires that the Missouri River had not occupied the Larb Hills portion of its channel prior to the existence of Lake Musselshell (Alden, 1932).

It is unknown whether the Missouri River channel east of UL Bend was established prior to, during or after the existence of glacial Lake Musselshell. If the Missouri River occupied the Larb Hills portion of its current channel prior to the existence of glacial Lake Musselshell, this outlet must have been blocked for the lake to form (Colton et al., 1961). In this case, drainage could have been under the ice like that of glacial Lake Missoula (Waitt, 1985; Table 7), or may have occurred in front of the ice sheet as soon as it receded.

Alternatively, W.C. Alden's map (1932) implies that the Missouri channel east of UL Bend was created during or after Lake Musselshell. Alden's field observations led him to place the local ice margin north of the modern Missouri channel. He attributed Lake Musselshell to an ice dam north of UL Bend that blocked the now-abandoned Sun Prairie channel of the Musselshell (Fig. 4). Based on Alden's ice margin, the Larb Hills were not glaciated when Lake Musselshell reached its maximum, so the lake would have overtopped the lowest pass in the Larb Hills and drained subaerially.

If ice extended farther south as proposed by Colton and others (1961), the lake water could have carved a subglacial or englacial channel through the Larb Hills. In order to have subglacial drainage, the hydrostatic pressure of the lake water would have lifted the ice sheet and decoupled it from its bed as happened repeatedly (≥40 times) in Lake Missoula (Waitt, 1985; Table 7). In order for the lake to drain englacially, the water would have carved an ice-marginal channel through the Larb Hills, similar to the channels carved in the foothills of the Highwood Mountains by the floodwaters of Lake Great Falls (Colton et al., 1961; Fullerton et al., 2004; Table 7).

The Cretaceous bedrock (Fig. 5) is easily eroded, so the incision from a single lake overflow would have probably been sufficient to establish a new course for the Missouri River. Upstream convergence of the lowest Musselshell River terraces (Fig. 13) implies a drop in base level since the last glaciation. This base level change could be the result of southward diversion of the Missouri River by the Late Wisconsin Laurentide ice sheet. Since Lake Musselshell seems to be a Late Wisconsin phenomenon, based on the surface exposure ages of ice-rafted boulders, the draining of Lake Musselshell – be it subglacial, englacial, or over a low bedrock pass – appears to be contemporaneous with, if not the cause of the river diversion.

Cat Creek Gravel

A thick deposit of gravel with giant cross-beds is located 0.5 km south of the hamlet of Cat Creek (Site K; Fig. 10). The deposit is 0.85 km long, 0.25 km wide, and is elongated in the direction of N10^{o}W (Fig. 26). The deposit stands out in relief on the landscape (Fig. 27a), and its crest is 890 m (2920 ft) above sea level. About 25 m of gravel is exposed in gravel pits, and gravel is still being mined from some pits (Fig. 27b).

The gravel occurs in continuous, planar cross-beds that are 0.2 to 1 m thick and dip at 20-30^o parallel to the long axis of the deposit (Fig. 28). Occasional intercalated sand beds are thinner (<0.2 m) and finely laminated (Fig. 28b). Strike and dip measurements taken in sand beds (Fig. 28b) ranged from N65-80^{o}W, 20^{o}SE. Individual cross-beds can be traced for more than 4 m in exposures, and the giant cross-beds probably exist over the entire length of the deposit.

Johnson and Smith (1964) mapped this deposit as Q_{tm6} (though it correlates better with Q_{tm5} based on its altitude and location relative to other terrace fragments; see the longitudinal profiles in Figs. 12-13). However, thickness and bedding characteristics imply that the process that deposited the gravel at Cat Creek is markedly different than the processes responsible for the terrace gravel. The terrace gravel in the study area is much thinner than that at Cat Creek: 1-7 m as opposed to $\geq$25 m. The beds of the terrace

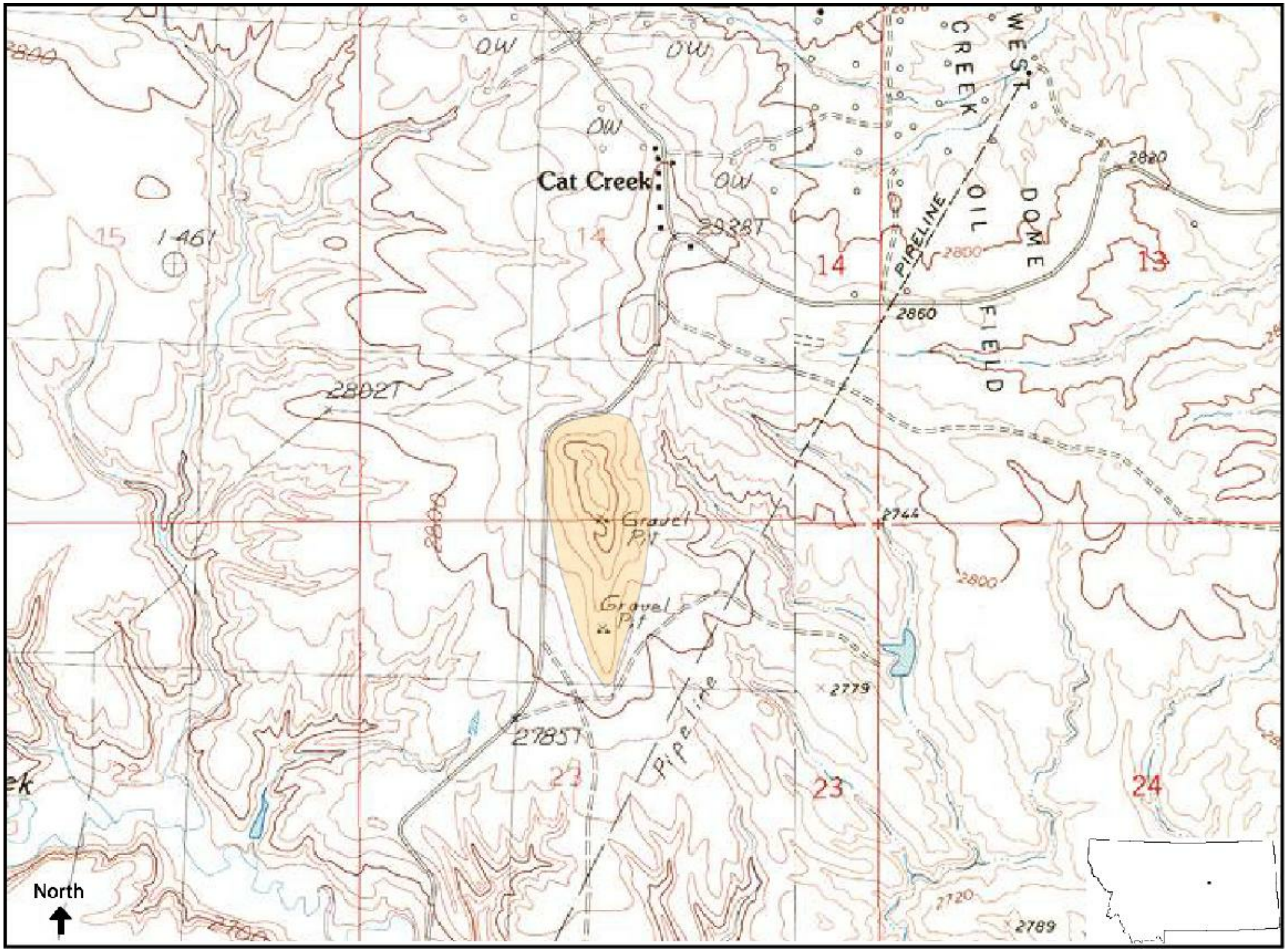

Figure 26. Topography of the Cat Creek gravel (shaded area). Scale is 1:24,000

Figure 27. Cat Creek gravel deposit: (a.) Looking northeast at the elongate Cat Creek gravel. Arrow points to the location where b. was taken. (b.) Operational gravel pit in the Cat Creek gravel (Site K). View is looking S/SE down the long axis of the deposit in which giant cross-beds also dip S/SE.

Figure 28. Cat Creek foreset beds: (a.) Recent exposure in a gravel pit. (b.) Close-up of the exposure in a. Strike and dips taken in the sand beds are S65-80^{o}W, 20^{o} SE.

deposits are flat-lying, while Cat Creek has steeply-dipping beds. No other deposits comparable in thickness and bedding character to the Cat Creek gravel have ever been reported in the basin.

The Cat Creek gravel is similar to the majority of the terrace gravel in terms of its rounding, sorting, and provenance. Like the terrace gravel, the gravel at Cat Creek is subrounded, imbricate, and primarily clast-supported, with a sandy matrix. The long axes of the gravel at Cat Creek are $\leq$12.5 cm, with an average length of 4.6 cm, similar to the size of the terrace gravel (Table 10). The Cat Creek gravel is from source areas in Montana, including the Judith, Snowy, Little Belt and northern Crazy Mountains, as well as local rock types (Appendix C, Tables 25-26). No gravel or boulders from the Canadian Shield were observed in or on the deposit, though some small boulders were found on its outer flanks. The possibility that the Cat Creek gravel is an ice-contact deposit, such as an esker, tunnel valley, or kame, was ruled out due to the absence of associated glacial boulders and cobbles.

The upper 0.5 m of the Cat Creek deposit is a cap of fine material with $\leq$20% gravel by volume. The cap has a thin A horizon and what, according to available field tests, is a B_k horizon. At least 25 m of gravel underlies the B_k horizon. The upper part of the gravel is considered a $2C_k$ horizon based on the abundant carbonate coats (<3 mm thick) on the bottom of the gravel. As with soils studied at Sites A-D and Y (Fig. 10; Table 11), the soil in the Cat Creek deposit has Stage I carbonate morphology. It has been shown that soil properties are not effective age indicators in the Musselshell basin, probably due to complex landscape evolution. Nonetheless, the lack of induration, and absence of carbonate coats thicker than 3 mm from the surface horizons down to 25 m depth in the Cat Creek gravel indicates that the gravel was probably not deposited during the Tertiary Period.

Such a narrow, voluminous deposit of well-sorted, apparently foreset-bedded gravel implies deposition by moving water confined by valley walls that suddenly lost competence. A logical inference, given the evidence for an ice-dammed lake in the valley, is that the Cat Creek gravel is part of a delta deposited at the margin of an intermediate lake stage. However, the valley walls that once held the hypothetical tributary that would have built this hypothetical delta are conspicuously absent. Also, no additional deltas or other lake-related deposits were identified at the same altitude (890 m). Hypotheses for the origin of the Cat Creek gravel are discussed further in Chapter 4.

Deep Coulee Deposit

A thick sequence of horizontally-laminated sediment is exposed in Deep Coulee (Figs. 29-31). The 0.42 km^2 deposit has a flat top and is incised approximately 11 m by the modern, intermittent stream (Fig. 29). The sediment can be traced for almost 2 km up Deep Coulee beginning near the Musselshell River. Johnson and Smith (1964) mapped this area as Cretaceous Bearpaw shale. The surface is lower, and therefore probably younger than remnants of terraces Q_{tm2-5} found nearby (Figs. 29 and 32; Johnson and Smith, 1964).

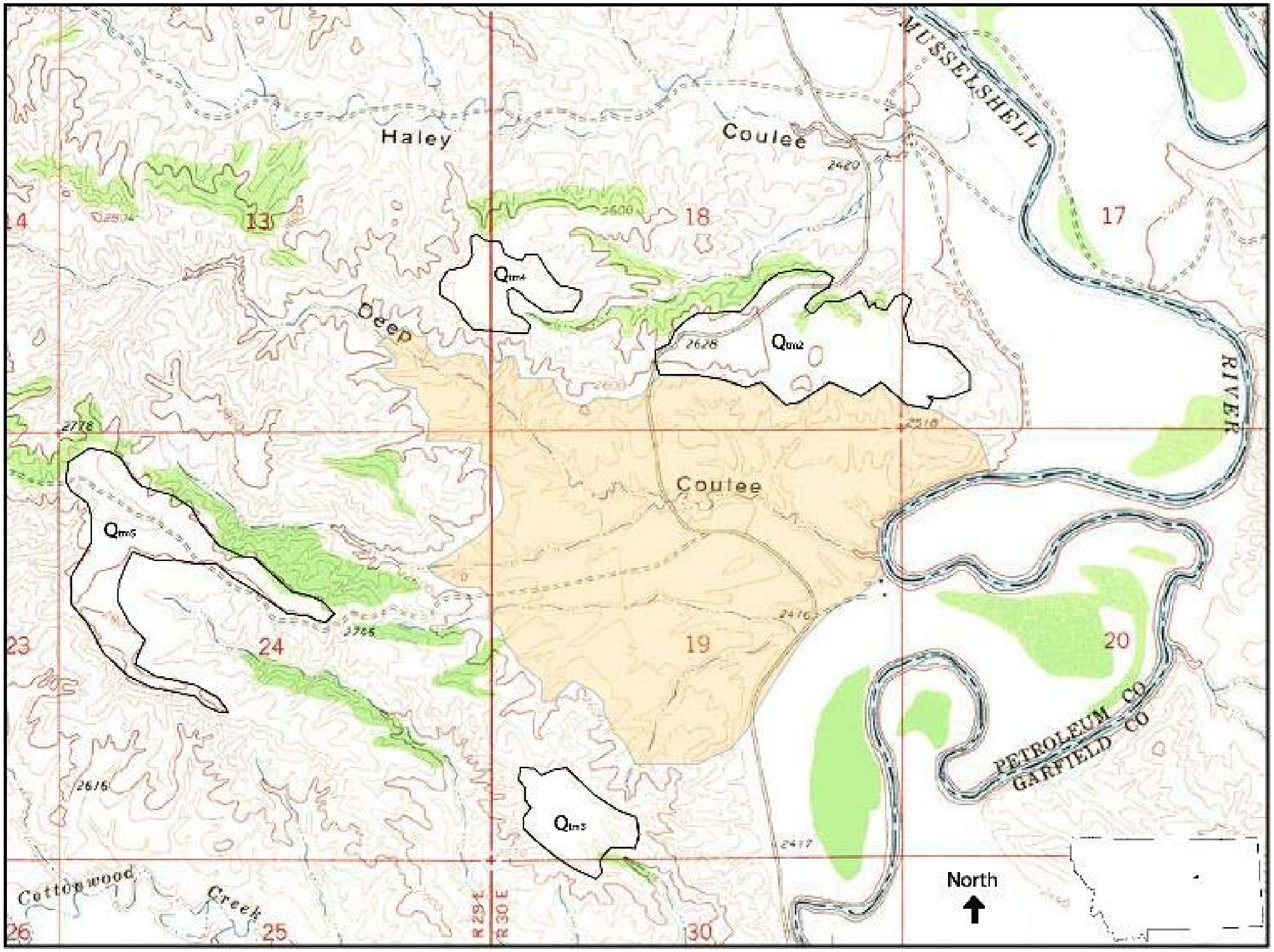

Figure 29. Topography of the Deep Coulee deposit and nearby Musselshell terraces. Scale is 1:24,000.

Figure 30. Laminated, fine-grained sediment exposed in the walls of Deep Coulee: (a.) The total thickness exposed is ~11 m. The cave, presumably formed by groundwater erosion, provided fresh exposures of the sediment. (b.) Close-up of finely-bedded sediment in the wall of the cave. Knife for scale.

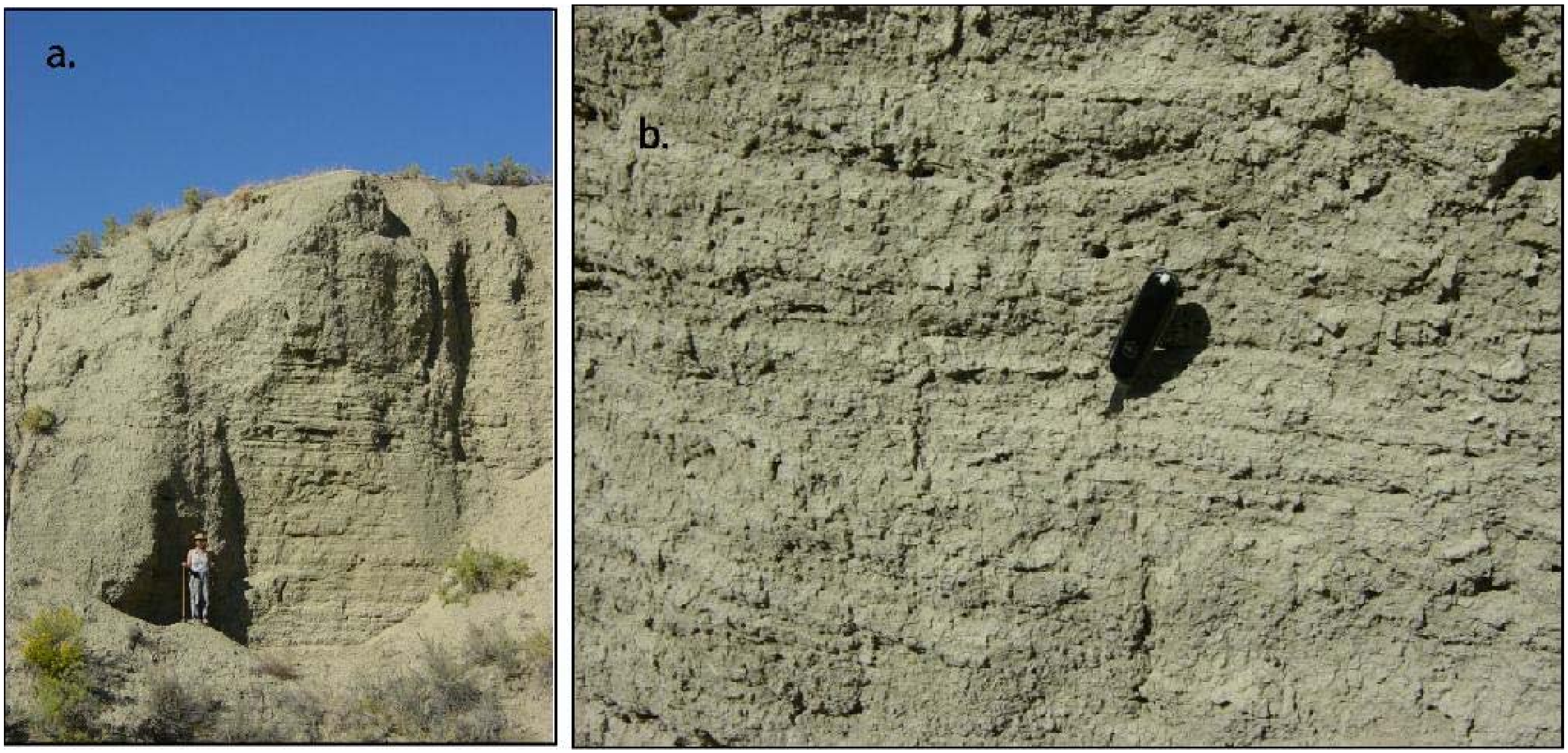

Figure 31. Rhythmites in Deep Coulee: (a.) Thick sequence of finely-bedded silt and sand. A continuous sheet of gravel is present at the bottom of this exposure. (b.) Close-up of the exposure in a. Knife for scale. Clays washed over the exposure from above gives the appearance that the deposit is composed largely of clay. Scraping of the exposure revealed that the beds are mostly silt and fine sand.

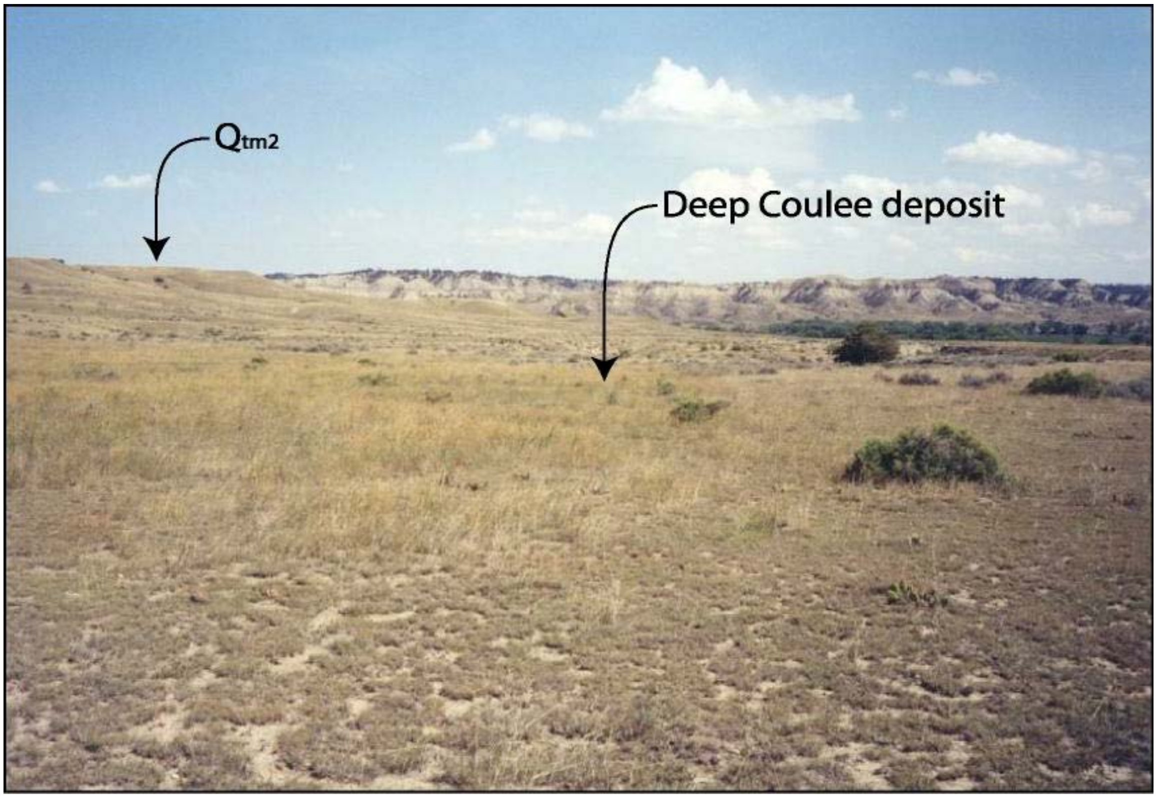

Figure 32. Flat top of the Deep Coulee deposit. Main coulee incision and exposures are off the picture to the right. The higher flat surface in the upper left of the photo is Q_{tm2}.

Most of the sediment exposed in Deep Coulee is rhythmically bedded fine silt and sand, but laterally continuous sheets of non-imbricated gravel are also present (Fig. 33). The gravel is mostly subrounded and of typical Musselshell River-type lithologies and sizes. Many clasts have carbonate coats on their tops and sides, indicating that they have been displaced from older deposits. Large (>20 cm) subangular slabs of locally-derived siltstone and sandstone were also observed. Recent erosion exposed fresh surfaces of the deposit. No major cut and fill features or buried soil horizons were recognized in the

Figure 33. Rhythmically-bedded fines and sheets of non-imbricated gravel in Deep Coulee: (a.) Silt and fine sand laminated in darker and lighter beds. (b.) Laminated fines underlain by a sheet of gravel. The author is pointing to the contact.

walls of Deep Coulee. All contacts appear conformable, with no significant intervening subaerial exposure. Ripple marks occur only on the centimeter scale. This deposit appears to have been formed entirely in standing water, rather than by fluvial processes.

An exotic boulder of Canadian Shield lithology 1 m tall and 1 m wide is exposed in the coulee wall (Fig. 34). The boulder is surrounded by sandy matrix-supported gravel. The lack of clay in the matrix is a sign that the boulder was not transported in a mudflow, as mudflows require cohesive sediment in order to generate high yield strength. The boulder may have been dropped by an iceberg, or rolled from a higher surface during the deposition of the sediment. However, deformation, as from the impact of a large ice-rafted dropstone, was not observed in the lower contact of the boulder with the underlying gravel, and the overlying gravel and sand, rather than being draped over the boulder, appears to have been deposited around the boulder.

Figure 34. Canadian Shield boulder exposed in the wall of Deep Coulee: (a.) Boulder (E108) is circled. (b.) Close-up view of the boulder. The surrounding sediment is gravel with a sand matrix. Tape measure is 0.3 m for scale.

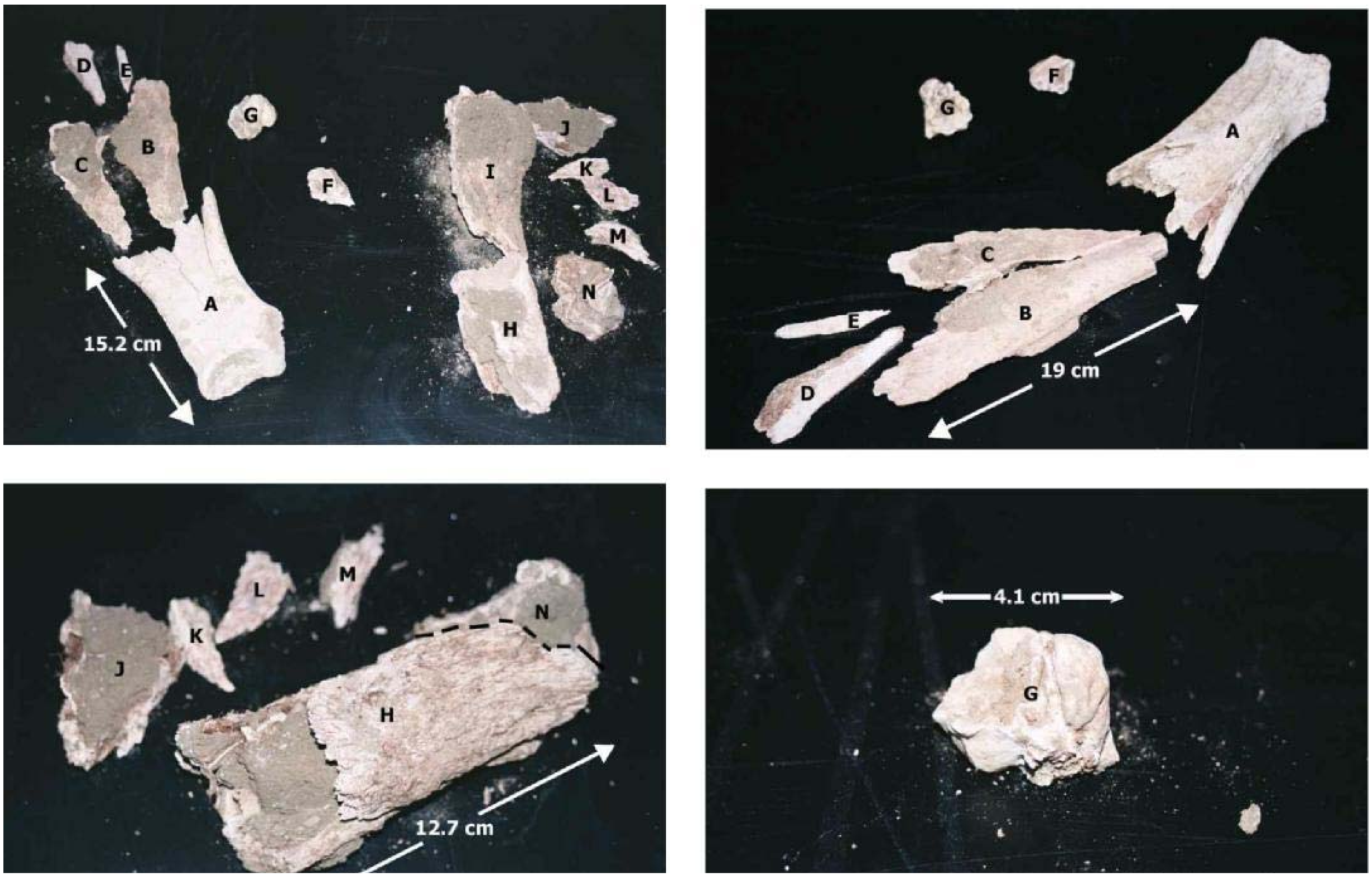

Figure 35. Photographs of bone samples A-N collected near the base of the exposure in Deep Coulee.

Two large, highly weathered exotic boulders (1.2x0.6x0.5 and 0.8x0.5x? m) were found in the coulee bottom. Six small (<0.3 m) and one large (0.45 m) Canadian Shield clasts were observed on the surface of the Deep Coulee sediments. The small clasts may have been in place, but the large boulder, which was unburied and next to a gravel road, displayed a carbonate coat on the side and scratch marks indicating that it had been moved by heavy machinery. Nonetheless, the presence of several erratics in and on the surface of the Deep Coulee sediment implies that this sediment was deposited during an interval when local ice-rafting was taking place. Other data from this study indicate a Late Wisconsin age for Lake Musselshell. Several pieces of mammal bone (Fig. 35) were found near the base of the outcrop, in one of the gravel sheets. A bone collagen age is in progress that will either support or contest a Late Wisconsin age for the Deep Coulee sediment.

Several other outcrops of a similar nature were observed nearby (Fig. 36; Table 14), but these were not as thoroughly described. In these cases, exposures were not as fresh or outcrops were not as well-exposed or extensive.

Figure 36. Twenty meters of laminated silt and fine sand with interbedded sheets of gravel. This face is exposed in the bluffs of the modern Musselshell River. See Table 14 for location. Note the person for scale.

TABLE 14. DESCRIPTION OF DEEP COULEE AND SIMILAR DEPOSITS.

Deposit	Location	Altitude	Notes
Deep Coulee	47° 08' 28" N 107° 58' 00" W	760 m (2494 ft)	11 m of laminated fine silt and sand with gravel sheets, exotic boulders and only minor cut and fill
Cottonwood Creek	47° 07' 12" N 107° 57' 28" W	732 m (2402 ft)	4.5 m of laminated fine sand with horizontal beds of tiny pebbles; deposits continue up valley
Musselshell	47° 02' 27" N 107° 55' 42" W	775 m (2543 ft)	20 m tall, 70 m wide and 30 m long; laminated grey silt and fine sand with bands of iron stain and interbedded gravels (subrounded, ≤12.5 cm and subangular, ≤45 cm)
River Rd.	47° 03' 15" N 107° 55' 56" W	762 m (2501 ft)	4.5 m of laminated silt and fine sand with two gravel beds
Long Coulee	47° 04' 00" N 107° 57' 30" W	791 m (2594 ft)	5 m of laminated silt and sand with 5-10 cm gravel beds (subrounded and subangular gravel, ≤30 cm); one subrounded exotic (15 cm long) buried 15 cm in deposit

Surface Exposure Ages of Musselshell Boulders

Five ^{21}Ne and 27 ^{10}Be surface exposure ages were calculated from the concentration of ^{21}Ne and ^{10}Be in the surface of ice-rafted boulders from the Musselshell basin. Theoretically, the concentration of these cosmogenic isotopes is directly related to the length of time that has elapsed since they were deposited by icebergs in glacial Lake Musselshell. However, only a select few of the ages actually serve to constrain the age(s) of the lake because of error from multiple sources (Table 8).

Cosmogenic ^{21}Neon Ages

Due to the limited number of samples that could be run at the USGS laboratory, only one boulder from each of the five altitude clusters was analyzed. The measured ^{21}Ne concentrations included both non-cosmogenic and cosmogenic components. Therefore, ages calculated from these data are greater than the exposure time of the boulder surfaces. The calculated ages ranged from 277 to 1036 ka and showed no correlation with altitude (Table 15). The ^{21}Ne results cannot be used to constrain the age(s) of Lake Musselshell.

^{10}Be analysis of the same five samples that were analyzed using ^{21}Ne resulted in ages that were not only one or two orders of magnitude younger, but also did not correlate chronologically with the ^{21}Ne ages (Table 16). This further supports the conclusion that the ^{21}Ne ages obtained are much greater than the actual surface exposure age and should be considered invalid.

Cosmogenic ^{10}Beryllium Ages

^{10}Be surface exposure ages were obtained on a total of 27 boulders, three from Cluster 1, four from Clusters 2 and 5, 11 from Cluster 3 and five from Cluster 4 (Fig. 21; Appendix G). The ages, once corrected for temporal variations in the geomagnetic field, ranged from 5.2$\pm$0.3 to 21.7$\pm$0.6 years (Table 17). The geomagnetically corrected ages will be used in the following discussion because these are considered the most reliable surface exposure ages possible, given the current understanding of past geomagnetic fluctuations. However, the ^{10}Be concentration and the non-geomagnetically corrected ages are also given

TABLE 15. RESULTS OF ^{21}NEON ANALYSIS OF FIVE BOULDER SURFACES.†

Sample, by altitude cluster	Mass (g)	$^{40}Ar/^{22}Ne$	$^{44}CO_2/^{22}Ne$	$^{20}Ne/^{22}Ne$, corrected	$^{21}Ne/^{22}Ne$, corr.	^{22}Ne (pcc/g)	Inclsn. ^{22}Ne (pcc/g)	$^{21}Ne_{ex}$ (pcc/g)	$^{22}Ne_{ex}$ (pcc/g)	$^{21}Ne_{ex}$ (at/g)	Prod. (at/g/y)	Age (ka)
1 E61 Grain	0.17285	10.043	1.622	10.043	0.0410	150.79	86.54	1.9618	-3.4207	$5.27*10^7$	97	543
E61 PDR	0.20181	9.680	2.797	9.680	0.0436	64.25		1.0024	0.8755	$2.70*10^7$	97	278
2 E54 Grain	0.15924	7.595	0.897	7.595	0.0597	293.82	167.87	9.3108	66.0018	$2.50*10^8$	102	2465
E54 PDR	0.19208	8.025	1.489	8.025	0.0591	125.95		3.9153	22.6952	$1.05*10^8$	102	1036
3 E33 Grain	0.15689	10.037	0.608	10.037	0.0463	266.23	158.43	4.8591	-5.9308	$1.31*10^8$	105	1241
E33 PDR	0.1930	10.323	1.345	10.323	0.0494	107.81		2.3016	-5.4927	$6.19*10^7$	105	588
4 E16 Grain	0.17527	9.551	1.871	9.551	0.0481	133.90	38.91	2.6969	3.5697	$7.25*10^7$	106	683
E16 PDR	0.21906	9.371	1.724	9.371	0.0475	94.99		1.8547	4.2507	$4.99*10^7$	106	469
5 E113 Grn	0.16347	10.386	1.432	10.386	0.0581	106.68	44.94	3.2056	-6.1082	$8.62*10^7$	109	794
E113 PDR	0.20901	11.300	1.892	11.300	0.0667	61.74		2.3901	-9.1772	$6.43*10^7$	109	592

†All results are for 30 minutes of fusion at 1600°C, blank sensitivity 3.14 fcc/cps, neon sensitivity 1.4E-19 mol/cps,.Ar^{++} 0.11158, CO_2^{++}=0.00955.

(Table 17), so that the ages could potentially be recalculated with improved geomagnetic data in the future.

TABLE 16. COMPARISON OF ^{21}NEON AND ^{10}BERYLLIUM AGES.

Cluster	Sample	^{21}Ne age (ka)	^{10}Be age (ka)
1	E61	278	7.6±0.4
2	E54	1036	9.6±0.5
3	E33	588	18.9±0.9
4	E16	469	19.7±0.8
5	E113	592	8.4±0.6

In general, boulders found at the lowest altitudes gave the youngest ages and the highest boulders gave the oldest ages, although there are numerous exceptions (Fig. 37). The ^{10}Be data, when plotted in the altitude clusters that were used for sampling purposes (Fig. 20) show, at most, two distinct groups of ages by altitude (Fig. 38). The boulders in Clusters 3-5 produced ages between 7.5 and 21.7 ka, while those in Clusters 1-2 are all $\leq$12.3 ka (Table 17). Because all of the ^{10}Be ages in Clusters 1-2 are viewed with caution because they have a moderate to high likelihood of prior burial, rolling, and surface-lowering (Table 18), the distinct age groups (Clusters 1-2 vs. Clusters 3-5) are most likely the result of erroneously low ages for all of the boulders sampled in the lowest two clusters. Therefore, the original hypothesis, that altitude clusters represented lake levels of distinct ages, is discarded. Multiple lakes may have existed, but apparently did not persist at a constant altitude for long enough to have an established iceberg grounding altitude.

TABLE 17. RESULTS OF ^{10}BE ANALYSIS OF 27 BOULDER SURFACES.

Cluster	Sample	^{10}Be (atoms/g)	Corrections		Exposure age (ka)	
			A†	B‡	Non-geomag. corr.§	Geomag. corr.#
1	E60	0.474±0.024	1.97	0.96	4.8±0.2	5.2±0.3
	E61	0.694±0.035	1.98	0.95	7.2±0.4	7.6±0.4
	E122	0.731±0.037	1.91	0.94	7.9±0.4	8.3±0.4
2	E54	0.955±0.048	2.07	0.98	9.2±0.5	9.6±0.5
	E45	0.972±0.049	2.08	0.95	9.5±0.5	10.0±0.5
	E62	1.186±0.059	2.08	0.95	11.7±0.6	12.3±0.6
	E32	0.751±0.038	2.07	0.97	7.3±0.4	7.7±0.4
3	E69	1.636±0.082	2.1	0.97	15.6±0.8	16.4±0.8
	E37	1.678±0.084	2.11	0.97	15.9±0.8	16.7±0.8
	E68	1.190±0.060	2.1	0.97	11.4±0.6	12.0±0.6
	E63	1.886±0.094	2.12	0.96	18.0±0.9	18.8±0.9
	E109	1.756±0.088	2.12	0.97	16.6±0.8	17.4±0.9
	E70	1.032±0.052	2.13	0.97	9.8±0.5	10.3±0.5
	E66	1.364±0.068	2.14	0.97	12.7±0.6	13.4±0.7
	E33	1.895±0.095	2.15	0.95	18.1±0.9	18.9±1.0
	E82	2.020±0.101	2.15	0.96	19.0±1.0	19.9±1.0
	E39	1.317±0.070	2.16	0.97	12.2±0.7	12.9±0.7
	E96	1.299±0.050	2.15	0.95	12.3±0.5	12.9±0.5
4	E28	1.805±0.053	2.16	0.97	16.8±0.5	17.6±0.5
	E100	0.756±0.050	2.16	0.95	7.1±0.5	7.5±0.5
	E101	1.609±0.069	2.16	0.97	15.0±0.6	15.8±0.7
	E16	2.015±0.077	2.17	0.96	18.8±0.7	19.7±0.8
	E102	1.174±0.049	2.17	0.96	11.0±0.5	11.6±0.5
5	E40	1.614±0.075	2.21	0.96	14.8±0.7	15.5±0.7
	E115	1.922±0.052	2.22	0.97	17.3±0.5	18.1±0.5
	E116	2.278±0.065	2.22	0.96	20.7±0.6	21.7±0.6
	E113	0.872±0.060	2.22	0.95	8.0±0.6	8.4±0.6

†A: Latitude/altitude correction (Stone, 2000).

‡B: Depth/topography correction (Nishiizumi et al., 1989; Brown et al., 1992).

§Using a SLHL production rate of 5.16 atoms/g/yr as discussed in Chapter 2.

#Corrected for variations of the magnetic field intensity and pole position (Nishiizumi et al., 1989; Ohno and Hamano, 1992; McEllhinny and Senanayake, 1982; Guyodo and Valet, 1999) using a SLHL production rate of 5.06 atoms/g/yr.

TABLE 18. QUALITATIVE ERROR ESTIMATES FOR ^{10}BE AGES.

Altitude Cluster	Sample	Likelihood of prior burial	Likelihood of prior rolling	Likelihood of surface lowering	^{10}Be age† (ka)	AMS error
1	E60	moderate	moderate	very low	5.2	±0.3
	E61	low	moderate	moderate	7.6	±0.4
	E122	moderate	high	low	8.3	±0.4
2	E54	moderate	moderate	low	9.6	±0.5
	E45	moderate	moderate	very low	10.0	±0.5
	E62	very low	moderate	moderate	12.3	±0.6
	E32	high	high	very low	7.7	±0.4
3	E69	low	high	moderate	16.4	±0.8
	E37	moderate	high	low	16.7	±0.8
	E68	low	high	very low	12.0	±0.6
	E63	**low**	**moderate**	**very low**	**18.8**	**±0.9**
	E109	**low**	**very low**	**low**	**17.4**	**±0.9**
	E70	**low**	**moderate**	**low**	**10.3**	**±0.5**
	E66	**low**	**very low**	**very low**	**13.4**	**±0.7**
	E33	**low**	**very low**	**low**	**18.9**	**±0.9**
	E82	**low**	**very low**	**low**	**19.9**	**±1.0**
	E39	low	high	low	12.9	±0.7
	E96	moderate	high	very low	12.9	±0.5
4	E28	high	low	moderate	17.6	±0.5
	E100	**low**	**low**	**moderate**	**7.5**	**±0.5**
	E101	low	high	low	15.8	±0.7
	E16	**low**	**low**	**low**	**19.7**	**±0.8**
	E102	high	low	low	11.6	±0.5
5	E40	low	high	moderate	15.5	±0.7
	E115	high	low	very low	18.1	±0.5
	E116	high	low	moderate	21.7	±0.6
	E113	moderate	high	moderate	8.4	±0.6

†Geomag. corr.; bold ages have lower ratings overall, as discussed in the text.

Many of the boulder ages are younger than any advance postulated for the Laurentide ice sheet in the United States (Bowen et al., 1986; Mickelson and Colgan, 2004). Evidence from eastern Alberta indicates that ice advancing from the north/northeast was gone from Montana by about 13 ka (Vreeken, 1989). Even if ice

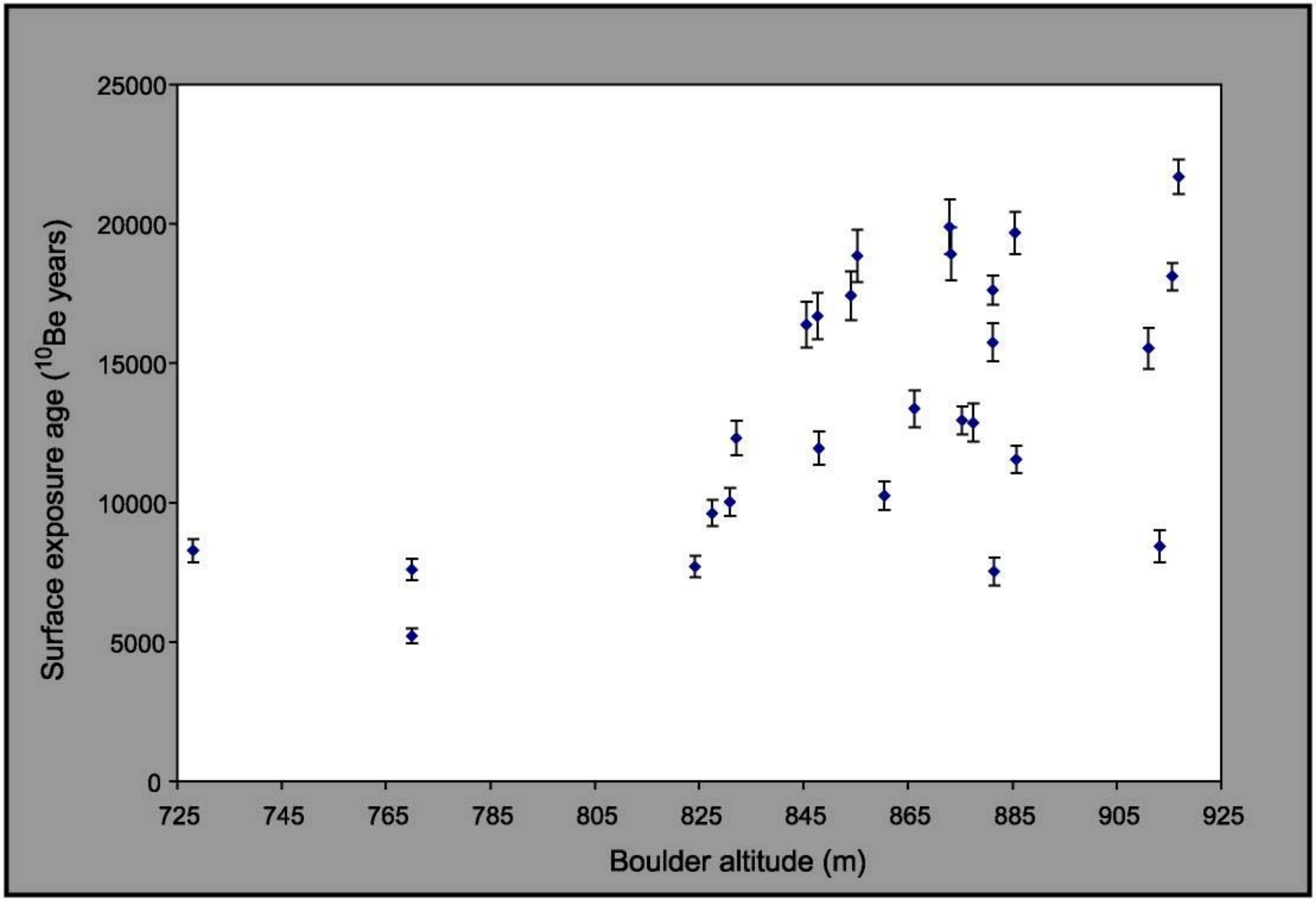

Figure 37. Geomagnetically corrected ^{10}Be data vs. boulder altitude. Error bars are for mass spec. error only.

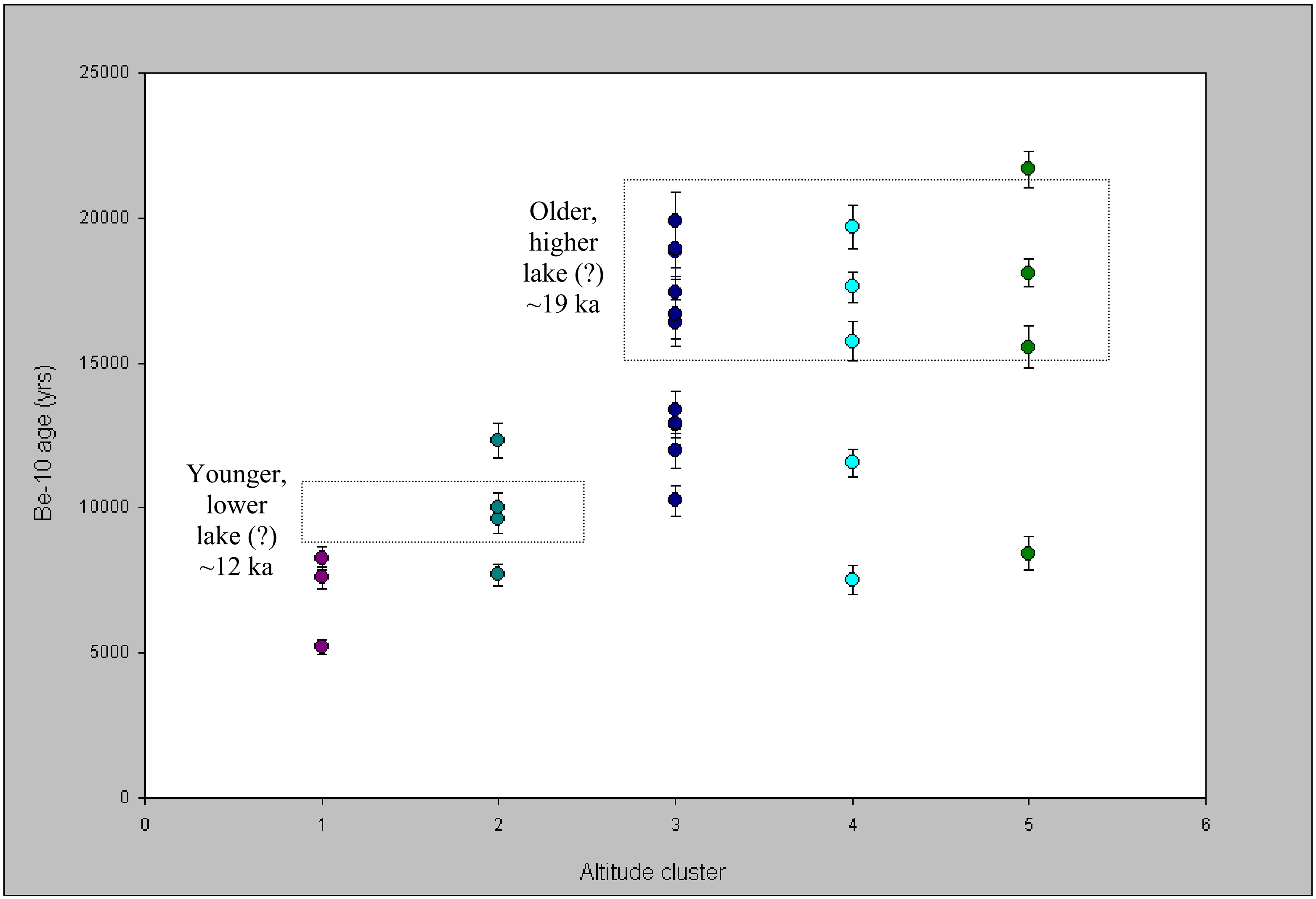

Figure 38. Geomagnetically corrected ^{10}Be ages by altitude cluster. Error bars are for AMS error only.

from western Alberta persisted somewhat longer, the Musselshell basin was most likely ice-free by at least 10 ka. Seven surface exposure ages are younger than 10 ka (Table 17), suggesting that they were affected by factors that would tend to decrease their age (Table 8).

The error given in Table 17 is only that associated with the function of the Accelerator Mass Spectrometer. Many additional error sources affect the ages (Table 8). Not including system-wide error sources discussed in Chapter 1, the error sources that are likely to have significantly affected the boulder ages in this study are irregular sample geometry, displacement, sediment shielding, erosion of the boulder surface, and inheritance from a previous exposure. All but the last of these would result in a surface exposure age that is younger than the age of Lake Musselshell (Table 8).

No correction or qualitative estimate was made to account for the irregular geometry of each sample. Masarik and Wieler (2003) show that irregular geometry may cause the ^{10}Be production rate to be underestimated by as much as 12%. There is no existing method to test for inheritance, but the oldest age, 21.7 ka, for E116, probably includes some inherited cosmogenic ^{10}Be because it exceeds the next oldest ages by >1.8 ka.

Displacement, shielding and surface-lowering were evaluated qualitatively and rated as described in Chapter 2. Approximately 55% of boulders found were on hillslopes or in gully bottoms (Fig. 39a-c) and 25% were found near a gravel or bladed two-track road. It is likely that only 20-30 of the boulders are in place – the remaining

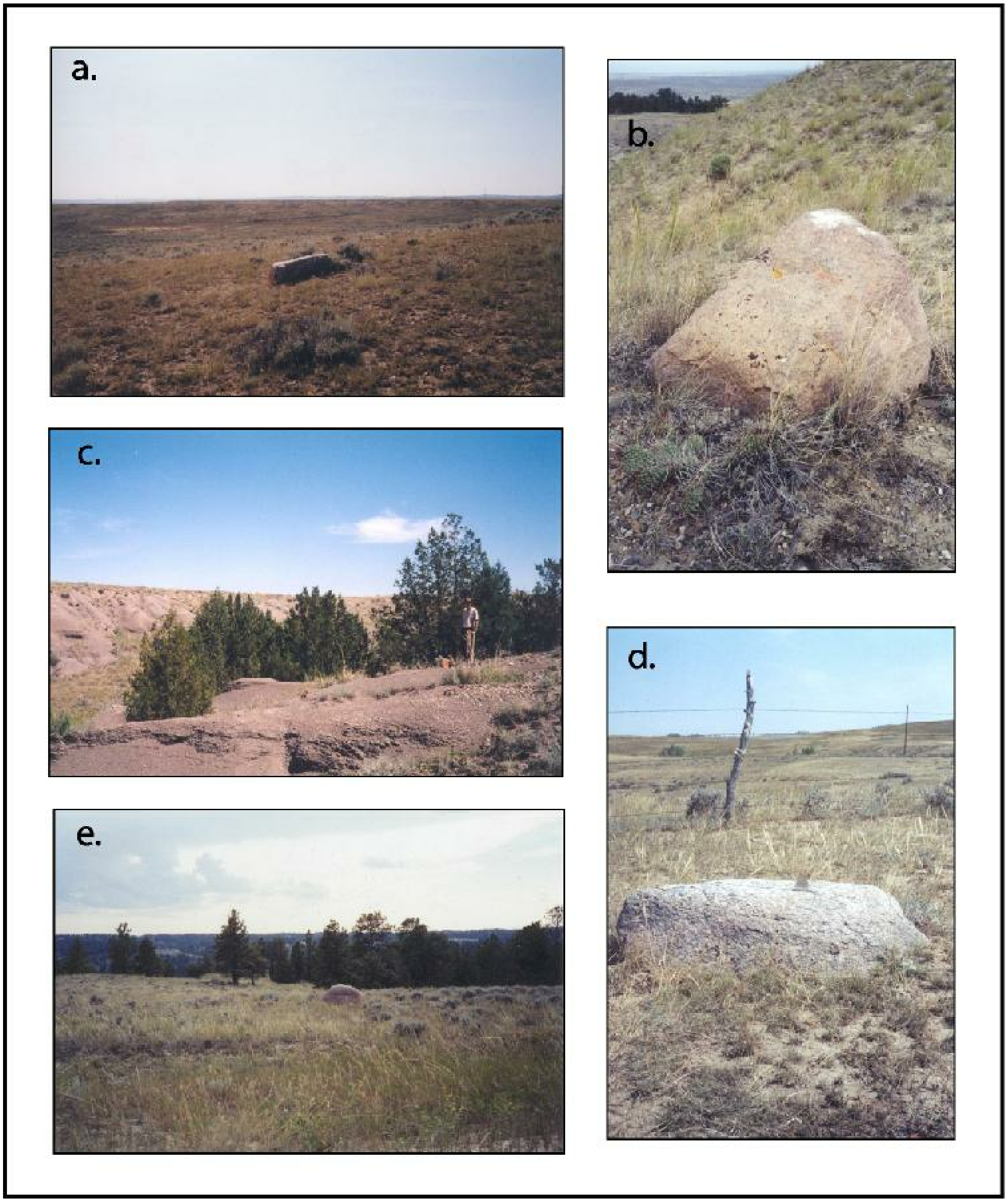

Figure 39. Landscape positions of ice-rafted boulders: (a.) E4 rests on a gentle hillslope. The gully bottom is visible in the upper left of the landscape. (b.) E40 is on a steep hillslope. (c.) E3 sits on bedrock in a gully wall. The boulder is to the left of the person, with a field notebook resting against it. They gully bottom is visible in the upper left of the landscape. (d.) E28 is partly buried, and its surface is low to the ground. (e.) E66 is large and on a relatively flat surface, making it a desirable candidate for sampling.

90-100 boulders were probably moved either by humans or by landscape erosion. Because many of the boulders have potentially moved or been moved since they were deposited, it was difficult to find samples suitable for surface exposure dating. In particular, surface exposure ages were obtained on many boulders that have a high likelihood of prior burial or rolling (Table 18). Samples were sometimes collected from boulders with high ratings because they had their original surfaces, were at key altitudes, or simply because they had the *least* undesirable surface available.

If all of the boulders that have one high or two moderate ratings are eliminated, the eight remaining exposure ages (in bold in Table 18) range from 7.5±0.5 to 19.9±1.0 ka. Five of these eight ages are fairly close (between 17.4±0.9 and 19.9±1.0 ka), with an average of ~19 ka. These can be used to constrain the age of Lake Musselshell. Two additional exposure ages (10.3±0.5 and 13.4±0.7 ka), with an average of ~12 ka, might have been deposited in a later stage of Lake Musselshell. E66, the boulder that produced a surface exposure age of ~13.4 ka, is the boulder with the lowest likelihood of prior burial, rolling or surface lowering of all 125 boulders observed in the Musselshell basin (Table 18). This lends additional credence to the idea of a lower lake around 11-14 ka. However, because there are only two reliable data points, the evidence for a lake around 12 ka is not as strong as that for the older (~19 ka) lake.

The young exposure age of 7.5±0.5 ka must not reflect the timing of deposition of boulder E100 in Lake Musselshell because the Laurentide ice sheet had receded completely from the United States by at least 10 ka (Bowen et al., 1986; Mickelson and Colgan, 2004). E100 must have been affected by one or more sources of uncertainty

(Table 8), though no evidence was found to indicate that the boulder had been buried, displaced or that its surface had eroded more than about 5 mm since it was deposited (Table 9; Table 18).

The fact that the five oldest of the remaining ages (Table 18) are fairly close (17.4$\pm$0.9 to19.9$\pm$1.0 ka) implies that these boulders do not carry a significant concentration of inherited ^{10}Be from a prior exposure. Though these are the most reliable surface exposure ages, they still must be considered minimum ages for Lake Musselshell. Some amount of post-depositional shielding, shifting of position, and/or surface-lowering has likely occurred for some or all of these samples. In addition, the samples collected were not infinitely flat, and the irregularity of the sample geometry, which can cause a surface exposure age to be younger than the actual exposure time (Masarik and Wieler, 2003), was not accounted for in any way. Viewed as minimum ages, the seven most reliable surface exposure ages record one, or possibly two episodes of ice-rafting in the Musselshell basin, around 18-21 and 11-14 ka (Fig. 38).

Summary

The Musselshell River terrace sequence consists of at least six high, unpaired gravel terraces (Q_{tm3-8}), two low, paired gravel terraces (Q_{tm2} and Q_{tm1}), and a very low (presumably Holocene) terrace of fine material. The three lowest gravel terraces (Q_{tm1-3}) converge upstream, while the gradients of the high terraces are parallel to the modern floodplain. The highest terraces (Q_{tm2-8}) have thin (~1-4 m) gravel deposits, while the lowest gravel terrace (Q_{tm1}) is nested inside Q_{tm2} and is potentially a valley fill. This terrace also contains a small amount of crystalline gravel from the Canadian Shield, while the others consist only of Montana-source gravel. A pilot study to test the usefulness of soil development as an age indicator in the Musselshell and tributary terrace sequences showed no conclusive trends.

Ice-rafted boulders located at and below 917 m provide an approximate elevation for the highstand of the lake, but additional physical evidence for Lake Musselshell remains elusive. Twenty-four meters of gravel with giant cross-beds near the town of Cat Creek and eleven meters of rhythmically-bedded silt and sand exposed in Deep Coulee may be related to the lake. However, no shorelines or varves were observed in the study area. Because proposed spillways to the southeast are higher than the highest ice-rafted debris, it is likely that Lake Musselshell drained out its northeast corner rather than southeast into the Yellowstone as proposed by previous workers (Alden, 1932; Colton, 1959).

Results of ^{21}Ne analysis were discounted because the non-cosmogenic ^{21}Ne was not removed. The only reliable ages for Lake Musselshell were from ^{10}Be analysis of glacial boulder surfaces. The twenty-seven ^{10}Be surface exposure ages were all between 5.2 and 21.7 ka, indicating that the Late Wisconsin (MIS 2) may have been the first time that ice-rafting occurred in the Musselshell basin. However, the exposure ages for many of the boulders are viewed with caution because of the potential for complex exposure histories or inheritance from a prior exposure. Young exposure ages are probably the result of rolling and, in some cases, temporary burial of many of the boulders after they were deposited in Lake Musselshell. Despite these issues, the fact that all of the ^{10}Be ages were below 21.7 ka is strong evidence that Lake Musselshell was a Late Wisconsin (MIS 2) phenomenon. No evidence was found for an older lake stage. Eight of the ^{10}Be ages may be more valid than the rest because these boulders did not appear to be greatly affected by displacement, prior burial or surface-erosion. These ages range from 7.5 to 19.9 ka.

DISCUSSION

In this chapter, the data collected during this investigation is discussed and compared with related work. From this discussion, conclusions are drawn about the extent and timing of glacial Lake Musselshell, the behavior of the southwestern Laurentide ice sheet, and Quaternary events on the Montana plains.

Extensive Late Wisconsin Ice Advance in Central Montana

Both the Musselshell River terraces and ice-rafted boulders of Lake Musselshell provided evidence that the Laurentide ice sheet extended into and/or dammed this valley during the Late Wisconsin. No evidence was found either in the terrace study or through surface exposure age dating of ice-rafted boulders for a pre-Late Wisconsin Lake Musselshell.

Age and Origin of Musselshell River Terrace Q_{tm1}

The lowest gravel terrace of the Musselshell, Q_{tm1}, appears to have formed under different circumstances than the older terraces Q_{tm2-8}. Of all of the terraces in the sequence, Q_{tm1} is the only one that is nested in the next older terrace. Q_{tm3-8} are unpaired, and each progressively younger terrace is located entirely to the east of the older terraces, indicating that the terraces were formed by lateral planation and concurrent, steady eastward downcutting punctuated by episodes of rapid downcutting (i.e. terrace abandonment). Additionally, the older terraces appear to be erosional rather than depositional valley fills (Mackin, 1937; Table 10). In contrast, the gravel of Q_{tm1} is thicker than that of the older terraces (Table 10) and displays the characteristics of a valley fill at Site H (Fig. 17). One theory for climatically-controlled alluvial terraces is that they are deposited during glacial conditions, when peak seasonal discharge and available bedload are high, and incised during the following interglaciation (Pierce and Scott, 1982; Reheis, 1984). The older Musselshell terraces may not have been entirely climate-driven. The steady eastward migration of the Musselshell River indicates that tectonic uplift in the Tertiary-age Judith and Snowy Mountains to the west may have played a role. However, it appears that the deposition of Q_{tm1} resulted mainly from the climate of the time.

Q_{tm1} is more deeply incised in the northern reach of the Musselshell, and there is evidence of a migrating knickpoint (Fig. 13). North of the knickpoint, >50 meters of incision has occurred. This amount of incision greatly exceeds the relief between any two of the older proposed terrace levels (Fig. 14). Post-glacial incision of Q_{tm1} by the Musselshell River was probably compounded by a drop in base level triggered by the southward diversion of and subsequent entrenchment by the Missouri River.

Finally, while exotic cobbles and boulders were observed on the surface of some of the higher terraces, Q_{tm1} (Sites M and H; Fig. 10) appears to be the only terrace that has Canadian Shield gravel incorporated in the deposit itself (Table 10). The incorporation of Shield clasts implies that the river was transporting reworked glacial debris for the first time during the deposition Q_{tm1}. Therefore, material transported by the

Laurentide ice sheet was initially deposited in the Musselshell basin prior to or during the deposition of Q_{tm1} but after the deposition of Q_{tm2}.

Because its deposition appears to be climatically driven, its abandonment may be related to the diversion of the Missouri River, and it contains exotic clasts, the age of Q_{tm1} is of particular interest. Unfortunately, the age of Q_{tm1} and the other terraces could not be determined by independent age controls. No ash or material suitable for radiocarbon analysis was found in association with the Musselshell River terraces during this study, and soil characteristics did not vary with age in a significant way (see Chapters 3-4). In other rivers in the western US, the lowest gravel terrace(s) were formed during the Late Wisconsin (Reheis, 1994; Chadwick et al., 1997). The height above drainage of the Late Wisconsin terraces in the northern Bighorn Basin (Reheis, 1984; Table 4) and the Wind River basin (Chadwick et al., 1997; Table 5) is ~6-15 m. This is comparable to the height of Q_{tm1} above the Musselshell River (12-17 m) in the stretch that is least incised by the modern Musselshell River (Table 2; Fig. 12). Therefore, Q_{tm1} is tentatively correlated with the Late Wisconsin stage (MIS 2), implying that the ice sheet was present in the Musselshell area during the Late Wisconsin.

<u>Upstream Convergence of the Musselshell River Terraces</u>

Significant knickpoint reduction is apparent in the gradient of the modern floodplain (Fig. 12-14). This incision was probably triggered when the Missouri River was diverted to the south of its former course in the Milk River valley and began to flow in its present channel (Fig. 4). As a result of the new, lower base level, the Musselshell

River terraces (at least Q_{tm1-3}) converge upstream and badlands have formed along the lowest 50 km stretch. Because Q_{tm1} converges upstream, alteration of the course of the Missouri River probably occurred during the Late Wisconsin stage. However, age control on the Musselshell River terraces is necessary to determine whether Q_{tm1} is in fact Late Wisconsin. In addition, more comprehensive longitudinal profiles, including locations and altitudes of terrace fragments north and south of the area covered by Johnson and Smith (1964; Fig. 2), would help to test the terrace correlations developed during this study (Fig. 13-14).

Surface Exposure Ages of Musselshell Boulders

Out of the twenty-seven ice-rafted boulders that were analyzed for cosmogenic ^{10}Be, only eight appeared to have a relatively low risk of prior burial, displacement or surface erosion (Table 18). The surface exposure ages of seven of these boulders (10.3±0.5 to19.9±1.0 ka) imply that Lake Musselshell existed around 18-21 ka (based on five exposure ages between 17.4±0.9 and 19.9±1.0 ka), and perhaps again around 11-14 ka, based on only two exposure ages (10.3±0.5 and 13.4±0.7 ka). The estimated ages for Lake Musselshell are considered minimum values.

A minimum age of 18-21 ka for Lake Musselshell is consistent with other ages presented for the maximum Late Wisconsin Laurentide ice sheet in the United States (Fig. 40a-c). According to the most widely cited interpretation, the Laurentide ice sheet reached its Late Wisconsin maximum in the United States between 21.5-22 ka B.P. (~25-

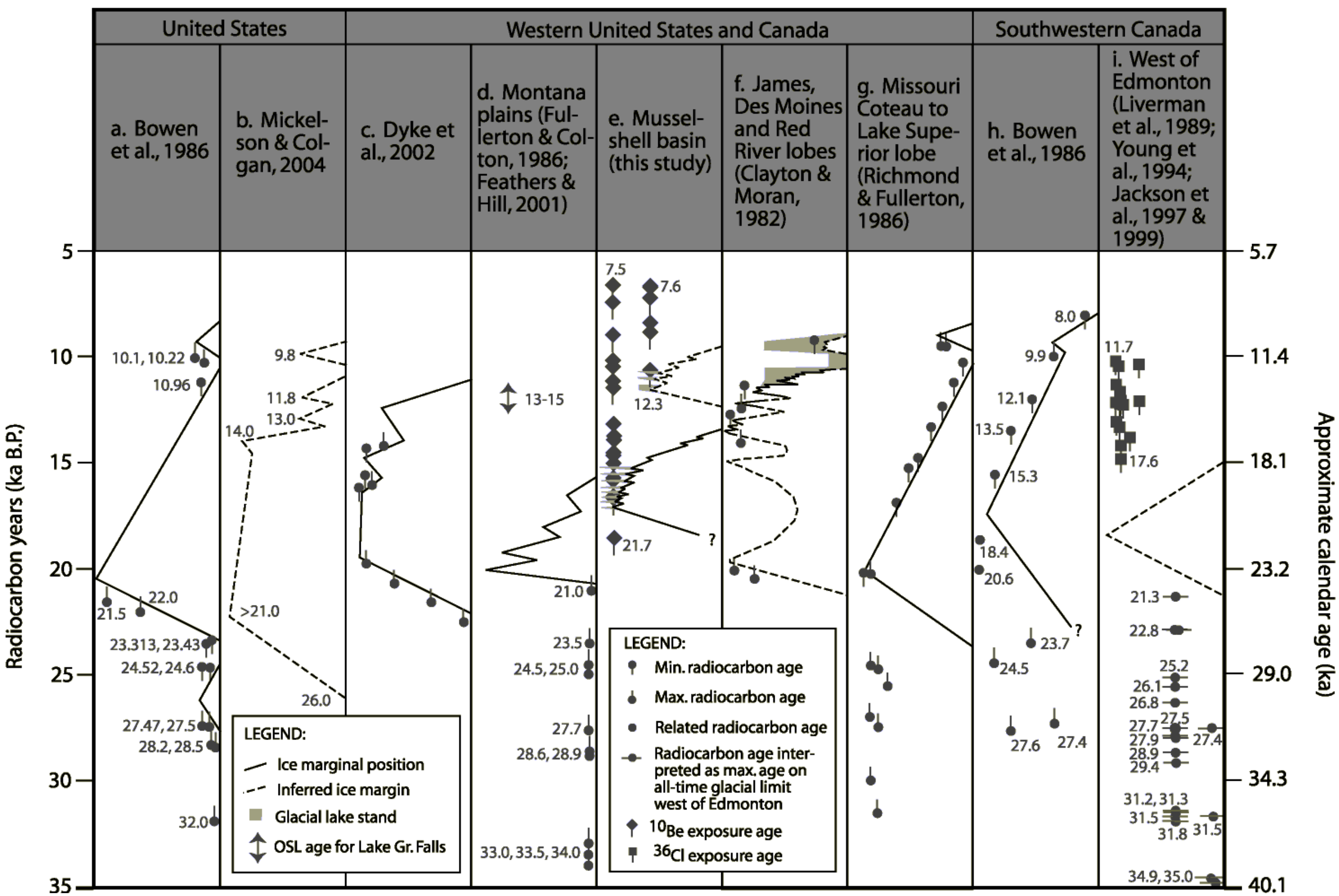

Figure 40. Time-distance diagrams for the southern margin of the Late Wisconsin Laurentide ice sheet. Discussed in text.

26 ka cal) and 10.96 ka B.P. (~13 ka cal; Richmond and Fullerton, 1986; Bowen et al., 1986; Fig. 40a). The western Laurentide ice sheet advanced prior to 21 ka B.P. (~24 ka cal) but reached its maximum late compared with the eastern ice sheet, at 14 ka B.P. (~17 ka cal; Mickelson and Colgan, 2004; Fig. 40b). Dyke and others (2002) ascertained from the radiocarbon database that the southwestern Laurentide ice sheet (from Montana/Alberta to Minnesota) reached its maximum around 19.5 ka B.P. (~ 23 ka cal) and remained there until 16.5 ka B.P. (~ 19 ka cal; Fig. 40c). Radiocarbon ages were calibrated using CALPAL (www.calpal-online.de) with an error of 0.1 ka.

On the Montana plains, Fullerton and Colton (1986) inferred a Late Wisconsin glacial maximum around 20 ka B.P. (~23 ka cal; Fig. 40d). All of the radiocarbon ages in Figure 41d are from neighboring states and provinces (Alberta, Saskatchewan and North Dakota) where tills have been correlated with those in Montana on the basis of their physical properties and weathering characteristics.

East of Montana, chronologies have been developed for the James, Des Moines and Red River lobes (North and South Dakota, Minnesota, and Iowa), including the stages of glacial Lake Agassiz (Clayton and Moran, 1982; Fig. 40f), and for the Missouri Coteau, James, Des Moines, Wadena, Rainy, and Lake Superior lobes (North and South Dakota to northwestern Wisconsin; Richmond and Fullerton, 1986; Hallberg and Kemmis, 1986; Matsch and Schneider, 1986; Fig. 40g). These are generally consistent with a Late Wisconsin glacial maximum around 18-21 ka or slightly before.

In southwestern Canada, (Fig. 40h), the generalized chronology of Bowen and others (1986; Fig. 40h) is consistent with data from this study. Maximum ages reported from Saskatchewan (~20 ka B.P.; ~23 ka cal), Manitoba (22.3 and 23.7 ka B.P.; ~26 and 28 ka cal), and southeastern Alberta (~24.5 ka B.P.; ~28 ka cal; Klassen, 1989) are older than the proposed age for Lake Musselshell (18-21 ka).

The complete absence of pre-Late Wisconsin ^{10}Be ages in a sample population of 27 suggests that glacial Lake Musselshell existed perhaps exclusively during the Late Wisconsin. A single, Late Wisconsin advance of the Laurentide ice sheet has been postulated for the area west of Edmonton, Alberta (Liverman et al., 1989; Young et al., 1994; Jackson et al., 1997; Jackson et al., 1999). The ice lobe investigated by these workers in southwestern Alberta is the same lobe that may have entered the Musselshell basin from the northwest (Fig. 7). Young and others (1994) concluded based on a set of radiocarbon ages (mostly from bones) that the only Laurentide ice sheet ever to reach southwestern Alberta arrived there after 21.3 ka B.P. (~25 ka cal; Fig. 40i). Jackson and others (1997, 1999) drew a similar conclusion based on ^{36}Cl surface exposure ages of boulders in till and the Foothills erratic train (Fig. 40i). The cosmogenic surface exposure ages are plotted as calendar ages (right axis) in Figure 40. The surface exposure ages provided a minimum age constraint of ~18 ka for the Late Wisconsin maximum of the Laurentide ice sheet in southwestern Alberta, and what Jackson and others (1997, 1999) consider to be the only ice sheet ever to have advanced into the area. D. Fullerton (oral comm., 2004) points out that pre-Late Wisconsin glaciations may have occurred in southwestern Alberta, but their deposits are probably buried.

A later Late Wisconsin stage for Lake Musselshell, postulated at approximately 11-14 ka, is consistent with the only other age for an ice-dammed lake on the Montana plains. Optically stimulated luminescence data (Feathers and Hill, 2001; Hill, 2001) from lake sediment in glacial Lake Great Falls (Fig. 1) implies damming of a lake in that basin around 13-15 ka (OSL data is plotted as calendar years in Fig. 40d). In addition, many workers show one or more readvances of the Laurentide ice sheet during late MIS 2 (Fig. 40a-c and f-h). Glacier Peak G tephra (11.2 ka B.P.; ~13 ka cal; Mehringer et al., 1984) was reported in deposits that immediately post-date what appears to be rapid deglaciation of southeastern Alberta (Vreeken, 1989). Thus, if the ice responsible for Lake Musselshell came from the north/northeast rather than the northwest (Fig. 7), the proposed late stage of Lake Musselshell must have existed prior to 13 ka.

The absence of shorelines, deltas and varved lake sediment in the Musselshell basin indicates multiple, short-lived lakes (Fig. 40e). However, the number of lake levels and the ice behavior shown on Figure 41e is illustrative only; the data is not detailed enough to resolve the number, duration or mechanism for the short-lived lake stands.

Multiple Short-Lived Stages of Lake Musselshell

The extent and surface exposure ages of ice-rafted debris indicate that one or more stages of Lake Musselshell existed at about 920 m during the Late Wisconsin. However, the former basin of Lake Musselshell lacks evidence for long-lived, stable lakes. The presence of slackwater deposits and the absence of shorelines, deltas, varved lake sediment, and iceberg grounding lines of distinct ages points to multiple, short-lived stages of Lake Musselshell that interacted with either a thin or surging ice sheet and with lakes to the west and east.

Absence of Common Lake-Related Features

The Musselshell basin lacks features that are common to many of the other ephemeral lakes that existed during the Late Wisconsin stage (Table 7). Many features, such as beaches, deltas, caves and wave-cut terraces, were eroded or deposited along the prominent shorelines of the relatively long-lived (1-3 ka) Lake Bonneville (Hamblin, 2003). Varved clay and silt has been identified in glacial Lake Great Falls (Smith, 1975). Even Lake Missoula, which existed for an average of only 30 years at a time, has well-preserved varves and wave-cut shorelines (Waitt, 1985).

During the Late Wisconsin, ample sediment of all sizes – from silt to large cobbles – would have been available to form varves and inflow deltas in Lake Musselshell. If a lake persisted long enough to form shorelines, varves, or deltas, these appear to have been removed or obscured by post-glacial processes. It seems more likely that the stage(s) of Lake Musselshell were extremely short-lived – perhaps only a few years long – so as not to build up seasonal varves, and that lake level constantly fluctuated, hindering the formation of distinct deltas, shorelines and iceberg grounding lines.

Presence of Slackwater Rhythmites

Instead of silt and clay couplets that are deposited seasonally in a typical glacial lake, thick sequences of rhythmically bedded silt and sand are exposed in the basin (Fig.

29-30). These rhythmites probably formed over the same span of time as Lake Musselshell, because exotic boulders are found both on top of and within the exposures in Deep Coulee. Two to three laterally continuous, horizontal sheets of gravel in a sandy matrix are interbedded with the rhythmites. The upper and lower contacts of the gravel with the rhythmites appear conformable (Fig. 33). All of the units seem to have been deposited in standing water with minimal to no intervening subaerial exposure. The rhythmic sediment and gravel sheets were probably laid down in temporary slackwater lakes, formed either by sudden drawdown of Lake Musselshell that occurred when the downstream ice dam failed or by hydraulically-controlled ponding of flood deposits from upstream.

In order to determine the timing of slackwater sedimentation in the Musselshell basin, collagen from the bone found in Deep Coulee (Fig. 35) will be dated using radiocarbon. Optically stimulated luminescence (OSL) ages from the Deep Coulee section would provide a second age control, and might indicate the length of time over which the sediment accumulated.

<u>Thin Ice Dam in the Larb Hills</u>

Historically, the western Laurentide ice sheet has been depicted as a thin equilibrium ice sheet with a low gradient and low basal shear stress (Mathews, 1974). If thin, slow-moving ice advanced across the Larb Hills and blocked the Missouri River to create Lake Musselshell, multiple lakes may have rapidly filled and drained subglacially, as happened in the Missoula basin (Waitt, 1985; Table 7). A thin ice dam would be particularly susceptible to hydraulic lifting by the rising lake water.

Glacial Surges and Catastrophic Drawdown of Lake Musselshell

If the southwestern Laurentide ice sheet was highly dynamic rather than in equilibrium as suggested above, it may have surged to its southernmost extent and/or readvanced rapidly multiple times during deglaciation (Fig. 40e). A series of short-lived or rapidly fluctuating lakes may have existed as a result of multiple surge events. Ice surges may have repeatedly advanced into the Musselshell watershed, dammed the lake and then stagnated and thinned rapidly. The thin, discontinuous ice would have floated relatively easily in the lake water, resulting in subglacial failure of the ice dam and a rapid drop in lake level. Sudden drawdown of the lake may have triggered current-generated sheetfloods that deposited the gravel and sand amidst the laminated silt and clay exposed in Deep Coulee.

Surge behavior has been inferred for Laurentide ice lobes in the central United States (Boulton and Clark, 1990; Mickelson and Colgan, 2004). The idea that the ice sheet also surged and then stagnated along its southwestern margin is well supported. There are very few well-developed or even identifiable end moraines on the Montana plains, indicating that the ice sheet did not tend to occupy the same ice-marginal position for an extended period of time. Much of the bedrock north of the study area is Cretaceous shale, which is particularly easy to deform. Given the low gradient of the land surface, the fine-grained bed material, and the absence of end moraines, it seems likely that the ice sheet did exhibit surge behavior in the Musselshell area.

Hydraulic Damming of Incoming Floods

Another mechanism that could have generated numerous, extremely short-lived lakes in the Musselshell basin is hydraulic damming of floodwaters released from upstream lakes. Rhythmites in exposures in Deep Coulee share some similarities with the Touchet beds rhythmites in the Pasco Basin. The Touchet beds were originally attributed to “Lake Lewis” (Table 7). However, the absence of other lake-related features that are commonly found in other ephemeral lakes (shorelines, inflow deltas and varves) spurred further investigation, which showed that no lake had existed in the Pasco Basin. Instead, the beds were attributed current flows, similar to turbidites, formed as a result of hydraulic damming of the floodwaters of glacial Lake Missoula. This water was backed up, but was draining continuously through a narrow constriction in the Columbia River (Wallula Gap).

The number of floods responsible for deposition of the Touchet beds is contended, but Waitt (1980) presented multiple avenues of evidence that each rhythmite is from a separate Lake Missoula jökulhlaup, and that brief periods of subaerial exposure occurred between deposition of each rhythmite. If this hypothesis is correct, each of forty rhythmites was probably laid down over the course of several hours. Thus, “Lake Lewis” was not really a lake, but an extremely short-lived slackwater environment that occurred multiple times in the same area. As shown by upstream paleocurrent indicators, the hydraulically-dammed water backflooded up basins upstream from Wallula Gap.

Nine or more wide, flat channels, some of which are now abandoned and perched in the foothills of the Highwood Mountains, were probably carved by ice-marginal release of jökulhlaups from glacial Lake Great Falls (Colton et al., 1961; Fullerton et al., 2004; Table 7). Incoming floods from glacial Lake Great Falls (and/or Lake Winifred, if it existed) would likely have entered the Musselshell basin through the spillways near Roy and traveled down what is now the channel of Box Elder Creek into the Musselshell and then the Missouri (Fig. 41). The large gravel deposits mapped as terraces of Musselshell tributaries from the west (Johnson and Smith, 1964; Table 3; Fig. 10) may be related to these hypothetical events. When the proposed floodwater reached the sag in the Larb Hills, its flow may have been constricted, forcing the water to backflood up the Musselshell, Missouri and their tributaries. Hydraulic damming could have only occurred if the narrow Larb Hills portion of the Missouri River channel was open. If this channel was blocked, the water would have simply added to the accumulation of a more long-lived Lake Musselshell that persisted for years rather than hours.

The Touchet beds are mostly fine sand to silt, rather than clay (Waitt, 1980), similar to the slackwater sediment in the Musselshell basin. However, the Touchet beds are thicker and do not include sheets of gravel like those found in the Musselshell basin. This may be because of the distance upstream of the Deep Coulee sediment from the Larb Hills constriction. Waitt (1980) notes that the thickness and grain size of the Touchet beds decreases upstream from Wallula Gap.

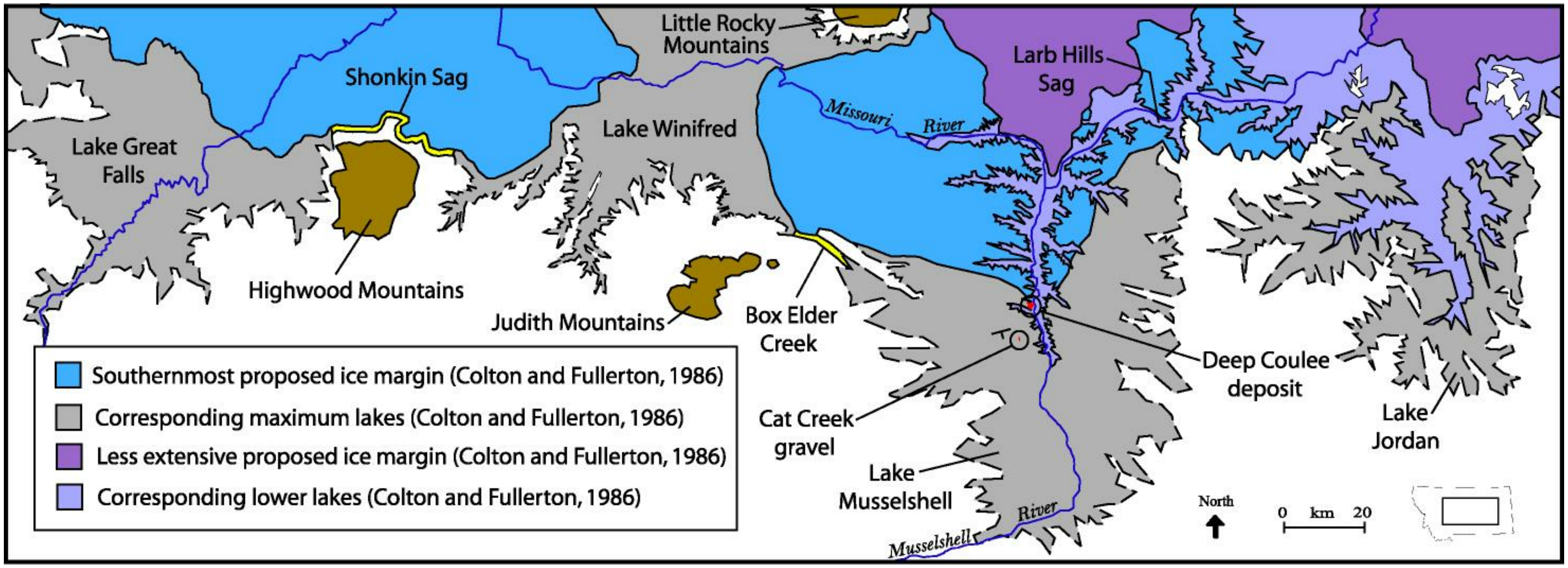

Figure 41. Potential interactions of glacial Lakes Great Falls, Winifred, Musselshell and Jordan. Deep Coulee and Cat Creek deposits shown for reference. The gravel at Cat Creek might have formed from floodwater entering through Box Elder Creek or by water backflooding up the Musselshell River. The strike and dip symbol shown is for Cat Creek (S 65-80° W, 20° SE). Additional field investigations are necessary to confirm the boundaries of the ice sheet and the other proglacial lakes shown in this diagram.

In addition to depositing slackwater sediment like that exposed in Deep Coulee, floods from Lakes Great Falls and Winifred may have rafted icebergs from these lake basins into the Musselshell. Ice-rafted boulders in the Pasco Basin ("Lake Lewis") were carried all the way from the western edge of Lake Missoula (Waitt, 1980). Since the volume of Lake Great Falls is approximately the same as that of the highstand of Lake Musselshell, the floods might initially have backfilled to the highest altitude reached by Lake Musselshell (~920 m).

If hydraulic damming occurred at the Larb Hills portion of the Missouri River channel, a delta such as the one downstream from Wallula Gap might be preserved downstream from the sag. Also, catastrophic floodwaters such as those from the draining of Lakes Missoula and Bonneville (Table 7) are capable of removing and locally redepositing sediment in giant ripple marks and other types of sub-fluvial bar forms. The 25 m of foreset-bedded gravel at Cat Creek is comparable in scale to cross-bedded sub-fluvial bar forms that were deposited during the backflooding of Lake Missoula and Lake Bonneville floodwater (Waitt, 1980). The foresets in the Cat Creek gravel dip south/southeast, indicating a paleocurrent opposite to the normal flow direction in the Musselshell River (Fig. 41). Therefore, this deposit could have been deposited by water flooding up the Musselshell River as a result of hydraulic damming.

<u>Interactions with Lake Jordan</u>

After the water of Lake Musselshell passed through the Larb Hills, it may have flowed down the modern Missouri channel without hindrance, or it may have been blocked by another ice dam on the eastern edge of the Lake Jordan basin. The elevation of erratic boulders in the Lake Jordan basin indicate that water in Lake Jordan was high enough to extend across the Larb Hills divide and create an upstream extension of Lake Jordan in the Musselshell basin (Colton and Fullerton, 1986). An understanding of the timing and extent(s) of Lake Jordan, as well as the other proglacial lakes on the Laurentide ice front in Montana, would augment the current study.

Potential Pre-Late Wisconsin Glaciation and Lake Damming

Boulders unearthed during the widening of Highway 19 south of Roy (Fig. 23) may be from an older glaciation (Fullerton and Colton, 1986; Fullerton et al., 2004; Fig. 8b), or from Late Wisconsin drainage of Lake Winifred or Lake Great Falls into Lake Musselshell (Colton and Fullerton, 1986). The boulders were not studied in enough detail to determine their age or mode of deposition. Whatever their origin, these boulders are a testament to the capability of the landscape to bury a large number of meter-size boulders without leaving any exposed.

Cat Creek Delta Remnant (?)

The 25 m thick Cat Creek gravel (Site K; Fig. 10) has consistent south/southeast-dipping cross-beds from one end of the deposit to the other (Fig. 28). It is difficult to interpret these steeply-dipping gravel beds as anything but foreset beds in a deposit of this thickness. The only Pleistocene event documented in the Musselshell basin that is capable of increasing base level enough to produce this volume of deltaic sediment is the rise of Lake Musselshell. However, a delta would normally be deposited as a valley fill in a channel, while this deposit now stands out in relief on the landscape (Fig. 26-27). Topographic inversion of this magnitude (>100 m) is unlikely to have occurred in just the last 20 ka. Therefore, the deposit might be a "delta remnant" from a pre-Late Wisconsin Lake Musselshell that was stable at 890 m. If so, the Cat Creek gravel would be the single piece of evidence for a lake of that age or at that altitude.

If the Cat Creek gravel is a delta remnant, other deltas (or delta remnants) at the same hypothetical lake level should also be preserved. Deposits of Q_{tm5}, which are at a similar altitude to Cat Creek (Fig. 13) were not exposed in gravel pits, and therefore their internal structure was not studied. Though it is likely that any known deposit of comparable thickness to the Cat Creek gravel would also be mined for gravel, it is possible that other flat-topped surfaces attributed to Q_{tm5} are actually deltaic in origin.

The Cat Creek gravel is located between Box Elder Creek, where water spilled into Lake Musselshell from higher glacial lakes, and the Larb Hills sag, where hydraulic damming may have caused backflooding into the Musselshell basin (Fig. 41). Therefore, the possibility that the Cat Creek deposit was formed in an unconfined channel during a flood cannot be ruled out. Thus, Cat Creek may have been deposited either

1. By Lake Great Falls or Winifred floodwaters.
    a. As a fan delta in Lake Musselshell.
    b. As a sub-fluvial bar form.
2. By a hydraulically-dammed backflood.
    a. As a sub-fluvial bar form.

The geographic position of the Cat Creek gravel and the dip direction of the foreset beds are compatible with any of these origins (Fig. 41).

It is quite likely that glacial meltwater flooded into the Musselshell basin during the Late Wisconsin. An MIS 2 stage has been demonstrated for Lake Great Falls (13-15 ka; Feathers and Hill, 2001; Hill et al., 2001) and catastrophic ice-marginal channels carved by Lake Great Falls outflow (Fullerton et al., 2004) indicate drainage down the Missouri River toward the Musselshell (Fig. 41). Additionally, evidence for a pre-Wisconsin flood event was not detected in the ^{10}Be surface exposure ages obtained for ice-rafted boulders in the Musselshell basin. It seems likely that incoming floods would have contributed at least a small percentage of the sample population. Previous workers have shown that the hydraulically-dammed flood deposits in the Pasco Basin ("Lake Lewis;" Table 7) include abundant meter-size boulders (Bjornstad et al., 2004). However, of the 27 boulders investigated in the Musselshell basin, none gave a surface exposure age older than 22 ka. Therefore, if the Cat Creek gravel is a flood deposit, it may be of Late Wisconsin age.

The Cat Creek gravel seems to be entirely from Montana sources (Appendix C, Table 27). The dip of the foresets implies that the water that deposited the Cat Creek gravel flowed from the north/northwest. If the Cat Creek gravel formed as a valley fill into a stable pre-Wisconsin stage of glacial Lake Musselshell, the gravel was probably deposited by a local-source (non-glacial) tributary flowing into the hypothetical lake from the north/northwest. The Judith Mountains are the most apparent choice (Fig. 41). However, shonkinite and quartzite and argillite from the Belt Supergroup were found in the delta, and these do not exist in the Judiths (Table 1). One possible source for the shonkinite and Belt clasts is a higher terrace of the Musselshell. Gravel from a higher Musselshell terrace (Q_{tm6-8}) may have been reworked by the tributary stream and deposited in the Cat Creek sediment. Alternatively, if the Cat Creek gravel is a flood deposit, the rock types in question could have been reworked locally or carried in with the floodwater, as both shonkinite and Belt Supergroup rocks are present upstream in the Missouri River watershed.

In conclusion, neither the boulders that were excavated from the roadbed along the Musselshell-Winifred divide, nor the Cat Creek gravel are necessarily pre-Late Wisconsin in age. Both could have been deposited either during the Late Wisconsin or during an older glaciation. No evidence was found aside from these two deposits for pre-Late Wisconsin glaciation of the Musselshell basin, though data from the river terraces, ice-rafted debris, and slackwater sediment indicate that Late Wisconsin glaciation did occur in the study area.

Summary

The Late Wisconsin (MIS 2) Laurentide ice sheet may have been the most extensive Late Pleistocene ice sheet that advanced into central Montana. Strong evidence was found only for Late Wisconsin glaciation at the southern edge of the ice margin in the Musselshell basin. Gravel from the Canadian Shield exists in the lowest (MIS 2?) gravel terrace of the Musselshell, but was not identified in the higher terraces. The seven most reliable ^{10}Be surface exposure ages of ice-rafted boulders indicate that the predominant, and probably the only stage(s) of Lake Musselshell existed during the Late Wisconsin, around 18-21 ka and possibly 11-14 ka. In addition, upstream convergence of Musselshell River terraces implies that the Missouri River may have first been displaced through the Larb Hills during the last glacial maximum.

Lake Musselshell rose as high as 917 m above sea level, but apparently did not persist at any one altitude for long enough to develop shorelines, deltas, varves or iceberg grounding lines. The Laurentide ice sheet consisted of multiple lobes that may have advanced asynchronously as rapid surges. Surging ice may have caused multiple lakes to fill and drain subglacially under stagnant ice. The drawdown from incomplete subglacial drainage of Lake Musselshell may have triggered currents that carried gravel sheetfloods out onto the remaining, very shallow lake.

Even after the Missouri River occupied its current channel through the Larb Hills east of UL Bend and the Larb Hills were ice-free, water may have ponded up in the Musselshell basin by a mechanism other than ice-damming. Although the Larb Hills were breached, the sag that formed might have greatly constricted the flow of any water entering the Musselshell basin catastrophically, from the draining of glacial lakes upstream. The water may have temporarily backflooded up the Musselshell River, creating a slackwater environment analogous to that in the Pasco Basin created by the floods of Lake Missoula ("Lake Lewis," Table 7; Waitt, 1980). Sheets of sand, silt and gravel exposed in Deep Coulee may be evidence for such hydraulic damming.

The possibility that pre-Late Wisconsin glaciation occurred in the Musselshell region cannot be wholly discounted. Deposits from older glaciations may be buried, eroded or difficult to discern in the modern landscape. Two deposits observed in the Musselshell basin during this study could be of Late Wisconsin or pre-Late Wisconsin age. The first is a deposit of glacial boulders, formerly buried 1-4 m deep, that were unearthed above 980 m in the upper reaches of Box Elder Creek. These could have been deposited by a pre-Late Wisconsin ice sheet or by either Late Wisconsin or pre-Late Wisconsin floodwaters from ice-dammed lakes upstream. Twenty-five meters of foreset-bedded gravel at Cat Creek may be a delta from an older stage of Lake Musselshell. A topographic inversion of >100 m is required for sediment deposited as a valley fill to become a local high point (Fig. 27). Because this amount of erosion is unlikely to have occurred over just the last 20 ka, this deposit is almost certainly not a Late Wisconsin-age delta. Alternatively, the Cat Creek gravel could be a fan delta or some type of sub-fluvial bar form similar to Lake Bonneville flood deposits (Waitt, 1985). If this is the case, the Cat Creek gravel could have been deposited during the Late Wisconsin by floodwaters from glacial lakes to the west that entered the Musselshell basin.

Conclusions

Glacial Lake Musselshell probably occurred as a series of short-lived lakes along the edge of the Late Wisconsin Laurentide ice sheet. One or more stages of the lake occurred between approximately 18 and 21 ka, and possibly also 11 to 14 ka. The stages of the lake were probably all below an altitude of about 920 m above sea level. However, the lack of well-developed shorelines, varves, and inflow deltas is an indication that the lake never persisted at the same elevation for very long. The multiple, brief stands of

Lake Musselshell could be the product of either a thin (equilibrium) or surging (disequilibrium) ice sheet or of hydraulic damming.

Drainage for Lake Musselshell was likely down the modern Missouri River channel, through a sag in the Larb Hills. The older (18-21 ka) lake(s) may have drained subglacially after decoupling a stagnant ice dam. Rapid subglacial drainage might have created a slackwater environment during which rhythmically bedded sheets of silt and sand and interbedded gravel sheets were deposited. However, some or all of the "lakes" may have been extremely short-lived slackwater environments formed when water from upstream glacial outburst floods was constricted passing through the Larb Hills. For hydraulic damming to occur, the Larb Hills channel would have had to be incised and ice-free prior to the outburst flood.

Upstream convergence of the Musselshell River terraces with the modern river gradient imply that the Missouri River may have only occupied its current channel south of the Milk River since the Late Wisconsin. This implies that the Late Wisconsin Laurentide ice sheet was the most extensive ice sheet north of the study area. Surface exposure ages of ice-rafted boulders and a glacial signal in only the lowest gravel terrace of the Musselshell (Q_{tm1}) are consistent with this idea. Though no conclusive evidence was found to support pre-Late Wisconsin glaciation in central Montana, older glaciations cannot be ruled out. High-altitude buried boulders and one potential valley fill delta may be from an older ice advance and/or stage of Lake Musselshell. However, these deposits are not necessarily pre-Late Wisconsin in age, and could both be related to Late Wisconsin jökulhlaups from glacial Lakes Great Falls and/or Winifred.

Events of considerable magnitude occurred in relatively rapid succession in the Musselshell basin during the last glacial maximum and the following interglacial stage. A surging and stagnating Laurentide ice sheet probably triggered the damming and release of multiple stages of Lake Musselshell over the course of a few thousand years. These may have interacted with other large lakes upstream and downstream through catastrophic outburst floods. Some of these lakes possibly lasted only a few years, or even a few days. When the ice was gone from the area, the Missouri River apparently began to entrench a new channel, triggering significant incision in the Musselshell River valley. Between the ice sheet, the ice-dammed lakes, and the rearrangement of drainage patterns, the plains and river valleys of central Montana have been shaped by an extraordinary sequence of geologic events over the last 20-25 ka.

REFERENCES CITED

Aguirre, E., and Pasani, G., 1984, Proposal of the ICS Working Group on the Pliocene/Pleistocene boundary concerning the definition of the Pliocene/Pleistocene boundary stratotype: Manuscript of the International Commission on Stratigraphy, 6 p.

Alden, W.C., 1932, Physiography and glacial geology of eastern Montana: US Geological Survey Professional Paper 174, 133 pages, 1 sheet.

Alt, D.D., and Hyndman, D.W., 1986, Roadside Geology of Montana: Missoula, Mountain Press Publishing Co., 429 p.

Andrews, J.T., 1975, Glacial Systems: An Approach to Glaciers and their Environments: North Scituate, Duxbury Press, 191 p.

Andrews, J.T., 1982, On the reconstruction of Pleistocene ice sheets: a review: Quaternary Science Reviews, v. 1, n. 1, p. 1-30.

Bachman, G.O. and Machette, M.N., 1977, Calcic soils and calcretes in the southwestern United States: US Geological Survey Open File Report 77-794, 163 p.

Baker, D.W. and Berg, R.B., eds., 1991, Guidebook to the central Montana alkalic province: geology, ore deposition and origin: Butte, Montana Bureau of Mines and Geology Special Publication 100, 201 p.

Bard, E., 1997, Nuclide production by cosmic rays during the last ice age: Science, v. 277, p. 532-533.

Benson, L., Madole, R., Phillips, W., Landis, G., Thomas, T., and Kubik, P., 2004, The probable importance of snow and sediment shielding on cosmogenic ages of north-central Colorado Pinedale and pre-Pinedale moraines: Quaternary Science Reviews, v. 23, p. 193-206.

Bergantino, R.N., 2001, oral communication, Montana Bureau of Mines and Geology, Butte, MT.

Bierman, P.R., Caffee, M.W., Davis, P.T., Marsella, K., Pavich, M., Colgan, P., Mickelson, D., and Larsen, J., 2002, Rates and timing of earth surface processes from *in situ*-produced cosmogenic Be-10, *in* Grew, E.S., ed., Beryllium: Mineralogy, Petrology and Geochemistry, Mineralogical Society of America and Geochemical Society of America, p. 147-205.

Bjornstad, B., Jennett, E., Gaston, J., and Kleinknecht, G., 2004, Erratic behavior on Rattlesnake Mountain, south-central Washington: The Pleistocene Post, Quarterly Newsletter of the Ice Age Floods Institute, New Series, v. 1, n. 1.

Booth, D.B., Troost, K.G., Clague, J.J., and Waitt, R.B., 2003, The Cordilleran ice sheet, *in* Gillespie, A.R. et al., eds., The Quaternary Period in the United States, Developments in Quaternary Science, v. 1: Amsterdam, Elsevier, p. 17-43.

Boulton, G.S., and Clark, C.D., 1990, A highly mobile Laurentide ice sheet revealed by satellite images of glacial lineations: Nature, v. 346, p. 813-817.

Bouyoucos, C.J., 1936, Directions for making mechanical analysis of soils by the Hydrometer Method: Soil Science, v. 42, n. 3.

Bowen, D.Q., Richmond, G.M., Fullerton, D.S., Sibrava, V., Fulton, R.J. and Velichko, A.A., 1986, Correlation of Quaternary Glaciations in the Northern Hemisphere: Quaternary Science Reviews, v. 5, p. 509-510, 1 plate.

Bradley, R.S., 1999, Paleoclimatology: Reconstructing climates of the Quaternary, second edition: San Diego, Academic Press, 613 p.

Brown, E.T., Brook, E.J., Raisbeck, G.M., Yiou, F., and Kurz, M.D., 1992, Effective attenuation lengths of cosmic rays producing ^{10}Be and ^{26}Al in quartz: Implications for exposure age dating: Geophysical Research Letters, v. 19, p. 369-372.

Buol, S.W., Hole, F.D., McCracken, R.J., and Southard, R.J., 1997, Soil Genesis and Classification, fourth edition: Ames, Iowa State University Press, 527 p.

Burns, J.A., and McGillivray, W.B., 1989, A new prairie dog, *Cynomys churcherii*, from the Late Pleistocene of southern Alberta: Canadian Journal of Zoology, v. 67, p. 2633-2639.

Busacca, A.J., Beget, J.E., Markewich, H.W., Muhs, D.R., Lancaster, N., and Sweeney, M.R., 2003, Eolian sediments, *in* Gillespie, A.R. et al., eds., The Quaternary Period in the United States: Amsterdam, Elsevier, p. 275-103.

Calhoun, F.H.H., 1906, The Montana Lobe of the Keewatin ice sheet: US Geological Survey Professional Paper 50, 62 p.

Cerling, T.E., and Craig, H., 1994, Geomorphology and *in situ* cosmogenic isotopes: Annual Review of Earth and Planetary Science Letters, v. 22, p. 273-317.

Chadwick, O.A., Hall, R.D., and Phillips, F.M., 1997, Chronology of Pleistocene glacial advances in the central Rocky Mountains: Geological Society of America Bulletin, v. 109, n. 11, p. 1443-1452.

Christiansen, E.A., 1968, Pleistocene stratigraphy of the Saskatoon area, Saskatchewan, Canada: Canadian Journal of Earth Sciences, v. 5, p. 1167-1173.

Cioppa, M.T., Karlstrom, E.T., Irving, E. and Barendregt, R.W., 1995, Paleomagnetism of tills and associated paleosols in southwestern Alberta and northern Montana: evidence for Late Pliocene-Early Pleistocene glaciations: Canadian Journal of Earth Sciences, v. 32, p. 555-564.

Clark, P.U., and Mix, A.C., 2001, Ice sheets and sea level of the Last Glacial Maximum: Quaternary Science Reviews, v. 21, p. 1-7.

Clark, P.U., Alley, R.A., and Pollard, D., 1999, Northern hemisphere ice-sheet influences on global climate change: Science, v. 286, p. 1104-1111.

Clark, P.U., Marshall, S.J., Clarke, G. K.C., Hostetler, S.W., Licciardi, J.M., and Teller, J.T., 2001, Freshwater forcing of abrupt climate change during the last glaciation: Science, v. 293, p. 283-287.

Clark, P.U., Clague, J.J., Curry, B.B., Dreimanis, A., Hicock, S.R., Miller, G.H., Berger, G.W., Eyles, N., Lamothe, M., Miller, B.B., Mott, R.J., Oldale, R.N., Stea, R.R., Szabo, J.P., Thorleifson, L.H., and Vincent, J.-S., 1993, Initiation and development of the Laurentide and Cordilleran ice sheets following the last interglaciation: Quaternary Science Reviews, v. 12, p. 79-114.

Clayton, L., and Moran, S.R., 1982, Chronology of Late Wisconsinan glaciation in middle North America: Quaternary Science Reviews, v. 1, n. 1, p. 55-82.

Colton, R.B., 1959, Additional evidence of glacial Lake Musselshell, MT: Geological Society of America Bulletin 70, 12, part 2, p. 1776.

Colton, R.B., 2001, written communication (map to accompany Colton and Fullerton, 1986 and notes from Colton, 1959 and Colton et al., 1961), US Geological Survey, Denver, CO.

Colton, R.B., and Fullerton, D.S., 1986, Proglacial lakes along the Laurentide ice sheet margin in Montana: Geological Society of America Abstracts with Programs, v. 18, n. 5, p. 347.

Colton, R.B., Lemke, R.W., and Lindvall, R.M., 1961, Glacial Map of Montana East of the Rocky Mountains: US Geological Survey Miscellaneous Investigations Series Map I-327, scale 1:500,000, 1 sheet.

Denton, G.H., and Hughes, T.J., eds., 1981, The Last Great Ice Sheets: New York, John Wiley and Sons, 484 p.

Dyke, A.S., Andrews, J.T., Clark, P.U., England, J.H., Miller, G.H., Shaw, J., and Veillette, J.J., 2002, The Laurentide and Innuitian ice sheets during the last glacial maximum: Quaternary Science Reviews, v. 21, p. 9-31.

Eberhardt, P., Eugster, O., and Marti, K., 1965, A redetermination of the isotopic composition of atmospheric neon: Z Naturforschung, v. 20a, p. 623-624.

Feathers, J.K., and Hill, C.L., 2001, Dating middle and late Wisconsin episode stratigraphic sequences in the Rockies and Missouri Plateau: luminescence and radiocarbon chronologies: Geological Society of America Abstracts with Programs, v. 33, n. 6, p. 287.

Finkel, R.C., April 2004, written communication, Lawrence Livermore National Laboratory, Center for Accelerator Mass Spectrometry, Livermore, CA.

Fullerton, D.S., 2004, oral communication, US Geological Survey, Denver, CO.

Fullerton, D.S. and Colton, R.B., 1986, Stratigraphy and correlation of the glacial deposits on the Montana plains: Quaternary Science Reviews, v. 5, p. 69-82, 1 plate.

Fullerton D.S., Colton, R.B., Bush, C.A., and Straub, A.W., 2004, Spatial and temporal relations of continental and mountain glaciations on the Northern Plains in Montana and North Dakota: U.S. Geological Survey Miscellaneous Investigations Series Map I-XXX with accompanying text, scale 1:1,000,000, 1 sheet.

Fulton, R.J., ed., 1989, Quaternary geology of Canada and Greenland, Geology of Canada, n. 1, Geological Survey of Canada (also Geological Society of America, The Geology of North America, v. K-1), 839 p.

Gile, L.H., Peterson, F.F., and Grossman, R.B., 1966, Morphological and genetic sequences of carbonate accumulation in desert soils: Soil Science, v. 101, n. 5, p. 347-360.

Glasgow, G.D.E., Wheatley, A.D., Bartlein, P.J., Anderson K.H., Anderson P.M., Edwards, M.E., Mock, C.J., Thompson, R.S., Webb, R.S., Webb III, T., and Whitlock, C., 1998, Paleoclimate simulations for North America over the past 21,000 years: process analysis of local climatic change: Quaternary Science Reviews, v. 17, n. 6, p. 549-585.

Goddard, E.N., 1988, Geologic Map of the Judith Mountains: US Geological Survey Miscellaneous I-Series Map, I-1729, scale 1:31,680, 1 sheet.

Gosse, J.C., and Phillips, F.M., 2001, Terrestrial *in situ* cosmogenic nuclides: theory and application: Quaternary Science Reviews, v. 20, p. 1475-1560.

Gosse, J.C., Evenson, E.B., Klein, J., and Sorenson, C., 2003, Cosmogenic nuclide glacial geochronology in the Wind River Range, Wyoming, *in* Easterbrook, D.J., ed., Quaternary Geology of the United States: Reno, International Quaternary Association, XVI INQUA Congress, INQUA 2003 Field Guide Volume, p. 49-56.

Gosse, J.C., Klein, J., Evenson, E.B., Lawn, B., and Middleton, R., 1995, Beryllium-10 dating of the duration and retreat of the last Pinedale glacial sequence: Science, v. 268, p. 1329-1333.

Graf, T., Kohl, C.P., Marti, K., and Nishiizumi, K., 1991, Cosmic-ray produced neon in Antarctic rocks: Geophysical Research Letters, v. 18, n. 2, p. 203-206.

Guyodo, Y., and Valet, J.P., 1999, Global changes in intensity of the Earth's magnetic field during the past 800 kyr: Nature, v. 399, p. 249-252.

Hallberg G.R., and Kemmis, T.J., 1986, Stratigraphy and correlation of the glacial deposits of the Des Moines and James Lobes and adjacent areas in North Dakota, South Dakota, Minnesota and Iowa: Quaternary Science Reviews, v. 5, p. 65-68, 1 plate.

Hamblin, K., 2003, Geology of Western Utah *in* Easterbrook, D.J., ed., Quaternary Geology of the United States: Reno, International Quaternary Association, XVI INQUA Congress, INQUA 2003 Field Guide Volume, p. 56-58.

Harden, J.W., 1982, A quantitative index of soil development from field descriptions: examples from a chronosequence in central California: Geoderma, v. 28, p. 1-28.

Harden, J.W., and Taylor, E.M., 1983, A quantitative comparison of soil development in four climatic regimes: Quaternary Research, v. 20, p. 342-359.

Harlan, S.S., 1986, Timing of deformation along the leading edge of the Montana Disturbed Belt, northern Crazy Mountains Basin, Montana [Master's thesis]: Bozeman, Montana State University, 87 p.

Hetzel, R., Niedermann, S., Ivy-Ochs, S., Kubik, P.W., Tao, M., and Gao, B., 2002, ^{21}Ne versus ^{10}Be and ^{26}Al exposure ages of fluvial terraces: the influence of crustal Ne in quartz: Earth and Planetary Science Letters, v. 201, p. 525-591.

Hill, C.L., 2001, Pleistocene mammals of Montana and their geologic context, *in* Hill, C.L., ed., Society of Vertebrate Paleontology 61st Annual Meeting Guidebook for the

Field Trips, Mesozoic and Cenozoic Paleontology in the Western Plains and Rocky Mountains: Bozeman, Museum of the Rockies Occasional Paper No. 3, p. 127-144.

Hopkins, D.M., 1975, Time-stratigraphic nomenclature for the Holocene epoch: Geology, v. 3, p. 10.

Izett, G.A., Pierce, K.L., Naeser, N.D., and Jaworowski, J., 1992, Isotopic dating of Lava Creek B tephra in terrace deposits along the Wind River, Wyoming: Implications for post 0.6 Ma uplift of the Yellowstone hotspot: Geological Society of America Abstracts with Programs, v. 24, n. 7, p. 102.

Jackson, L.E., 1980, Glacial history of the Alberta portion of the Kananaskis Lakes map area: Canadian Journal of Earth Sciences, v. 17, p. 459-477.

Jackson, L.E., and Phillips, F.M., 2003, Cosmogenic ^{36}Cl dating of the all time limit of glaciation, Del Bonita upland, Alberta/Montana border and insights into changing extents and ice-flow patterns in successive continental ice sheets: Eos. Trans. American Geophysical Union, Fall Meeting Supplement, v. 84, n. 46, Poster H42C-1086.

Jackson, L.E., Phillips, F.M., and Little, E.C., 1999, Cosmogenic ^{36}Cl dating of the maximum limit of the Laurentide ice sheet in southwestern Alberta: Canadian Journal of Earth Sciences, v. 36, p. 1347-1356.

Jackson, L.E., Phillips, F.M., Shimamura, K., and Little, E.C., 1997, Cosmogenic ^{36}Cl dating of the Foothills erratics train, Alberta, Canada: Geology, v. 25, n. 3, p. 195-198.

Jackson, L.E., Jr., Rutter, N.W., Hughes, O.L., and Clague, J.J., 1989, Glaciated fringe, *in* Fulton, R.J., ed., Quaternary geology of Canada and Greenland, Geology of Canada, n. 1, Geological Survey of Canada (also Geological Society of America, The Geology of North America, v. K-1), p. 63-68.

Jenny, H., 1941, Factors of Soil Formation: New York, McGraw-Hill, 281 p.

Johnson, W.D., and Smith, H.R., 1953-1956, unpublished field notes with accompanying aerial photographs: Denver, US Geological Survey Field Records Library NO-7417, 152 p.

Johnson, W.D., and Smith, H.R., 1964, Geology of the Winnett-Mosby area, Petroleum, Garfield, Rosebud, and Fergus Counties, Montana: US Geological Survey Bulletin 1149, 91 pages.

Karlstrom, E.T., 1999, Evidence for coalescence of Laurentide and Rocky Mountain glaciers east of Glacier National Park, Montana: Physical Geography, v. 20, n. 3, p. 225-239.

Karlstrom, E.T., 2000, Fabric and orientation of multiple diamictons within the pre-Illinoian Kennedy Drift east of Waterton-Glacier International Peace Park, Alberta, Canada, and Montana, USA: Geological Society of America Bulletin, v. 112, n. 10, p. 1496-1506.

Kaufman, D.S., Porter, S.C., and Gillespie, A.R., 2003, Quaternary alpine glaciation in Alaska, the Pacific northwest, Sierra Nevada, and Hawaii, *in* Gillespie, A.R. et al., eds., The Quaternary Period in the United States, Developments in Quaternary Science, v. 1: Amsterdam, Elsevier, p. 77-103.

Klassen, R.W., 1989, Quaternary geology of the southern Canadian Interior Plains, *in* Fulton, R.J., ed., Quaternary Geology of Canada and Greenland: Geological Survey of Canada, p. 138-173.

Kohl, C.P., and Nishiizumi, K., 1992, Chemical isolation of quartz for measurement of in situ-produced cosmogenic nuclides: Geochimica et Cosmochimica Acta, v. 56, p. 3583-3587.

Kutzbach, J.E., and Wright, H.E., 1985, Simulation of the climate of 18,000 years BP: Results for the North American North Atlantic European sector and comparison with the geologic record of North America: Quaternary Science Reviews, v. 4, p. 147-187.

Lal, D., 1991, Cosmic ray labeling of erosion surfaces: *in situ* nuclide production rates and erosion models: Earth and Planetary Science Letters, v. 104, p. 424-439.

Licciardi, J.M., Clark, P.U., Brook, E.J., Pierce, K.L., Kurz, M.D., Elmore, D., and Sharma, P., 2001, Cosmogenic ^{3}He and ^{10}Be chronologies of the late Pinedale northern Yellowstone ice cap, Montana, USA: Geology, v. 29, n. 12, p. 1095-1098.

Little, E.C., Jackson, L.E., James, T.S., Hicock, S.R., and Leboe, E.R., 2001, Continental/Cordilleran ice interactions: a dominant cause of westward super-elevation of the last glacial maximum continental ice limit in southwestern Alberta, Canada: Boreas, v. 30, p. 43-52.

Liverman, D.G.E., Catto, N.R., and Rutter, N.W., 1989, Laurentide glaciation in west-central Alberta: a single (Late Wisconsinan) event: Canadian Journal of Earth Sciences, v. 26, p. 266-274.

Machette, M.N., 1985, Calcic soils of the southwestern United States, *in* Weide, D.L., ed., Soils and Quaternary Geology of the Southwestern United States: Geological Society of America Special Paper 203, p. 1-21.

Mackin, J.H., 1937, Erosional history of the Big Horn Basin, Wyoming: Geological Society of America Bulletin, v. 48, p. 813-893.

Masarik, J., and Wieler, R., 2003, Production rates of cosmogenic nuclides in boulders: Earth and Planetary Science Letters, v. 216, p. 201-208.

Masarik, J., Kollar, D., and Vanya, S., 2000, Numerical simulation of *in situ* production of cosmogenic nuclides: Effects of irradiation geometry: Nuclear Instruments and Methods in Physics Research B, v. 172, p. 786-789.

Mathews, W.H., 1974, Surface profiles of the Laurentide ice sheet in its marginal areas: Journal of Glaciology, v. 13, p. 37-43.

McElhinny, M.W., and Senanayake, W.E., 1982, Variations in the geomagnetic dipole 1: The past 50,000 years: Journal of Geomagnetism and Geoelectricity, v. 34, n. 1, p. 39-51.

Mehringer, P.J., Sheppard, J.C., and Foit, F.F., 1984, The age of the Glacier Peak tephra in west-central Montana: Quaternary Research, v. 21, p. 36-41.

Mickelson, D.M., and Colgan, P.M., 2003, The southern Laurentide ice sheet, *in* Gillespie, A.R. et al., eds., The Quaternary Period in the United States, Developments in Quaternary Science, v. 1: Amsterdam, Elsevier, p. 1-16.

Montana Natural Resources Information System (NRIS) web site, 2004, http://nris.state.mt.us/gis/gisdatalib/downloads/windspeed.gif: Helena, Montana State Library.

Niedermann, S., 2002, Cosmic-ray-produced noble gases in terrestrial rocks: Dating tools for surface processes, *in* Porcelli, D. et al., eds., Noble gases in Geochemistry and Cosmochemistry, Geochemical Society of America and Mineralogical Society of America, p. 731-784.

Niedermann, S., Graf, T., Kim, J.S., Kohl, C.P., Marti, K., and Nishiizumi, K., 1994, Cosmic-ray-produced ^{21}Ne in terrestrial quartz: the neon inventory of Sierra Nevada quartz separates: Earth and Planetary Science Letters, v. 125, p. 341-355.

Nishiizumi, K., Winterer, E.L., Kohl, C.P., Klein, J., Middleton, R., Lal, D., and Arnold, J.R., 1989, Cosmic ray production of ^{10}Be and ^{26}Al in quartz from glacially polished rocks: Journal of Geophysical Research, v. 94, p. 17907-17915.

Ohno, M., and Hamano, Y., 1992, Geomagnetic poles over the past 10,000 years: Geophysical Research Letters, v. 19, n. 16, p. 1715-1718.

Osborn, G., Jackson, L.E., Barendregt, R., Enkin, R., Young, R., Wilson, P., 2000, Geologic constraints on archeological interpretations of a Late Wisconsinan site at Varsity Estates, Calgary, Alberta: Quaternary International, v. 68-71, p. 209-215.

Owen, L.A., Finkel, R.C., Caffee, M. W., and Gualtieri, L., 2002, Timing of multiple late Quaternary glaciations in the Hunza Valley, Karakoram Mountains, northern Pakistan: Defined by cosmogenic radionuclide dating of moraines: Geological Society of America Bulletin, v. 114, n. 5, p. 593-604.

Palmquist, R.C., 1983, Terrace chronologies in the Big Horn Basin, Wyoming: Wyoming Geological Association 34th Annual Field Conference Guidebook, p. 217-231.

Phillips, F.M., Zreda, M.G., Gosse, J.C., Klein, J., Evenson, E.B., Hall, R.D., Chadwick, O.A., and Sharma, P., 1997, Cosmogenic ^{36}Cl and ^{10}Be ages of Quaternary glacial and fluvial deposits of the Wind River Range, Wyoming: Geological Society of America Bulletin, v. 128, n. 11, p. 1453-1463.

Pierce, K.L., 2003, Pleistocene glaciations of the Rocky Mountains, *in* Gillespie, A.R., et al., eds., The Quaternary Period in the United States: Amsterdam, Elsevier, p. 63-76.

Pierce, K.L., and Morgan, L.A., 1992, The track of the Yellowstone hot spot: Volcanism, faulting and uplift, *in* Link, P.K., et al., eds., Regional Geology of Eastern Idaho and Western Wyoming: Geological Society of America Memoir 179, p. 1-53.

Pierce, K.L., and Scott, W.E., 1982, Pleistocene episodes of alluvial-gravel deposition, southeastern Idaho, *in* Bonnichsen, B. and Breckenridge, R.M., eds., Cenozoic Geology of Idaho, Idaho Bureau of Mines and Geology Bulletin 26, p. 685-702.

Poreda, R.J., and Farley, K.A., 1992, Rare gases in Samoan xenoliths: Earth and Planetary Science Letters: v. 113, p. 129-144.

Porter, K.W., 1990, Reconnaissance geologic map of the Grassrange-Winnett area, central Montana: Montana Bureau of Mines and Geology Open File Report 229, scale 1:100,000, 1 sheet.

Porter, K.W., and Wilde, E.M., 1999, Geologic map of the Musselshell 30’ x 60’ Quadrangle, central Montana: Montana Bureau of Mines and Geology Open File Report 386, scale 1:100,000, 1 sheet.

Porter, K.W., Wilde, E.M. and Vuke, S.M., 1993, Preliminary geologic map of the Big Snowy Mountains 30'x60' Quadrangle, Montana: Montana Bureau of Mines and Geology Open File Report 341, 1:100,000, 1 sheet.

Reeves, F., 1931, Geology of the Big Snowy Mountains, Montana: US Geological Survey Professional Paper 165-D, p. 135-149, 4 plates.

Reheis, M.C., 1984, Chronologic and climatic control on soil development, Northern Bighorn Basin, Wyoming and Montana [Ph.D. Thesis]: Boulder, University of Colorado, 346 p.

Reheis, M.C., 1987, Soils in granitic alluvium in humid and semiarid climates along Rock Creek, Carbon County, Montana: US Geological Survey Bulletin 1590-D, 71 p.

Richmond, G.M. and Fullerton, D.S., 1986, Summation of Quaternary glaciations in the United States of America: Quaternary Science Reviews, v. 5, p. 3-10.

Ritter, D.F., Kochel, R.C., and Miller, J.R., 2002, Process Geomorphology: New York, McGraw Hill, 560 p.

Roberts, S.M., ed., 1986, Belt Supergroup: a guide to Proterozoic rocks of western Montana and adjacent areas: Butte, Montana Bureau of Mines and Geology Special Publication 94, 311 p.

Smith, H.R., 1962, Geology of the Melstone-Sumatra area in central Montana: US Geological Survey Oil and Gas Investigations Map, scale 1:63,360, 1 sheet.

Smith, R.M., 1975, Geotechnical properties of glacial Lake Great Falls sediments in the Missouri River canyon, Montana [Master's Thesis]: Moscow, University of Idaho, 122 p.

Soil Survey Staff, 1993, Soil Survey of Petroleum County, Montana: US Department of Agriculture, Soil Conservation Service, 321 p.

Soller, D.R., 1992, Text and References to accompany "Map showing the thickness and character of Quaternary sediments in the glaciated United States east of the Rocky Mountains:" US Geological Survey Bulletin 1921, 54 p.

Soller, D.R., 1994, Map showing the thickness and character of Quaternary sediments in the glaciated United States east of the Rocky Mountains - northern plains states (west of 102^{o} West longitude): US Geological Survey Miscellaneous Investigations Series Map I-1970-D, scale 1:1,000,000, 1 sheet.

Springer, M.E., 1958, Desert pavement and vesicular layer of some soils of the desert of the Lahontan Basin, Nevada, USA: Soil Science Society of America Proceedings, v. 22, p. 63-66.

Stalker, A.M., 1977, The probable extent of Classical Wisconsin ice in southern and central Alberta: Canadian Journal of Earth Sciences, v. 14, p. 2614-2619.

Stone, J.O., 2000, Air pressure and cosmogenic isotope production: Journal of Geophysical Research, v. 105, p. 23 753-23 759.

Sugden, D.E., 1978, Glacial erosion by the Laurentide ice sheet: Journal of Glaciology, v. 20, n. 83, p. 367-391.

Taylor, R.L., Ashley, J.M., Chadwick, R.A., Custer, S.G., Lageson, D.R., Locke, W.W., Mogk, D. W., Schmitt, J.G., and Erickson, J.B., undated, Geological Map of Montana and Yellowstone National Park: Bozeman, Department of Earth Sciences, Montana State University, 1 sheet.

Teller, J.T., Sun, S., and Wolfe, B., 1990, Catastrophic flooding into Lake Agassiz: Canadian Quaternary Association-American Quaternary Association First Joint Meeting Programme and Abstracts, p. 32.

Thackray, G.D., Lundeen, K.A., and Borgert, J.A., 2004, Latest Pleistocene alpine glacier advances in the Sawtooth Mountains, Idaho, USA: reflections of midlatitude moisture transport at the close of the last glaciation: Geology, v. 32, n. 3, p. 225-228.

United States Geological Survey, November 1999, Map Accuracy Standards: USGS Fact Sheet 171-99.

Vreeken, W.J., 1989, Late Quaternary events in the Lethbridge area, Alberta: Canadian Journal of Earth Science, v. 26, p. 551-560.

Waitt, R.B., 1980, About forty last-glacial Lake Missoula jökulhlaups through southern Washington: Journal of Geology, v. 88, p. 653-679.

Waitt, R.B., 1985, Case for periodic, colossal jökulhlaups from Pleistocene glacial Lake Missoula: Geological Society of American Bulletin, v. 96, p. 1271-1286.

Wegmann, R., 2002, oral communication, Natural Resources Conservation Service, Roundup, MT.

Wilde, E.M., and Bergantino, R.N., 1992, Preliminary geologic map of the Sand Springs 30’ x 60’ Quadrangle: Montana Bureau of Mines and Geology Open File Report 304, scale 1:100,000, 1 sheet.

Weed, W.H., 1899, Description of the Little Belt Mountains Quadrangle, Montana: US Geological Survey Geologic Atlas Folio, 11 p.

Young, R.R., Burns, J.A., Rains, R.B., and Schowalter, D.B., 1999, Late Pleistocene glacial geomorphology and environment of the Hand Hills region and southern Alberta, related to Middle Wisconsin fossil prairie dog sites: Canadian Journal of Earth Sciences, v. 36, p. 1567-1581.

Young, R.R., Burns, J.A., Smith, D.G., Arnold, L.D. and Rains, B.R., 1994, A single, Late Wisconsin, Laurentide glaciation, Edmonton area and southwestern Alberta: Geology, v. 22, n. 8, p. 683-686.

Young, R.R., Burns, J.A., Smith, D.G. and Sjogren, D.B., 1996, Pleistocene fluvial geomorphology of the Edmonton area: implications for Laurentide glaciation on the Alberta plains: Geological Society of America Abstracts with Programs, v. 28, n. 7, p. 471.

APPENDIX A:

SAMPLE PREPARATION FOR COSMOGENIC ^{21}NE ANALYSIS.

1. Cut each sample to a uniform depth (3 cm) using a table saw.
2. Weigh the sample.
3. Run sample through the jaw crusher and pulverizer until all grains are smaller than 600 μm (30-mesh).
4. Sieve in sieve shaker using 40-, 50- and 60-mesh sieves.
5. Continue processing the 425-600 μm (40-mesh) grain size. Set aside the other grain sizes in case they are needed later.
6. Use a hand magnet covered in a piece of wax paper to remove the majority of the magnetic minerals.
7. Rinse the sample in distilled water and dry it on a hot plate.
8. Run the sample through the Frantz Isodynamic Separator from low to high voltage in order not to clog the magnet. Once the maximum voltage (150 V) is reached, adjust the tilt in increments from 15^{o} to 3^{o}.
9. Immerse the sample in 10% hydrochloric acid (HCl) and place in an ultrasonic bath for 30 minutes.
10. Repeat HCl sonication (Step 9) until the HCl comes out clean.
11. Sonicate in distilled water to remove acid residues.
12. Dry on a hot plate and place sample in a labeled film canister for transport to chemistry lab.
13. Treat each sample with 15% hydrofluoric acid (HF) for 30 minutes under a fume hood.
14. Rinse fifteen times with tap water.
15. Dry using ethyl alcohol (anhydrous ethanol).
16. Perform LST (a solution of lithium heteropolytungstates in water) heavy liquid separation.
    a. Fill a flask with LST to test the density. A chip of silica with density 2.582 should float slowly and steadily up from the bottom of the flask. Since LST is expensive, it is reused many times and, over time, evaporation or dilution can change its density.
    b. Place a glass funnel with a funnel stopper on a ring stand with a petri dish underneath the funnel opening to catch any drips.
    c. Fill the funnel half full with LST.
    d. Pour in the sample and fill the funnel with LST, mixing sample well. Cover the funnel with a petri dish to prevent evaporation.
    e. Wait 10-20 minutes while the minerals separate.
    f. Assemble filter apparatus . The flask should be labeled "LST clean."
    g. When the minerals have stopped rising and falling, remove the funnel from the ring stand and empty the contents of the bottom of the funnel (the minerals that sank in the liquid and any accompanying LST) into the filter apparatus.
    h. Suck the LST through a 541 grade Whatman filter paper using a General Electric standard vacuum unit ($\geq$10 psi).

i. Attach a new flask, labeled "Clean wash," to the filter apparatus. Rinse the sample with distilled water and filter again to save as much LST as possible. This very dilute LST can later be reconstituted to the proper density for reuse.
j. Detach the clamp and carefully remove the filter paper. Using distilled water, rinse the sample into a beaker labeled "Heavy."
k. Clean the filter apparatus thoroughly to prevent contamination.
l. Repeat the process for the "Light" mineral fraction left in the funnel. Rinse the funnel with distilled water into the filter apparatus after attaching the flask labeled "Clean wash."
m. Rinse the light and heavy mineral fractions five times with tap water, three times with distilled water, and twice with ethanol. Leave to dry on evaporating dishes.

17. Run sample through a small Frantz Isodynamic Separator up to -4^{o} tilt and 175 amps to remove remaining feldspars.
18. Sonicate overnight in distilled water, then again overnight hydrosilicic acid. The Branson sonicator used had a hose and drain mechanism that cycled the water through to keep the temperature low and approximately constant.
19. Rinse samples thoroughly and dry.
20. Hand-pick approximately 0.2 g of individual quartz grains under a binocular microscope.
21. Place each sample in a small foil boat for processing in the mass spectrometer.
22. Load targets into the extraction line for the Noble Gas Mass Spectrometer.

APPENDIX B:

SAMPLE PREPARATION FOR COSMOGENIC ^{10}BE ANALYSIS.

1. Measure and record the maximum thickness of the sample.
2. Wrap the sample well in plastic bags or tape.
3. Smash the sample with a hammer until the largest pieces are $\leq$~8 cm, a size that will not jam the Jaw Crusher.
4. Run the sample once through a Braun Chipmunk Jaw Crusher.
5. Beginning on a coarse setting, run the sample several times through a Bico Pulverizer (Type UA) until the average grain size is 250-500 μm.
6. Separate the sample into three size fractions, <250 μm, 250-500 μm and >500 μm, in a sieve shaker. Continue processing only the 250-500 μm sample.
7. Using a small MATLAB program, calculate the minimum mass of pure quartz necessary to obtain an age. Inputs to the program are latitude, altitude, and estimated age of the sample, erring on the young side. Younger rocks have accumulated smaller amounts of cosmogenic beryllium, and therefore the isotope is more difficult to detect against background Be levels. Output is the Be ratio compared to a background of 2×10^{-14} and assuming use of 350 ppm Be carrier. Be ratios that are at least an order of magnitude greater than background are easily readable. Assume that the bulk sample will be reduced to 20-30% of its original mass, so to obtain 20-30 g of pure quartz, begin with 90-100 g of bulk mineral.
8. Leach the sample in HCl to remove organics and carbonate residues.
   a. Prepare a solution of 6N HCl and 0.03% hydrogen peroxide (H_2O_2). For 100 g of rock, use 1 L of solution and prepare in a 5 L beaker using 500 ml of MilliQ water, 500 ml of 12M HCl, and a pipette full (3 ml) of H_2O_2, added in that order.
   b. Pour in the sample cautiously, watching for a reaction.
   c. Place on a hot plate at setting 2-3, cover with a watch glass, and set the timer to heat for 12 hours.
9. Drain and rinse the sample three times with MilliQ water, then rinse into a 250 ml beaker and drain. Use a plastic disposable pipette to suck the excess water from the sample and place in the drying oven at 100° C.
10. Weigh the dry sample and split into 30 g fractions. Record all weights and proportions on a data sheet.
11. Perform the first hydrofluoric acid leaching on each 30 g fraction.
    a. Use large (~4 L) Teflon beakers with lids for the leaching. The recipe for the first HF leach is 1% HF, 1% HNO_3, 7.5 g quartz/L acid solution. For 30 g of rock, use 3660 ml of MilliQ water, 83 ml of HF, and 54 ml of HNO_3.
    b. Add the sample after the water and before the acids. Pour the acids under a fume hood. Wear nitrile gloves and apron, and a face shield in addition to the basic lab coat and safety glasses whenever working with HF. Hydrofluoric acid is a bone-seeking acid, and if one is exposed to it, the fluorine will bind with bone calcium and can potentially cause death.
    c. Stir the solution with a stirring rod to prevent separation caused by the high density of the acid.
    d. Label the lid and place on the beaker.

   e. Place the beaker in the ultrasonic bath at sub-boiling temperature (90°C) for nine hours.
   f. After the leaching, drain the sample and rinse once with MilliQ. Rinse into a 250 ml beaker and place in the drying oven.
12. Determine the dry weight and calculate the proportion for the second HF leach. The recipe for both the second and third HF leach is 1% HF, 1% HNO_3, 15 g quartz/L acid solution.
   a. Place the appropriate amounts of water, HF and HNO_3 in a large Teflon beaker with a labeled lid.
   b. Sonicate the beaker for nine hours at sub-boiling.
   c. Dry (in the same 250 ml glass beaker as in Step 11f) and weigh.
13. Run the sample through a Frantz Isodynamic Separator at maximum voltage (~150 V) and 12° tilt.
14. Measure the new weight and determine the proportions for a third and final HF leach.
   a. Prepare the beakers for the third leach in the same fashion as for the second HF treatment.
   b. Sonicate for nine hours, again at sub-boiling.
   c. Dry and weigh samples as before.
15. In order to determine the purity of the quartz thus far, perform an Atomic Absorption Spectrometer reading of representative samples.
   a. Weigh out approximately one gram of each sample on the precision balance and place in a small Teflon beaker with 10 ml of 1:1 HNO_3 and 10 ml of HF.
   b. Heat the beaker on a hot plate (setting 3-4), and add HF in 10 ml increments until the quartz is dissolved.
   c. Dry down the solution and add 5 ml of HNO_3 to the residue.
   d. Fume off the HNO_3 and repeat with another 5 ml HNO_3. After the second fume, the HF should have been removed and the dry residue is ready for dilution with 1 ml 6M HCl and 9 ml MilliQ water. HF and HCl should not be mixed.
   e. Run this liquid through the AAS, where the aluminum within is ionized in a nitrous oxide-driven flame. The AAS measures the wavelength of the light absorbed by the flame. A coarse estimate of the aluminum content of the pure quartz is obtained with the AAS. Aluminum is the primary impurity in pure quartz, possibly because of feldspar inclusions, and high aluminum counts can interfere with the Accelerator Mass Spectrometer's ability to measure Be and Al ratios. If the aluminum content is <100ppm, proceed with the quartz dissolution process.
16. Prepare seven samples and one blank with beryllium and aluminum carrier and dissolve on a hot plate.
   a. Carefully weigh each sample on a precision balance.
   b. Measure the predetermined amount of pure quartz from step 7 into a Teflon beaker and set aside, covered with a non-static-producing cover such as a Kim wipe, to keep out dust. In this study, ≤30 g of quartz (whatever was available after the leaching process) was used for each sample.

c. Take each sample individually and add the beryllium and aluminum carriers. Do this very carefully, as the weight of carrier added is a crucial piece of data in analyzing the AMS results.
   i. Tare a small plastic crucible on the precision balance.
   ii. Using a plastic disposable pipette, place approximately one gram of beryllium carrier in the crucible and record its precise weight.
   iii. Pour the carrier into the Teflon beaker containing the sample.
   iv. Rinse the crucible three times with MilliQ water to ensure that every last drop of carrier is added to the sample.
   v. Add approximately one gram of aluminum carrier to the sample in the same manner.

d. Fit the samples with Teflon tops so as to prevent evaporation during heating. Perform the same procedure for the blank, beginning with an empty Teflon beaker.

e. Move all eight beakers to a hot plate under a fume hood, and add HF (5 ml acid/g quartz) and HNO_3 (0.3 ml acid/g quartz).

f. Leave the hot plate on setting 2-4 for 24-48 hours until the quartz is dissolved. Periodically check the beakers with a Teflon stirring rod to determine if dissolution has occurred. Use extreme caution during the dissolution process, as hot, concentrated HF is dangerous.

g. If some solid residue remains when all of the quartz is dissolved, centrifuge the portion of the solution containing the solid and remove the residue from the process.

17. Take an aliquot of each sample for potential use in future ^{26}Al dating.
    a. Transfer the quartz solution to a plastic bottle and determine and record its mass.
    b. Set aside 10% of the solution by mass in an aliquot bottle.
    c. Rinse the rest of the liquid back into the Teflon beaker and place uncovered on the hot plate on setting 4 until the liquid evaporates.

18. Fume samples three times with perchloric acid. Perchloric acid is used, because of its high boiling point, to remove the fluorides left over from the HF used in dissolution. Sulfuric acid also has a boiling point high enough to remove the fluorides, but its boiling point is close to the melting point of Teflon, and therefore the samples must be more closely monitored. Fluorides form strong complexes that interfere with the anion/cation column work, so these have to be removed before proceeding. Some perchlorate complexes can be explosive, so use a special hood with the capability for a daily wash-down.
    a. For the first perchloric treatment, add 10 ml of 1:1 nitric acid and 3 ml of perchloric acid to the dried down residue from the dissolution process.
    b. Swirl to dissolve the residue and leave on a hot plate (setting 4) to dry down for approximately two hours.
    c. When dry, add water from a wash bottle to mobilize the residue and to rinse the sides, which because they are cooler than the bottom of the beaker during heating

on the hot plate might provide a place for fluorides to condense during the drying down process.

d. Add 1-2 ml of perchloric acid to each beaker and dry down the samples again.
e. Repeat a third time with 1 ml of perchloric acid.
f. NOTE: The nitric acid used in the first perchloric fume may be extraneous to the procedure. It was introduced in order to help drive off some other residuals when processing bulk basalts. When using pure quartz rather than bulk basalt, the nitric acid does not appear to serve any purpose, but since it is currently being used in the procedure, it is discussed in these methods.

19. Prepare the dried down residue for anion column work.
    a. Heat and dilute the residue with approximately 6 ml of 9 N HCl.
    b. Once the residue is dissolved in the HCl, transfer the solution with a pipette to a 10 ml test tube.
    c. Centrifuge the test tube for 2 minutes to ensure that only aqueous state materials are placed in the ion separation columns.
20. Condition the anion column and run the sample through. The main function of the anion column is to strip the sample of negatively charged ions, primarily iron chlorocomplexes (i.e. Fe_3Cl_4 and $Fe_3Cl_6^{3-}$) and minor amounts of manganese, cobalt and chromium. Since beryllium and aluminum are not transition metals, they pass through the anion column.
    a. For an anion column whose resinous area has a volume of 20 ml, the column is conditioned using 60 ml (3 column volumes) 9 N HCl. This is done immediately before use so that the column has a strong positive charge.
    b. Place a small quartz beaker under the tip of the column to collect the drips.
    c. Transfer the 6 ml of sample solution (approximately 1/3 of a column volume) to the conditioned anion column using a pipette. Take care not to pipette the centrifuged residue or disturb the resin bed.
    d. Once the column has stopped dripping, run 34 ml 9N HCl through the column and collect in the same quartz beaker, for a total of 2 column volumes of 9N.
    e. Dry down the sample solution.
    f. Run 80 ml (4 column volumes) of 0.1 N HCl through the column and collect in 100 ml bottles and set aside as the "anion reject" fraction of each sample.
    g. NOTE: During the night, a small amount of water should be placed on top of the resin and the column valve should be closed to prevent the resin from drying out.
21. Prepare the dried down anion sample for cation column work.
    a. Add three milliliters of 1 N (0.5 M) sulfuric acid (H_2SO_4) to the dry sample.
    b. Heat the mixture on a hot plate until the sample is completely dissolved and white SO_4 fumes are produced.
    c. Remove the quartz beaker from the heat and add 1 ml of MilliQ water to cool it.
    d. Add one to three drops of hydrogen peroxide (H_2O_2). The H_2O_2 turns yellow in the presence of titanium.
    e. Add two more ml of MilliQ water and pipette the solution into a 10 ml test tube.

f. Dilute the solution with MilliQ to 6 ml by first pipetting the appropriate amount of water into the quartz beaker to rinse it and then transferring the rinse solution to the test tube.
g. Centrifuge the test tube in preparation for the cation column.

22. Run the sample through the cation column. The purpose of the cation column is to separate the desired cations (Be and Al) from the other cations in the sample. The sample is added, and as the column work progresses the concentration of the acid used is increased, thereby increasing the H+ concentration. The competition by the H+ drives each ion present in the sample off of the resin in sequence, according to their binding strength.
    a. Place a bottle labeled "Ti reject" under the column to collect the drips.
    b. Introduce the sample to the column via pipette.
    c. Since ions such as sodium and titanium have a lesser charge than Be and Al, they are less attracted to the negative charge of the cation column and will come off in a less concentrated acid. In order to collect the unwanted ions that have a lower positive charge than Be, add 120 ml (6 column volumes) of 0.5 N H_2SO_4 to the column.
    d. Remove the Ti bottle and place a quartz beaker labeled "Be" under the column.
    e. Beryllium is the next weakest binder. To maximize the amount of Be collected, pass seven column volumes of 1 N HCl through the column.
    f. When the quartz beaker becomes ¾ full, switch it with a plastic bottle and place it on a hot plate and begin drying it down. Periodically transfer additional solution from the bottle to the quartz beaker.
    g. Collect a "Be reject" fraction in another plastic bottle by running 3 column volumes of 1 N HCl through the column. This fraction may also contain other ions with a binding strength intermediate to Be and Al, such as Mg and Fe.
    h. Aluminum binds strongly to the resin column. Collect the aluminum fraction last by passing four column volumes of 2.5 N HCl through the column. This solution is dried down for preparation for ^{26}Al dating.
    i. NOTE: Save all fractions from the column separation process until the results of the AMS measurements are read and it is determined that the sample does not need to be rerun.
23. Condition the cation column immediately after use.
    a. Run ten column volumes of 6 N HCl and then three column volumes of MilliQ water through the column.
    b. Collect this liquid in a waste bottle and dispose of in a waste drum.
24. Precipitate the beryllium oxide in the dry Be fraction.
    a. Dissolve the residue in 1 ml 6N HCl.
    b. Add a few drops (1-3) of H_2O_2 to see if any titanium remains in the mixture.
    c. Pipette the solution into a 10 ml test tube.
    d. Use approximately 1 ml of water to rinse the beaker. Pipette this rinse water into the test tube.

   e. Add 1:1 NH_4OH in increments to the test tube to turn the solution basic, thereby forcing the precipitation of beryllium oxide.
      i. Add 0.5 ml of NH_4OH.
      ii. Mix the test tube on a vortex and inspect for tiny blebs of precipitate. Beryllium oxide is gelatinous and is usually white. Upon centrifuging, it will form a plug in the bottom of the test tube.
      iii. If BeO_2 is not apparent and after a few minutes the test tube does not smell of ammonia, add additional NH_4OH in 0.5 ml increments until precipitation is achieved.

25. Centrifuge the test tube for two minutes and drain off the liquid with a pipette into a waste beaker.
26. Rinse the beryllium plug twice with 6 ml of MilliQ water. Vortex, centrifuge and drain with a pipette each time.
27. Pipette the clean, drained plug into a tiny quartz crucible.
28. Rinse the test tube and pipette repeatedly with 3 drops of water that was then added to the crucible.
29. Place the crucible in one of the fitted slots to dry in an oxide drying plate for six hours at $90^{o}C$.
30. Remove the dried crucibles from the heating plate with tweezers to avoid contamination, place in a metal rack, and cover with quartz lids.
31. Place the rack in a furnace and ignite at $750^{o}C$ for five minutes.
32. Remove the rack from the oven with metal tongs and take off the lids with tweezers.
33. Place each crucible inside a glass vial with a plastic lid. Label both the lids and vials with the sample number.
34. Prepare the ^{10}Be target.
    a. Thoroughly and frequently clean the workspace with isopropyl alcohol to avoid contamination.
    b. Remove the crucibles from the vials with tweezers.
    c. Grind the beryllium powder inside them as fine as possible with a small metal rod.
    d. Mix with a small scoop of niobium powder. The purpose of the niobium powder is to aid with the initial ionization in the AMS. Niobium is a good electrical conductor.
    e. Pour the contents of the crucible onto a labeled metal target resting on a metal holder.
    f. Pound the sample down into a small hole in the top of the target using a hammer and the metal rod.
    g. Place the packed target in a labeled plastic vial with a labeled plastic screw-on top.
35. Load the targets on the wheel.
36. Analyze the wheel of targets in the Accelerator Mass Spectrometer.

APPENDIX C:

PROVENANCE AND CLAST SIZE DATA AT SITES E-Z.

Site E. Modern Musselshell alluvium (Q_{al}) on gravel bar south of Rt. 200
Latitude/Longitude: 46° 59' 36" N 107° 53' 19" W
Altitude: 763 m
Height above the Musselshell River: 0 m

TABLE 19. COBBLE COUNT AND CLAST SIZE DATA AT SITE E.

Lithology	Number
Limestone	21
Argillite (Belt Supergroup)	7
Chert	5
Salt and pepper sandstone	6
Quartz sandstone	3
Quartzite (Belt Supergroup)	13
Igneous trachytes and syenties (MT alkalic province)	40
Green (fenite or tinguaite)	1
Shonkinite	4
Total	100

Size	Number
≤ 2 cm	28
≤ 5 cm	40
≤ 7.5 cm	17
≤ 10 cm	9
≤ 12.5 cm	6
Total	100

Avg. size: 5.5 cm

Also at Site E. Lowest terrace of the Musselshell, exposed in streamcuts
Height above the Musselshell River: Approximately 1.5-2 m
Correlation: Mapped as Q_{al} by Johnson and Smith (1964); herein designated the lowest Musselshell terrace (probably Holocene in age) based on grain size and height above river
Surface of the deposit: Swampy, with some alluvial cobbles (≤8 cm long axis) strewn about. These may have been lowered from a higher terrace or may have worked their way up through the terrace. Deposit is generally flat-lying with two small rises (90 cm and 30 cm) between the river and a gravel road.

Stratigraphy of the deposit:

0-25 cm	Fine sand and silt; finely laminated; cross-beds (?)
25-28 cm	Buried A horizon – contains basically intact woody plant parts (largest one is 2” in diameter and >5” long)
28-33 cm	Laminated fines with bright orange (Fe?) streaks
33-46 cm	Salt layer; 1 small (2 cm) alluvial cobble at 15” depth
46-51 cm	Laminated fines
51-53 cm	Buried A horizon
>53 cm	Sequence repeats; hard to tell how many times

Site F. Musselshell River terrace (Q_{tm2}) exposed in gravel pit north of Rt. 200
Latitude/Longitude: 47° 00' 04" N 107° 54' 01" W
Altitude: 791 m
Height above the Musselshell River: 28 m

TABLE 20. COBBLE COUNT AND CLAST SIZE DATA AT SITE F.

Lithology	Number	Size[†]	Number
Limestone	40	≤ 2 cm	22
Local limestone	5	≤ 5 cm	54
Argillite (Belt Supergroup)	10	≤ 7.5 cm	20
Chert	9	≤ 10 cm	4
Salt and pepper sandstone	3	≤ 12.5 cm	0
Quartz sandstone	0	Total	100
Igneous trachytes and syenites (MT alkalic province)	29	[†]clasts up to 7" were observed but not counted at this site	
Quartzite (Belt Supergroup)	1		
Green (fenite or tinguaite)	2		
Shonkinite	0	Avg. size: 5.0 cm	
Tooth/bone/petrified wood	1		
Total	100		

Site G. Musselshell River terrace (Q_{tm2}) exposed in road cut on River Rd.
Latitude/Longitude: 47° 03' 29" N 107° 56' 09" W
Altitude: 799 m
Height above the Musselshell River: 49 m

TABLE 21. COBBLE COUNT AND CLAST SIZE DATA AT SITE G.

Lithology	Number
Limestone	27
Local limestone and siltstone	8
Argillite (Belt Supergroup)	5
Chert	7
Salt and pepper sandstone	3
Quartz sandstone	1
Igneous trachytes and syenites (MT alkalic province)	38
Quartzite (Belt Supergroup)	0
Green (fenite or tinguaite)	2
Shonkinite	0
Ironstone	4
Conglomerate (Belt Supergroup)	2
Hard (cherty) dolostone	2
Tooth/bone/petrified wood	1
Total	100

Size	Number
≤ 2 cm	34
≤ 5 cm	36
≤ 7.5 cm	20
≤ 10 cm	3
≤ 12.5 cm	3
≤ 15 cm	3
22.5 cm	1
Total	100

Avg. size: 5.3 cm

Site H. Musselshell River terrace (probably Q_{tm1}) exposed in Browning gravel pit
Latitude/Longitude: 47° 12' 45" N 107° 57' 06" W
Altitude: 775 m
Height above the Musselshell River: 59 m

TABLE 22. COBBLE COUNT AND CLAST SIZE DATA AT SITE H.

Lithology	Number	Size	Number
Limestone	19	≤ 2 cm	30
Local limestone and siltstone	11	≤ 5 cm	37
Argillite (Belt Supergroup)	11	≤ 7.5 cm	19
Chert	6	≤ 10 cm	9
Salt and pepper sandstone	12	≤ 12.5 cm	2
Quartz sandstone	3	≤ 17cm	2
Igneous trachytes and syenites (MT alkalic province)	19	50 cm	1
Quartzite (Belt Supergroup)	3	Total	100
Green (fenite or tinguaite)	1		
Shonkinite	1	Avg. size: 5.9 cm	
Coal (local)	1		
Black and white granite	1		
Pink, black and white granite	5		
Pink gneiss	2		
Black and white gneiss	1		
Biotite schist	1		
Ironstone	2		
Marble (?)	1		
Total	100		

Site I. Musselshell River terrace (probably Q_{tm2}) exposed in Dutton's hidden gravel pit
Latitude/Longitude: 47° 03' 54" N 107° 57' 35" W
Altitude: 809 m
Height above the Musselshell River: 63 m

TABLE 23. COBBLE COUNT AND CLAST SIZE DATA AT SITE I.

Lithology	Number	Size	Number
Limestone	24	≤ 2 cm	35
Local sandstone and siltstone	10	≤ 5 cm	55
Argillite (Belt Supergroup)	15	≤ 7.5 cm	8
Chert	17	≤ 10 cm	2
Salt and pepper sandstone	1	Total	100
Quartz sandstone	1		
Igneous trachytes and syenites (MT alkalic province)	28	Avg. size: 4.3 cm	
Quartzite (Belt Supergroup)	1		
Green (fenite or tinguaite)	1		
White limestone	1		
Tooth/bone/petrified wood	1		
Total	100		

Site J. Musselshell River terrace (Q_{tm3}) exposed in gravel pit on south side of River Rd.
Latitude/Longitude: 47° 03' 41" N 107° 56' 21" W
Altitude: 821 m
Height above the Musselshell River: 75 m

TABLE 24. COBBLE COUNT AND CLAST SIZE DATA AT SITE J.

Lithology	Number	Size	Number
Limestone	30	≤ 2 cm	35
Local limestone and siltstone	6	≤ 5 cm	47
Argillite (Belt Supergroup)	5	≤ 7.5 cm	14
Chert	6	≤ 10 cm	4
Salt and pepper sandstone	9	≤ 12.5 cm	0
Quartz sandstone	4	Total	100
Igneous trachytes and syenites (MT alkalic province)	37		
Quartzite (Belt Supergroup)	3	Avg. size: 4.5 cm	
Total	100		

Site K. Cat Creek gravel exposed in Ahlgren/county gravel pit
Latitude/Longitude: 47° 03' 21" N 108° 00' 30" W
Altitude: 885 m
Height above the Musselshell River: 134 m

TABLE 25. COBBLE COUNT AND CLAST SIZE DATA AT SITE K.

Lithology	Number	Size	Number
Limestone	25	$\leq$ 2 cm	34
Local limestone and siltstone	7	$\leq$ 5 cm	49
Argillite (Belt Supergroup)	12	$\leq$ 7.5 cm	10
Chert	9	$\leq$ 10 cm	7
Salt and pepper sandstone	5	$\leq$ 12.5 cm	0
Quartz sandstone	3	Total	100
Igneous trachytes and syenites (MT alkalic province)	31		
Quartzite (Belt Supergroup)	2	Avg. size: 4.6 cm	
Green (fenite or tinguaite)	0		
Shonkinite	2		
Tooth/bone/petrified wood	4		
Total	100		

Site description by W. D. Johnson, unpublished field notes: S 1/2 sec. 14 and N 1/2 sec. 23, T15N, R29E. 18.3+ m of subrounded gravel exposed in pits mined for cement aggregate and road ballast. Lenses of very coarse sand and fine sand to silt that generally dip to the southeast at ~25°.

TABLE 26. COBBLE COUNT DATA AT SITE K FROM JOHNSON AND SMITH.

Lithology	Number	% of total	
Limestone	22	42	Size: $\leq$12.5 cm
Sandstone	8	15	
Shale	1	2	
Igneous	8	15	
Ironstone	7	14	
Quartzite	6	12	
Total	52	100	

Site L. Highest Musselshell River terrace (Q_{tm8}), no good exposure
Latitude/Longitude: 47° 00' 03" N 108° 02' 11" W
Altitude: 957 m
Height above the Musselshell River: 198 m

TABLE 27. COBBLE COUNT AND CLAST SIZE DATA AT SITE L.

Lithology	Number	Size	Number
Argillite (Belt Supergroup)	1	≤ 2 cm	3
Igneous trachytes and syenites (MT alkalic province)	1	≤ 5 cm	2
Green (fenite or tinguaite)	3		
Total	5	Avg. size: 3.2 cm	

Site M. Musselshell River terrace (probably Q_{tm1}) exposed in gravel pit west of Lower River Rd.
Latitude/Longitude: 47° 06’ 29” N 107° 57’ 27” W
Altitude: 779 m
Height above Musselshell River: 44 m
Provenance: Mostly typical Musselshell lithologies. However, abundant local shale clasts (2.5-8 cm long), flat shaley limestone clasts (<20 cm long), and two Canadian Shield clasts (one granite and one gneiss, both 15 cm long and subrounded) were present.

Site N. Gravel deposit exposed in road cut east of Dovetail Rd.
Latitude/Longitude: 47° 18' 18" N 107° 57' 30" W
Altitude: 707 m
Height above Musselshell River: 17 m
Provenance: Mostly typical Musselshell lithologies, with two Canadian Shield boulders (0.2 m in diameter) buried 0.2 m in the deposit.

*NOTE: There is no Site O.

Site P. Musselshell River terrace (Q_{tm2})
Description: 1.5-2 m thick gravel deposit (Johnson and Smith, 1953-1956)
Location: NW 1/4 sec. 32 T16N R30E

TABLE 28. COBBLE COUNT AND CLAST SIZE DATA AT SITE P FROM JOHNSON AND SMITH (1953-1956).

Lithology	Number	% of total
Limestone	10	40
Sandstone	1	4
Chert	2	8
Igneous	12	48
Total	25	100

Size	Number
≤ 2 cm	17
≤ 5 cm	5
≤ 7.5 cm	2
≤ 10 cm	1
≤ 12.5 cm	0
Total	25

Avg. size: 3.4 cm

Site Q. Musselshell River terrace (Q_{tm2})
Description: 1.5-2 m thick gravel deposit (Johnson and Smith, 1953-1956)
Location: NW 1/4 sec. 16 T15N R30E

TABLE 29. COBBLE COUNT AND CLAST SIZE DATA AT SITE Q FROM JOHNSON AND SMITH (1953-1956).

Lithology	Number	% of total
Limestone	6	24
Sandstone	2	8
Chert	2	8
Igneous	10	40
Mudstone	2	8
Siltstone	3	12
Total	25	100

Size	Number
≤ 2 cm	22
≤ 5 cm	1
≤ 7.5 cm	2
≤ 10 cm	0
Total	25

Avg. size: 2.6 cm

Site R. Musselshell River terrace ($Q_{t3or4?}$)
Description: Highest gravel terrace in vicinity; represents divide between Elk and McDonald Creeks (Johnson and Smith, 1953-1956)
Location: NE 1/4 sec. 28 T14N R26E

TABLE 30. COBBLE COUNT AND CLAST SIZE DATA AT SITE R FROM JOHNSON AND SMITH (1953-1956).

Lithology	Number	% of total	Size	Number
Limestone	8	16	≤ 2 cm	29
Sandstone	26	52	≤ 5 cm	10
Chert	8	16	≤ 7.5 cm	7
Igneous	1	2	≤ 10 cm	1
Conglomerate sandstone	1	2	≤12.5 cm	1
Calcite	2	4	>12.5 cm	2
"Coprolitic"	1	2	Total	50
Ironstone	1	2		
Chalcedony	2	4		
Total	50	100	Avg. size: 4.4 cm	

Site S. Musselshell tributary terrace ($Q_{t?}$)
Description: None given (Johnson and Smith, 1953-1956)
Location: Questionable; on road, ca. N 1/2 sec. 10 T13N R25E

TABLE 31. COBBLE COUNT AND CLAST SIZE DATA AT SITE S FROM JOHNSON AND SMITH (1953-1956).

Lithology	Number	% of total	Size	Number
Limestone	10	40	≤ 2 cm	16
Sandstone	3	12	≤ 5 cm	6
Chert	3	12	≤ 7.5 cm	0
Igneous	3	12	≤ 10 cm	1
Quartz	1	4	>10 cm	2
Ironstone	5	20	Total	25
Total	25	100		
			Avg. size: 4.0 cm	

Site T. Musselshell tributary terrace (Q_{t2or1})
Description: Lower terrace gravel; ~2.5 m thick (Johnson and Smith, 1953-1956)
Location: sec. 7 T13N R27E

TABLE 32. COBBLE COUNT AND CLAST SIZE DATA AT SITE T FROM JOHNSON AND SMITH (1953-1956).

Lithology	Number	% of total	Size	Number
Limestone	33	82.5	≤ 2 cm	29
Sandstone	3	7.5	≤ 5 cm	4
Chert	2	5	≤ 7.5 cm	1
Calcite	1	2.5	≤ 10 cm	4
Agate?	1	2.5	>10 cm	2
Total	40	100	Total	40

Avg. size: 3.9 cm

Site U. Musselshell tributary terrace (Q_{t2})
Description: ~1.8 m thick gravel deposit north of McDonald Creek (Johnson and Smith, 1953-1956)
Location: NE 1/4 sec. 1 T14N R27E

TABLE 33. COBBLE COUNT AND CLAST SIZE DATA AT SITE U FROM JOHNSON AND SMITH (1953-1956).

Lithology	Number	% of total	Size	Number
Limestone	49	81.7	≤ 2 cm	43
Sandstone	4	6.7	≤ 5 cm	12
Chert	2	3.3	≤ 7.5 cm	0
Igneous	2	3.3	≤ 10 cm	3
"Igneous granitic"†	2	3.3	≤12.5 cm	1
Concretion	1	1.7	20 cm	1
Total	60	100	Total	60

†granitic clasts are 2 cm and 10 cm long

Avg. size: 3.5 cm

Site V. Musselshell tributary terrace (Q_{tm2or1})

Site description: 2.4 m of gravel interbedded with yellowish-grey fine to medium sand; gravel is well-sorted and well-rounded to subangular (Johnson and Smith, 1953-1956)

Location: sec. 35 T13N R30E

TABLE 34. COBBLE COUNT DATA AT SITE V FROM JOHNSON AND SMITH.

Lithology	Number	% of total	
Limestone	15	27.3	Size: ≤15 cm
Sandstone	7	12.7	
Chert	5	9.1	
Igneous	25	45.5	
Ironstone	3	5.5	
Total	55	100	

Site W. Mapped as a Musselshell River terrace (Q_{tm3}) by Johnson and Smith (1964)

Description: "On high terrace…gravel is predominantly of angular pebbles of sandstone (locally derived), some ironstone and fragments of limestone and calcite. Some angular cobbles and boulders of local sandstone." - W.D. Johnson, unpublished field notes (1953-1956)

The gravel pit marked in this section was revisited by Nicole Davis on 8/22/02. Two abandoned, overgrown trenches could not have yielded much gravel, though a local rancher reported that these pits were used for the original highway. Trenches appeared to be cut in fine sediment ("gumbo") with some angular local bedrock chunks. Two well-rounded quartzite cobbles (8 and 15 cm long) were found at the site. No cobble count was performed.

Location: NE 1/4 sec. 8 T14N R31E

Site X. Musselshell River terrace (Q_{tm2})

Description: 2.7 m of subangular to subrounded pebbles and some scattered cobbles (Johnson and Smith, 1953-1956)

Location: sec. 34 T15N R30E

TABLE 35. COBBLE COUNT DATA AT SITE X FROM JOHNSON AND SMITH.

Lithology	Number	% of total	
Limestone	18	56.3	Size: Mostly <5 cm
Sandstone	7	21.9	
Quartzite	2	6.3	
Igneous	5	15.6	
Total	32	100	

Site Y. Musselshell River terrace (Q_{tm7})

Description: 0.3-.76 m of yellowish-grey to light olive-grey highly calcareous fine sandy clay with thin lenses and stringers of bedded gravels. Clay shows columnar jointing and "strongly resembles glacial till." Clay overlies 2.4 m of "roughly bedded" gravel, granules and coarse sand. Gravels are subangular to subrounded, with some well-rounded pieces. -W.D. Johnson, unpublished field notes (1953-1956)

Revisited by Nicole Davis on 8/27/02. 3 m of gravel overlain by 0.6 m of pebbly silt with soil development. No cobble count was performed.

Location: NE 1/4 sec. 2, T14N, R29E

TABLE 36. COBBLE COUNT DATA AT SITE Y FROM JOHNSON AND SMITH.

Lithology	Number	% of total	
Limestone	14	24.1	Size: 2.5-12.5 cm
Sandstone	4	6.9	
Shale	2	3.4	
Igneous	26	44.8	
Ironstone	9	15.5	
Quartzite	3	5.2	
Total	58	100	

Site Z. Musselshell tributary terrace (Q_{t1})

Description: Lowest terrace on McDonald Creek. 2.8 m of bedded gravel with sand matrix and a few thin beds of sand underlain by 1.4 m of yellowish-grey calcareous clayey silt. Gravels are subangular to subrounded, with a few well-rounded clasts. (Johnson and Smith, 1953-1956)

Location: sec. 6 T14N R28E

TABLE 37. COBBLE COUNT DATA AT SITE Z FROM JOHNSON AND SMITH.

Lithology	# of clasts	% of total
Limestone	28	57.1
Sandstone	7	14.3
Chert	1	2.0
Igneous	8	16.3
Ironstone	5	10.2
Total	49	100

Size: Mostly 2.5-5 cm; all $\leq$15 cm

APPENDIX D:

SOIL DESCRIPTIONS AT SITES A-D FROM FIELD NOTES.

Site A.	0-10 cm	A – mollic epipedon, loamy texture
Q_{tm2}	10-43 cm	B_t – moderately-developed clay films
	43-69 cm	B_k – strongly effervescent, carbonate filaments
	>69 cm	2C – coarse-clast alluvium

Local rock type: Judith River Formation
Lithology of cobbles: limestone, alkaline intrusives, chert, calcareous sandstone
Vegetation: sage, grasses and prickly pear cactus
Location: 46^o 56’ 19” N 107^o 55’ 51” W, 817 m (2680 ft)

Site B.	0-20 cm	A – mollic epipedon, loamy texture
Q_{tm2}	20-38 cm	B_t – well-developed clay films
	38-45 cm	B_y – non-effervescent, gypsum filaments (white-yellow)
	45-$\geq$76 cm	B_{ky} – strongly effervescent, gypsum filaments

Local rock type: Colorado shale
Lithology of cobbles: alkaline intrusives, limestone, chert, sandstone
Vegetation: sage, grasses, prickly pear cactus, moss and some lichen
Location: 47^o 00’ 12” N 107^o 54’ 17” W, 798 m (2618 ft)

Site C.	0-10 cm	A – mollic epipedon, high organic matter (OM) content
Q_{tm7}	10-28 cm	B_t – limited accumulation of organic matter evident, very compact and heavy soil, abundant high chroma mottles, moderately-developed clay films
	28-43 cm	B_k – strongly effervescent, carbonate filaments (white)
	43-$\geq$89 cm	B_{k2} – strongly effervescent, carbonate filaments, OM lenses

Local rock types: Eagle Sandstone and Claggett Shale
Lithology of cobbles: alkaline intrusives, chert
Vegetation: sage, grasses, prickly pear cactus, moss and some lichen
Location: 47^o 00’ 14” N 108^o 00’ 53” W, 941 m (3086 ft)

Site D.	0-6 cm	A – ochric epipedon(?), loamy texture
Q_{t2}	6-27 cm	B_t – well-developed clay films, blocky structure
	27-71 cm	B_k – strongly effervescent, carbonate filaments (white)
	71-$\geq$122 cm	B_{ky} – gypsum filaments (white-yellow)

Local rock type: Cretaceous Colorado Group
Lithology of cobbles: alkaline intrusives, limestone, sandstone
Vegetation: sage, grasses and prickly pear cactus
Location: 47^o 05’ 45” N 108^o 20’ 03” W, 901 m (2955 ft)

APPENDIX E:

SOIL TEXTURE, PH AND DRY COLOR AT SITES A-D.

TABLE 38. SOIL TEXTURE AND SELECTED HYDROMETER ANALYSIS DATA.

Site	Horizon[†]	Adjusted 40-second reading	Adjusted 2-hour reading	% Sand	% Silt	% Clay
A	A	28.1	10.6	43.9	35.0	21.1
	B_t	32.6	17.6	34.9	30.0	35.1
	B_k	28.4	17.6	43.2	21.7	35.1
B	A	27.7	5.6	44.5	44.4	11.1
	B_t	34.2	20.6	31.5	27.4	41.1
	B_y	32.6	4.6	34.9	56.0	9.1
	B_{ky}	32.1	14.6	35.9	35.0	29.1
C	A	22.6	7.6	54.9	30.0	15.1
	B_t	32.5	23.6	35.0	17.9	47.1
	B_k	30.1	17.6	39.9	25.0	35.1
	B_{k2}	34.1	20.6	31.7	27.1	41.1
D	A	24.8	9.6	50.4	30.5	19.1
	B_t	33.7	24.6	32.5	18.4	49.1
	B_k	26.6	16.6	46.9	20.0	33.1
	B_y	26.1	4.6	47.8	43.1	9.1

[†]Determined in the field; see Table 39 for corrections based on texture data.

TABLE 39. SOIL TEXTURE, pH, AND DRY COLOR.

Site	Horizon[†]	Texture[‡]	pH	Dry color[§]	Local rock type(s)
A	A	loam	7.4	2.5 YR 5/3	Judith River formation
	B_t	clay loam	7.4	5Y 4/4	
	B_{tk}	clay loam	8.4	10 YR 5/2	
B	A	loam	6.8	10 YR 4/3	Colorado shale
	B_t	clay	8.6	2.5 YR 3/3	
	$2BC_y$	silt loam	8.4	10 YR 4/3	
	$3Bt_{ky}$	clay loam	8.8	2.5 YR 3/3	
C	A	sandy loam	7.0	10 YR 4/2	Eagle sandstone and Claggett shale
	B_t	clay	8.0	7.5 YR 4/3	
	B_{tk}	clay loam	8.6	2.5 YR 4/3	
	B_{tk2}	clay	8.5	2.5 YR 5/3	
D	A	loam	6.6	10YR 4/2	Colorado shale
	B_t	clay	7.4	10 YR 4/3	
	B_{tk}	sandy clay loam	8.4	10 YR 4/2	
	$2BC_y$	loam	8.2	10 YR 4/1	

[†]Modified in light of texture data in Table 38.
[‡]Determined from data in Table 38 and a standard soil texture triangle.
[§]All values are probably darker than the actual dry color because analysis was performed indoors.

APPENDIX F:

LATITUDE, LONGITUDE, ALTITUDE, LITHOLOGY AND SIZE OF ALL BOULDERS MAPPED AS PART OF THIS STUDY.

Sample name	North Latitude[†]			West Longitude[†]			Altitude (m)	Lithology	Length (m)	Width (m)	Height (m)
	Degrees	Minutes	Seconds	Degrees	Minutes	Seconds					
E1	46	59	34	107	53	04	765±3	Pink granite	1.1	0.6	0.6
E2	47	00	24	107	57	23	867±6	Pink gneiss	1.2	0.6	0.3
E3	47	00	11	107	55	42	814±6	Foliated pink granite	0.8	0.6	0.5
E4	47	00	12	107	59	07	892±6	Foliated pink granite	0.9	0.6	0.3
E5	46	59	51	107	58	06	891±3	Pink granite	0.4	0.2	0.2
E6	46	59	52	107	58	08	892±3	Pink granite	0.8	0.5	0.2
E7	46	59	52	107	58	10	896±3	Pink gneiss	0.4	0.4	0.1
E8	46	59	50	107	58	15	895±3	Pink gneiss	0.8	0.8	0.3
E9	46	59	53	107	58	22	891±3	Pink granite	0.5	0.3	0.1
E10	46	59	55	107	58	18	887±3	Pink granite	0.4	0.2	0.1
E11	46	59	55	107	58	18	887±3	Pink granite	0.6	0.3	0.2
E12	46	59	55	107	58	17	885±3	Fossiliferous limestone	0.3	0.3	0.1
E13	46	59	54	107	58	17	885±3	Foliated pink granite	0.5	0.3	0.2
E14	46	59	54	107	58	17	885±3	Biotite schist	0.4	0.2	0.1
E15	46	59	54	107	58	17	885±3	Foliated pink granite	0.3	0.2	0.2

[†]Datum is NAD 83.

Sample name	North Latitude†			West Longitude†			Altitude (m)	Lithology	Length (m)	Width (m)	Height (m)
	Degrees	Minutes	Seconds	Degrees	Minutes	Seconds					
E16	46	59	54	107	58	17	885±3	Foliated pink granite	1.0	0.6	0.6
E17	46	59	54	107	58	17	885±3	Pink granite	0.3	0.3	0.1
E18	46	59	54	107	58	17	885±3	Foliated pink granite	0.5	0.3	0.2
E19	46	59	54	107	58	16	884±3	Pink gneiss	0.2	0.2	0.1
E20	46	59	54	107	58	12	893±3	Foliated pink granite	0.2	0.2	0.1
E21	46	59	55	107	58	11	892±3	Foliated pink granite	0.3	0.2	0.2
E22	46	59	52	107	58	02	885±3	Foliated pink granite	0.6	0.5	0.2
E23	47	02	35	108	04	56	891±3	Fossiliferous limestone	0.3	0.3	0.2
E24	47	02	40	108	04	55	882±3	Pink gneiss	0.3	0.2	0.2
E25	47	02	31	108	04	55	894±3	White gneiss	0.5	0.5	0.2
E26	47	02	31	108	04	55	894±3	White gneiss	0.3	0.3	0.2
E27	47	02	31	108	04	55	894±3	Pink granite	0.2	0.1	0.1
E28	47	05	29	108	07	22	881±3	Pink gneiss	0.9	0.7	0.2
E29	47	05	51	108	06	47	886±3	Pink granite	0.3	0.2	0.2
E30	47	07	15	108	05	12	890±3	Pink gneiss	0.6	0.6	0.2

†Datum is NAD 83.

Sample name	North Latitude†			West Longitude†			Altitude (m)	Lithology	Length (m)	Width (m)	Height (m)
	Degrees	Minutes	Seconds	Degrees	Minutes	Seconds					
E31	47	07	16	108	05	11	892±3	White granite	0.3	0.2	0.2
E32	47	07	30	108	03	09	824±6	Pink granite	0.6	0.6	0.2
E33	47	06	50	108	02	48	873±3	Pink granite	0.9	0.6	0.6
E34	47	06	52	108	02	47	874±3	Foliated pink granite	0.9	0.6	0.2
E35	47	07	22	108	01	32	836±3	Foliated pink granite	1.1	1.1	0.8
E36	47	07	22	108	01	36	840±3	Shonkinite	0.3	0.2	0.2
E37	47	07	01	108	02	03	848±3	Pink granite	0.7	0.6	0.3
E38	47	05	45	108	00	47	877±3	Shonkinite (?)	0.9	0.6	0.3
E39	47	05	45	108	00	47	878±3	Pink granite	0.8	0.5	0.5
E40	47	01	19	108	00	45	911±3	Pink granite	0.6	0.5	0.5
E41	47	01	26	108	01	20	882±3	Pink gneiss	0.8	0.5	0.5
E42	47	01	42	108	01	13	868±3	Pink granite	0.7	0.5	0.2
E43	47	00	14	107	54	02	802±6	Biotite schist	0.5	0.5	0.2
E44‡	47	03	43	107	57	38	814±6	Light pink granite	0.5	0.2	0.2

†Datum is NAD 83.
‡Postprocessed differential correction not applied to this sample.

Sample name	North Latitude[†]			West Longitude[†]			Altitude (m)	Lithology	Length (m)	Width (m)	Height (m)
	Degrees	Minutes	Seconds	Degrees	Minutes	Seconds					
E45[‡]	47	03	51	107	57	46	831±6	Pink gneiss	0.9	0.6	0.4
E46[‡]	47	03	52	107	57	45	828±6	Shonkinite	0.9	0.5	0.3
E47	47	03	52	107	57	44	826±6	Pink gneiss	0.6	0.5	0.2
E48	47	03	52	107	57	44	826±6	Pink gneiss	0.4	0.2	0.2
E49	47	03	52	107	57	42	823±6	Pink granite	0.4	0.2	0.2
E50	47	03	53	107	57	42	820±6	Pink granite	0.2	0.2	0.2
E51	47	03	53	107	57	41	815±6	Pink gneiss	0.6	0.3	0.3
E52	47	03	53	107	57	41	817±6	Pink granite	0.9	0.6	0.2
E53	47	03	52	107	57	42	823±6	Pink gneiss	0.6	0.5	0.2
E54	47	03	51	107	57	39	828±6	Pink granite	0.7	0.6	0.3
E55	47	03	51	107	57	39	829±6	White granite	0.8	0.4	0.2
E56	47	03	49	107	57	40	836±6	Foliated pink granite	0.8	0.5	0.3
E57	47	03	46	107	57	26	830±6	Pink gneiss	0.6	0.3	0.3
E58	47	07	01	107	56	51	777±6	Pink gneiss	0.3	0.3	0.2

[†]Datum is NAD 83.
[‡]Postprocessed differential correction not applied to this sample.

Sample name	North Latitude[†]			West Longitude[†]			Altitude (m)	Lithology	Length (m)	Width (m)	Height (m)
	Degrees	Minutes	Seconds	Degrees	Minutes	Seconds					
E59	47	07	00	107	56	51	777±6	Pink gneiss	0.6	0.5	0.3
E60	47	06	59	107	56	42	770±6	Pink gneiss	0.8	0.5	0.3
E61	47	09	33	107	57	50	770±6	Pink gneiss	1.1	0.6	0.6
E62	47	10	40	107	57	28	832±6	Pink gneiss	1.5	1.1	1.1
E63	47	10	41	107	57	48	855±6	Pink granite	1.2	0.6	0.6
E64	47	10	47	108	00	36	865±6	Pink gneiss	1.1	0.8	0.6
E65	47	11	04	108	01	22	879±6	Pink granite	1.5	1.1	0.9
E66	47	10	24	108	00	06	866±6	Foliated pink granite	1.4	0.9	0.9
E67	47	03	54	107	58	40	859±6	Foliated pink granite	0.8	0.6	0.3
E68	47	04	33	107	58	13	848±6	Pink granite	1.0	0.7	0.7
E69	47	04	34	107	58	18	846±6	Pink gneiss	0.9	0.8	0.8
E70	47	05	24	107	59	48	860±6	Pink granite	1.1	0.8	0.5
E71	47	01	27	108	16	43	927±3	White gneiss	0.6	0.5	0.3
E72	46	58	54	108	00	19	913±3	Pink granite	0.6	0.5	0.3
E73	46	55	55	108	09	21	897±3	Pink/white gneiss	0.8	0.8	0.4

[†]Datum is NAD 83.

Sample name	North Latitude†			West Longitude†			Altitude (m)	Lithology	Length (m)	Width (m)	Height (m)
	Degrees	Minutes	Seconds	Degrees	Minutes	Seconds					
E74	46	57	20	108	00	12	894±3	Pink granite	1.3	1.0	0.6
E75	47	07	21	107	52	22	886±3	Pink granite	0.5	0.3	0.3
E76	47	07	23	107	52	43	896±6	Foliated pink granite	0.8	0.6	0.3
E77	47	07	38	107	54	16	882±6	Pink granite	0.9	0.6	0.3
E78	47	08	09	107	53	12	882±6	No data	0.8	0.5	0.4
E79	47	08	24	107	53	06	887±6	Pink granite	0.8	0.5	0.5
E80	47	08	26	107	53	31	883±6	Pink gneiss	0.9	0.6	0.6
E81	47	08	42	107	53	45	883±6	Pink gneiss	0.9	0.6	0.3
E82	47	09	06	107	54	27	873±6	Pink gneiss	0.9	0.6	0.5
E83	47	15	55	107	56	52	726±6	Pink gneiss	1.2	0.9	0.6
E84	47	20	53	108	08	16	910±6	Pink gneiss	0.7	0.5	0.6
E85	47	20	56	108	08	20	917±6	White granite	0.5	0.3	0.3
E86	47	18	5	107	59	33	856±6	Schist-gneiss	0.9	0.9	0.5
E87	47	18	15	107	58	25	780±6	Pink gneiss	1.5	0.9	0.9
E88	47	24	40	108	08	20	874±3	Pink granite	0.9	0.9	0.6

†Datum is NAD 83.

Sample name	North Latitude†			West Longitude†			Altitude (m)	Lithology	Length (m)	Width (m)	Height (m)
	Degrees	Minutes	Seconds	Degrees	Minutes	Seconds					
E89	47	24	40	108	08	21	871±3	Pink gneiss	1.2	0.9	0.3
E90	47	24	38	108	08	19	869±3	Pink gneiss	1.2	1.2	0.8
E91	47	24	29	108	03	01	869±3	White granite	1.4	0.8	0.6
E92	47	03	45	108	00	24	886±3	Foliated pink granite	0.9	0.9	0.6
E93	47	08	28	107	58	03	763±6	Light pink gneiss	0.5	0.5	0.3
E94	47	10	41	108	04	47	908±6	Pink gneiss	0.5	0.2	0.2
E95	47	09	28	108	09	02	879±6	No data	0.5	0.5	0.3
E96	46	55	26	107	51	20	875±3	Pink gneiss	0.6	0.3	0.3
E97	46	55	28	107	51	21	871±3	Pink ?	0.6	0.6	0.3
E98	46	55	29	107	51	23	867±3	Pink granite	0.9	0.6	0.5
E99	46	54	59	107	51	22	883±3	Foliated pink granite	1.1	0.9	0.8
E100	46	55	01	107	51	23	881±3	Pink granite	0.6	0.6	0.5
E101	46	55	08	107	50	23	881±3	Pink granite	0.9	0.8	0.8
E102	46	55	15	107	50	20	886±3	Pink gneiss	0.6	0.6	0.2
E103	46	55	27	107	50	51	868±3	Pink gneiss	0.5	0.3	0.2

†Datum is NAD 83.

Sample name	North Latitude[†]			West Longitude[†]			Altitude (m)	Lithology	Length (m)	Width (m)	Height (m)
	Degrees	Minutes	Seconds	Degrees	Minutes	Seconds					
E104	46	55	16	107	51	10	899±3	Pink gneiss	0.6	0.6	0.2
E105	47	20	58	107	52	56	832±6	Pink gneiss	0.6	0.5	0.3
E106	47	20	49	107	52	38	833±6	Foliated pink granite	1.5	1.5	1.5
E107	47	03	41	107	43	23	875±3	Pink gneiss	0.9	0.6	0.5
E108	47	08	27	107	57	56	751±6	Pink granite	0.9	0.9	0.2
E109	47	09	50	107	58	53	854±6	Pink granite	1.2	0.9	0.9
E110	47	13	14	108	01	01	871±6	Pink gneiss	0.8	0.8	0.2
E111	47	10	06	108	02	59	886±6	Pink granite	0.6	0.3	0.5
E112	47	08	45	108	00	40	885±6	Pink gneiss	1.2	0.6	0.6
E113	46	58	50	107	32	45	913±3	Pink granite	0.9	0.6	0.4
E114	47	08	35	107	58	28	775±6	Gneiss	1.2	0.6	0.5
E115	46	59	30	107	33	29	916±3	Pink granite	0.5	0.3	0.1
E116	46	59	30	107	33	28	917±3	Black/pink gneiss	0.4	0.3	0.1
E117	47	04	00	107	57	28	794±6	Foliated pink granite	1.2	1.1	0.3

[†]Datum is NAD 83.

Sample name	North Latitude[†]			West Longitude[†]			Altitude (m)	Lithology	Length (m)	Width (m)	Height (m)
	Degrees	Minutes	Seconds	Degrees	Minutes	Seconds					
E118[§]	47	04	02	107	57	28	810±6	Foliated pink granite	0.9	0.6	0.3
E119[§]	47	04	02	107	57	29	810±6	Foliated pink granite	0.6	0.6	0.3
E120[§]	47	04	02	107	57	24	789±6	White gneiss	0.9	0.6	0.6
E121[#]	47	07	57	107	53	03	883±6	No data	1.2	0.9	0.3
E122[#]	47	15	54	107	56	52	725±6	Pink granite	0.8	0.6	0.3
E123[#]	47	15	55	107	56	51	736±6	No data		No data	
E124[#]	47	15	55	107	56	51	736±6	No data		No data	
E125[#]	47	08	50	107	53	47	871±6	No data	0.9	0.6	0.6

[†]Datum is NAD 83.
[§]The latitude and longitude of these boulders was approximated from the 1:24,000 topographic maps.
[#]Latitude and longitude data collected using a Magellan GPS as opposed to the Trimble Explorer.

APPENDIX G:

DETAILED DESCRIPTIONS OF SAMPLES COLLECTED FOR SURFACE EXPOSURE AGE DATING.

TABLE 40. DESCRIPTION OF SAMPLES FROM ALTITUDE CLUSTER 1.

Sample name	Latitude/ Longitude	Elevation (m)	Size (m)	Comments
E60	47° 6.99' N 107° 56.70' W	772	0.76 x 0.53 x 0.30	Gneiss; original surface; no lichen; located on the crest of an east-west trending ridge that juts out into the center of a meander of the Musselshell River to the east; maximum sample depth=5cm
E61†	47° 9.54' N 107° 57.83' W	770	1.07 x 0.61 x 0.61	Gneiss; lichen on sides; partly buried; surface is rough but not pitted; located at the intersection of two unpaved roads on the lower part of a ridge on the north side of Haley Coulee; max. sample depth=7 cm
E122	47° 15.9' N 107° 56.87' W	728	0.76 x 0.61 x 0.30	Granite; still retains a rounded shape; located on a shallow colluvial slope on the edge of the modern floodplain of the Musselshell approximately 25 m from a steep bluff; potentially exhumed from bluff; topographic shielding from bluff accounted for in MATLAB program; max. samp. depth=7 cm

TABLE 41. DESCRIPTION OF SAMPLES FROM ALTITUDE CLUSTER 2.

Sample name	Latitude/ Longitude	Elevation (m)	Size (m)	Comments
E54†	47° 3.85' N 107° 57.65' W	828	0.69 x 0.61 x 0.30	Granite; lichen on the north side; located on a ridge on the south side of Long Coulee; surface is covered in gravel including exotic lithologies; tends to shatter; polished, maybe by the wind; max. sample depth=3 cm; sample dips $\leq 10^{o}$
E45	47° 3.85' N 107° 57.76' W	831	0.91 x 0.61 x 0.46	Blebby gneiss; very lichen covered on north side; located on the same surface as E54; clearly exfoliating on the sides, though the top may be original surface; 4 mm white weathering rind; max. sample depth=6 cm
E62	47° 10.67' N 107° 57.46' W	832	1.52 x 1.07 x 1.07	Gneiss; lichen covered, bumpy surface; located next to a two-track road on a gentle slope at the head of a modern coulee; rolling is possible (round shape); wooded area; max. sample depth=7 cm
E32	47° 7.49' N 108° 3.14' W	824	0.61 x 0.61 x 0.23	Granite with 0.5 cm quartz band on top; located on a hillside on the edge of a modern coulee bottom (has probably been lowered since deposition); smooth, possibly original surface, not pitted; striated (possibly formerly buried); max. sample depth=4.5 cm

TABLE 42. DESCRIPTION OF SAMPLES FROM ALTITUDE CLUSTER 3.

Sample name	Latitude/ Longitude	Elevation (m)	Size (m)	Comments
E69	47° 4.57' N 107° 58.30' W	846	0.91 x 0.76 x 0.76	Gneiss; lichen covered; rough surface; located on a gentle bedrock-floored slope north of Long Coulee; wooded area; max. sample depth=4 cm
E37	47° 7.01' N 108° 2.05' W	848	0.69 x 0.61 x 0.30	Granite; some pitting; surface is flat w/ parallel raised ridges; located on a gentle slope at the head of a gully; max. sample depth=3.5 cm
E68	47° 4.55' N 107° 58.21' W	848	0.99 x 0.69 x 0.69	Granite; lichen on top and downhill side but not on rough uphill side; hardly buried and has a round shape (may have rolled some); the top surface is very polished and shiny (may be a ventifact coating on a glacial surface); 0.25 mm weathering rind; wooded area; max. sample depth=4.2 cm
E63	47° 10.68' N 107° 57.80' W	855	1.22 x 0.61 x 0.61	Granite; some lichen; some original surface sampled; located next to a two-track road on the crest of a ridge; 3.5 mm black weathering rind with underlying rust layer; wooded area; max. sample depth=5 cm
E109	47° 9.84' N 107° 58.89' W	854	1.22 x 0.91 x 0.91	Granite; lichen covered; partly buried; located on a ridge north of Haley Coulee; max. sample depth=4 cm
E70	47° 5.41' N 107° 59.80' W	860	0.91 x 0.91 x 0.61	Granite; lichen covered; located on a gentle slope; max. sample depth=4.5 cm
E66	47° 10.41' N 108° 0.09' W	866	1.37 x 0.91 x 0.91	Granite; original surface; located on a ridge but next to a bladed road; not very buried; carbonate coat exposed and tilted; this rock was probably displaced when the road was made, but I was able to correct for this in sampling by using the carbonate coat to identify the former top; max. depth=3.5 cm
E33†	47° 6.83' N 108° 2.80' W	873	0.91 x 0.61 x 0.61	Granite; lichen covered; looks smooth and polished, even striated, where not broken; carbonate coat visible and tilted; the rock was displaced but I corrected for this in sampling; tilt in sample surface corrected in MATLAB program; located on a ridge next to a two-track road; wooded area; max. depth=6.5 cm
E82	47° 9.10' N 107° 54.45' W	873	0.91 x 0.61 x 0.46	Gneiss; some lichen; grusified but preserves original round shape; 2 mm weathering rind; located on a ridge top next to two-track road; max. sample depth=5 cm
E39	47° 5.75' N 108° 0.78' W	878	0.76 x 0.46 x 0.46	Granite; two carbonate coats at right angles to each other; some polished surface but mostly fractured; located next to two-track road on a broad ridge; max. sample depth=4 cm
E96	46° 55.44' N 107° 51.34' W	875	0.61 x 0.30 x 0.30	Gneiss; original surface; not buried; max. sample depth=6 cm

TABLE 43. DESCRIPTION OF SAMPLES FROM ALTITUDE CLUSTER 4.

Sample name	Latitude/ Longitude	Elevation (m)	Size (m)	Comments
E28	47° 5.48' N 108° 7.37' W	881	0.91 x 0.76 x 0.23	Blebby gneiss; little lichen; partly buried; bumpy, exfoliated surface; rounded shape; located on a gentle slope between a ridge and the headwaters of Cat Creek; max. sample depth=4.5 cm
E100	46° 55.02' N 107° 51.38' W	882	0.61 x 0.61 x 0.46	Granite; pegmatitic; partly buried; located on a low ridge; max. sample depth=6 cm
E101	46° 55.14' N 107° 50.38' W	881	0.91 x 0.76 x 0.61	Granite; very smooth surface; 1 cm^2 of original surface – rest of sample lowered by 2mm; partly buried; located on a slope between a ridge and a gully; max. sample depth=4.5 cm
E16†	46° 56.90' N 107° 58.29' W	885	0.99 x 0.61 x 0.61	Gneiss; lichen on all sides; slightly buried; located on gentle slope between a ridge and a gully; max. sample depth=5 cm
E102	46° 55.26' N 107° 50.34' W	886	0.61 x 0.61 x 0.23	Gneiss; smooth surface; located on a ridge; max. sample depth=5.5 cm

TABLE 44. DESCRIPTION OF SAMPLES FROM ALTITUDE CLUSTER 5.

Sample name	Latitude/ Longitude	Elevation (m)	Size (m)	Comments
E40	47° 1.31' N 108° 0.75' W	911	0.61 x 0.46 x 0.46	Granite; slightly buried; not much lichen; some pitting and exfoliation; located on a ridge that is being cut into by a modern coulee; max. sample depth=5.5 cm
E115	46° 59.50' N 107° 33.48' W	916	0.46 x 0.30 x 0.08	Granite; no lichen; almost completely buried; some original surface; 2 mm weathering rind (black then white then yellow); located on the flats at the headwaters of a modern coulee; max. sample depth=3.5 cm
E116	46° 59.50' N 107° 33.46' W	917	0.38 x 0.30 x 0.08	Gneiss; almost completely buried; half black, half pink; rough surface; located in close proximity to E115; max. sample depth=5 cm
E113†	46° 58.83' N 107° 32.75' W	913	0.91 x 0.61 x 0.38	Granite; very buried; rough surface; rounded shape; located down in the coulee by an old spring; max. sample depth=6 cm

†Also sampled for ^{21}Ne analysis